Polarons

Recent
Progress and
Perspectives

Amel Laref
Editor

NOVA

POLARONS

RECENT PROGRESS AND PERSPECTIVES

PHYSICS RESEARCH AND TECHNOLOGY

Additional books and e-books in this series can be found on Nova's website under the Series tab.

POLARONS

RECENT PROGRESS AND PERSPECTIVES

AMEL LAREF
EDITOR

NOTICE TO THE READER

Published by Nova Science Publishers, Inc. † New York

CONTENTS

PREFACE

In this book, the modern developments of polaron and its applications in condensed matter physics and materials sciences, will be exposed. Polarons are an excessively prosperous and profound arenas which are still very active research. The exploration of polarons and bipolarons in magnetic semiconductors and transition metal oxides has renewed interest in the current research related to the contemporary materials. A luminous guidance on various kinds of polaron forms will be discerned theoretically and experimentally in various classes of materials. This book supplies the recent scrutiny and advancement of polaron physics in multifunctional materials, conducting the reader to the comprehension from single-polaron problems to multi-polaron systems. The primary target of the book is to offer the reader a thorough overview about the contemporary advances in the polarons properties of various systems. The book covers broad spectrum of disciplines of polarons performed by well-acknowledged international researchers who are active in this area and will assist scientists with a background in solid state physics and materials sciences. Special emphasis is provided to understand and to describe many interesting phenomena related to polarons problems in advanced materials. Moreover, current importance and ultimate prospects for the supplementary evolution of polarons are addressed. The scope involves a description of many compelling phenomena in manganites, colossal magnetoresistance oxides, high-temperature superconductors, ferromagnetic oxides, conducting polymers, inorganic and organic semiconductors, ferrites, glasses-ceramics, and semiconducting of low-dimensionality, such as, heterostructures, quantum wells, quantum well wires, and quantum dots. The overview of the underlying physical concepts, experimental methods, and applications of polarons are represented. A numerous of new physical phenomena in various materials will be described on the basis of single and multi-polaron theories. Appealing electronic transport and optical mechanisms will be emphasized from the emergence of polarons. The principles prevailing polaron and multi-polaron formations and their applicability into wide spectrum of physical aspects of advanced materials with reduced dimension, like transport through nanowires are also discussed. Novel theoretical models based on the polaron phenomena are needed to promote better comprehension of the fundamental physics of advanced materials. This could aid more practical exploitation in prospective application devices. This book reviews the recent advancement in the field of polarons, going beyond their fundamental description to the numerous of vigorous routes of research. Overall, this book will serve as valuable reference for students, researchers, material and chemical engineers to comprehend the

polaron properties in advanced materials and its ongoing breakthrough. The book composes normally into sixteen chapters.

In the chapter 1 of the book, a special emphasis is devoted to Electron Paramagnetic Resonance (EPR) spectroscopy of polarons in conjugated polymers and their nanocomposites. The focus of this chapter is on the utilization of EPR technique combined with the spin label and probe, steady-state microwave saturation, saturation transfer and conductometric methods for the investigation of conjugated polymers. The author reviews the key experimental methodological approaches basically developed for the scrutiny of various organic condensed systems.

Chapter 2 reviews tight-binding models for the charge transport in organic semiconductors. This chapter is dedicated to an exposition of the most basic description regarding the Tight-Binding models of charge transport in organic semiconductors. Moreover, the physical aspects of some valuable applications are succinctly discussed about the recombination process between quasi-particles in organic-based optoelectronic devices.

Chapter 3 is addressed to the manifestations of polaron effect on charge transport property for organic semiconductors. In this chapter, the researchers are primarly concerened to explain the polaron effect on the charge transport of organic semiconductors. Several kinds of theoretical models of polaron effect on the charge transport property in organic semiconductors has been discussed in details. The authors aimed that their contexts can be beneficial for ameliorating polaron effect in organic materials and for serving to the progress of novel organic devices with high performance.

Chapter 4 scrutinizes the recent results about the polarons in electrochemically doped non-degenerate π-–conjugated polymers. The authors reported that the produced quasiparticles, such as polarons and bipolarons can be directly inspected by employing the experimental techniques. The polaron and bipolaron effects on these systems would provide a vision to alter light-to-current conversion processes in organic materials and many other next generation devices of organic electronics.

Chapter 5 focuses on the anharmonicity, soliton-assisted transport and electron surfing, as a generalization of polaron transport with practical consequences. The authors discussed a generality of the polaron theory to involve soliton assisted transport. A novel filed effect transistor based upon the solectron concept (SFET) is shortly exposed. The researchers suggested that SFET provides a thoroughly new idea to create computer elements permitting the switching with three orders a magnitude reduction in energy consumption which would be useful as a valuable energy reductions in the digital computers, server farms, and smart phones.

Chapter 6 delineates the polarons in the functionalized nanowires. The authors discussed their self-consistent theoretical approach that is evolved to portray the electronic spectra in functionalized semiconducting nanowires. The quantization, localization and polaron formation have been explored for an uncompensated charge carrier in a functionalized nanowire.

Chapter 7 describes the bound polarons and exciton-phonons coupling in semiconductor nanostructures. This chapter offers an overview of the contemporary advancement in the description of polaronic effects on confined impurities and excitons in semiconductor nanostructures and their pertinence to ameliorating electronic and excitonic characteristics in these systems. The researchers expose important theoretical frameworks, presently promoted

in scrutiny, taking into account the interactions between charge carriers and optical phonons in semiconductor of low-dimensional structures.

Chapter 8 overviews the electrical and structural study of compounds with modulated scheelite-type structure at high temperature. The authors revised and discussed the electrical properties of scheelites and related compounds. They explained the polaronic mechanisms which are correlated with the thermal dependence of the crystal structure.

Chapter 9 reports the unravelling effects of polaron conduction on mixed conductivity glasses. In the current chapter, the authors are principally concerned to discuss the electrical properties of glasses. They characterized and examined the electrical response of uncommon oxide glasses. According to their finding, it was viable to demonstrate the presence of ion-polaron entity in modified tellurite glassy matrices.

Chapter 10 characterizes the small polaron hopping conduction mechanism in based V_2O_5-glass-ceramic nanocomposites. In this chapter, the compositional dependence of the nanostructural and transport properties of V_2O_5-based glasses and corresponding glass-ceramic nanocomposites have been outlined by the researchers in view of Mott's small polaron hopping (SPH) model. They also elucidated the mechanism of electrical conduction of these glasses and the corresponding glass-ceramic nanocomposites.

Chapter 11 explores the polaron in perovskite manganites. This chapter deals with the polaron concept, types and mechanisms in perovskite manganites and its effect on their transport properties. The polaron effect has a main contribution in the magneto-transport correlation in manganites, such as phenomena as colossal magnetoresistance. The authors exhibited the polaron contribution in manganite phenomena and its impact on the magneto-transport correlation.

Chapter 12 discusses the correlated polarons in mixed valence oxides. In this chapter, the authors elucidated the transport properties of some mixed valence oxides compounds by means of correlated polaron theory accounting for the colossal magnetoresistance in manganites. They suggested that the correlated polaron model was extended to transport in the normal state of high temperature copper oxide superconductors.

Chapter 13 covers the polarons and bipolarons in colossal magnetoresistive manganites. In this chapter, the researchers reviewed some unconventional oxygen-isotope effects in doped manganites. According to their results, the detected large unconventional isotope effects notably evince the formation of polarons/ bipolarons to be related to strong electron-phonon coupling, which is pertinent to the fundamental physics of manganites and significant for the emergence of colossal magnetoresistance.

Chapter 14 discusses polaronic high-temperature superconductivity in bismuthates and cuprates. The authors illustrated the experimental evidences for the polaronic Cooper pairs in both bismuthate and cuprate superconductors. They stated that the substantial enhancement of the effective density of states to be connected to the lattice polaronic effect and this will conduct to the increase of the effective electron-phonon coupling constant to a value inevitably for the inspected superconducting transition temperature in bismuthates.

Chapter 15 outlines the polarons in ferrites. These magnetic materials illustrate striking features that are useful in the electronic devices. The researchers discussed their latest results on the ferrite systems of interest with emphasis on polaron models. Ferrites which are ferromagnetic semiconductors opened a novel perspective in material physics and the demand for high resistivity ferrites conducted to the synthesis of various ferrites.

Chapter 16 provides an overview on the magnetic polarons in EuTe: early and modern discoveries in magnetic order control in semiconductors. In this chapter, the authors discuss the evolution of the theoretical modeling for magnetic polarons and the background experimental measurements, with emphasis to the EuTe magnetic polaron. The advancement of spintronic devices, magnetic polarons are also very appealing in a more basic perspective, conveying information about the physics of the exchange interactions and its dynamics, which is a broad area in material science and solid state physics.

Chapter 1

EPR SPECTROSCOPY OF POLARONS IN CONJUGATED POLYMERS AND THEIR NANOCOMPOSITES[*]

Victor I. Krinichnyi[†]

Institute of Problems of Chemical Physics,
Chernogolovka, Russian Federation

ABSTRACT

The past two decades have seen extraordinary progress in synthesis and study of organic conjugated polymers and their nanocomposites. This caused by large prospects of utilization of such systems in molecular electronics and spintronics. One of the main scientific goals is to reinforce human brain with computer ability. However, a convenient modern computer technology is based on three-dimensional inorganic crystals, whereas human organism consists of biological systems of lower dimensionality. So, the combination of a future computer based on biopolymers with organic conjugated polymer semiconductors of close dimensionality is expected to increase considerably a power of human apprehension. This is why understanding the major factors determining specific spin charge transfer processes in conjugated polymers is now a hot topic in organic molecular science.

The charge in such systems is transferred by topological excitations, spin polarons and spinless bipolarons, characterized by high mobility along polymer chains. This stipulated the utilization of Electron Paramagnetic Resonance (EPR) spectroscopy as a unique direct tool for more efficient study and monitoring of spin reorganizing, relaxation and dynamics processes carrying out in polymer systems with such charge carriers. It was demonstrated that the method allows to obtain qualitative new information on spin-modified polymer objects and to solve various scientific problems.

The focus of the present chapter is on the use of EPR technique in combination with the spin label and probe, steady-state microwave saturation, saturation transfer and

---

[*] This chapter is dedicated to the veteran of the World War II, designer Grigori T. Rudenko.
[†] Corresponding Author Email: Email: kivirus@gmail.com; Web: http://hf-epr.awardspace.us.

conductometric methods in the study of initial and treated conjugated polymers. It covers a wide range of specific approaches suitable for analyzing of processes carrying out in polymer systems with paramagnetic adducts providing readers with background knowledge and results of the latest research in the field. It reviews the main experimental methodological approaches originally developed for the study of various organic condensed systems.

The chapter is organized as following. The first part includes the fundamental properties of conjugated polymers with topological quasi-particles, polarons and bipolarons, as charge carriers. The second part is devoted to an original data obtained at X-band to D-band (30 − 2-mm, 9.7 – 140 GHz) EPR study of the nature, relaxation and dynamics of polarons stabilized and initiated in widely used conjugated polymers and their nanocomposites. The third part reveals the possibility to handle of charge transport in some polymer composites with spin-spin exchange which can be used in the further creation of novel elements of molecular electronics and spintronics. Finally, theoretical and experimental background necessary for EPR study of the main magnetic resonance, relaxation and dynamics parameters of polaron quasi-particles in organic compounds are described shortly in the Appendix.

1. INTRODUCTION

Basic features of polarons were well recognized a long time ago and have been described in a number of review publications (Emin 2013, Chatterjee and Mukhopadhyay 2018). Nevertheless, interest in the study of polarons has recently increased because they are important to the understanding of properties of the microcosm and even the space.

Fundamental electron–phonon interactions have been shown to be relevant in many inorganic and organic semiconductors, giant magnetoresistance oxides, and transport of Cooper pairs in high-temperature superconductors and free charges through nanowires and quantum dots are often governed by libration displacements of environmental ions. Charge transport in organic semiconductors is also sensitive to polaronic effects, which is particularly relevant in the design of organic components of molecular electronics. When charge carriers, polaron or electron, are formed in a polymer system, the surrounding ions can interact with them. The ions can adjust their positions slightly, balancing their interactions with the charge carriers and the forces that hold the ions in their stable positions. This adjustment of positions leads to a polarization locally centered on the charge carrier. Besides, such a quasi-particle can be formed as topological distortion separating two conformational forms of conjugated polymers (Lu 1988). There can be formed "large" and "small" polarons, defined by whether or not the polarization cloud is much larger than the atomic spacing in the material. Polarons are a useful way to understand charge transport in conjugated polymer semiconductors which are very squishy, deformable systems held together by van-der-Waals rather than covalent bonding.

1.1. Properties of Conjugated Polymers

A wide class of electronic materials, organic conjugated polymers, attracts during the past decades great attention due to their unique capabilities, namely, flexible, solution processable, lightweight, and tunable electronic properties (Wan 2008, Heeger, Sariciftci, and Namdas

2010, Launay and Verdaguer 2013, Kobayashi and Müllen 2015, Kondawar and Sharma 2017). The particular interest to such systems was initiated at 1964 by the Little hypothesis (Little 1964) on principal possibility of synthesis of high-temperature superconductors based on conjugated polymers. This caused by large prospects of utilization of such systems in molecular electronics. Organic semiconductors have been widely investigated in recent years also in the context of spintronics. One of the main scientific goals is to reinforce human brain with computer ability. However, a convenient modern computer technology is based on three-dimensional inorganic crystals, whereas human organism consists of biological systems of lower dimensionality. So, the combination of a future computer based on biopolymers with organic conducting polymers of close dimensionality is expected to increase considerably a power of human apprehension. Understanding the major factors which govern specific spin charge transfer processes in conjugated polymers is now a hot topic in organic molecular science. This is why the investigation of conjugated polymers and their nanocomposites has generated entirely new scientific conceptions and a potential for their perspective application as active material for creation of novel components of organic molecular electronics.

Figure 1 shows room temperature (RT) direct current (*dc*) conductivity σ_{dc} of some conjugated polymers in comparison with that of convenient insulators, semiconductors and conductors. The structures of some conjugated polymers used as active matrix in molecular electronics are schematically presented in the Figure as well. The principal *x*-axis of polymers' chain is shown to be chosen parallel to their longest molecular *c*-axis, the *y*-axis lies in the C-C-C plane, and the *z*-axis is perpendicular to *x*- and *y*-axes. These polymers initially synthesized as films or powders are insulators with *dc* conductivity near $10^{-15} - 10^{-10}$ S/m. This parameter can be varied controllable by more than 12 orders of magnitude by chemical or electrochemical oxidation or reduction of their chains. Electron transfer upon such polymer doping leads to the increase of *dc* conductivity up to ~ $10^{-3} - 10^2$ S/m (semiconductor regime) or even up to ~ $10^4 - 10^8$ S/m (metal regime) (Salamone 1996, Nalwa 1997, Scotheim, Elsenbaumer, and Reynolds 1997). The analogous effect can also be achieved by somewhat physical effect on the polymer, e.g., by laser radiation. This leads to the formation of quasi-particles, polarons, on the polymer chains due to their topological distortion (Lu 1988). Conjugated polymers have a highly anisotropic quasi-one-dimensional (Q1D) π-conjugated structure with charge carriers on delocalized polarons which makes such systems fundamentally different from traditional inorganic semiconductors, for example, silicon and selenium, and from well-known convenient insulating polymers, e.g., polyethylene, polyvinyl chloride and polystyrene. Electronic properties of such systems strongly depend on their structure, morphology and quality, whereas the type of their conductivity is governed by the nature of the introduced counter-ion (Menon et al. 1997, Wessling 1997). The introduction of anions, e.g., HSO_4^- BF_4^-, ClO_4^-, I_3^-, $FeCl_4^-$ into a polymer induces a positive charge on a polymer chain and thus leads to *p*-type conductivity of the polymer. Conductivity of *n*-type is realized under polymer doping by Li^+, K^+, Na^+ and ions of other alkali metals.
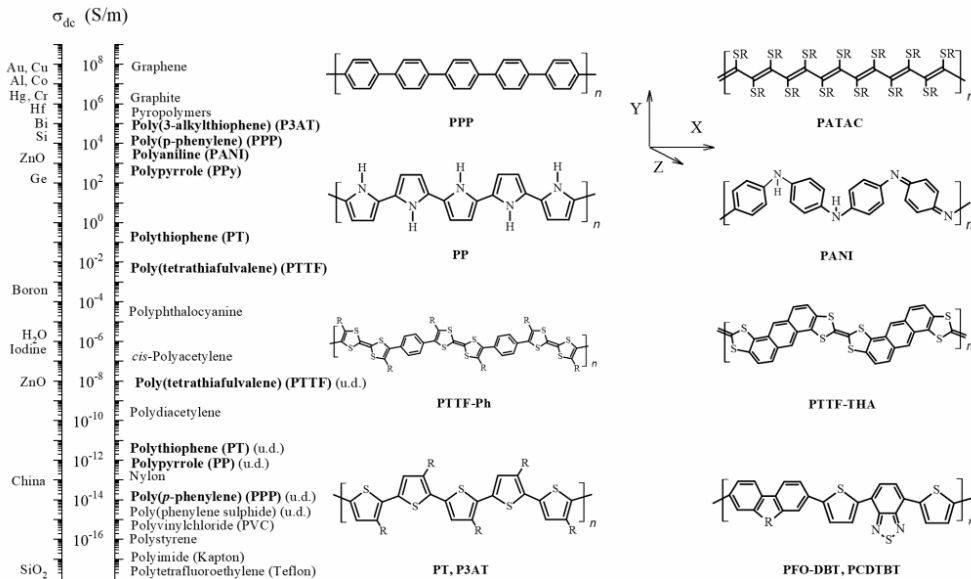
Figure 1. Room temperature (RT) direct current (*dc*) conductivity σ_{dc} of undoped (u.d.) and highly doped conducting polymers (Nalwa 1997) in comparison with that of some convenient polymers and metals. The structures of poly(*p*-phenylene) (PPP). poly(*bis*-alkylthioacetylene) (PATAC, R ≡ CH$_3$, C$_2$H$_5$, C$_3$H$_7$), polypyrrole (PPy), polyaniline (PANI), polytetrathiafulvalene linked *via* phenyl (PTTF-Ph, R ≡ H, CH$_3$, C$_2$H$_5$) and tetrahydroanthracene (PTTF-THA) bridges, polythiophene (PT), poly(3-alkylthophene) (P3AT, R ≡ C$_m$H$_{2m+1}$).poly[2,7-(9,9-dioctylfluorene)-alt-4,7-bis(thiophen-2-yl)benzo-2,1,3-thiadiazole] [PFO-DBT, R ≡ >C=(C$_8$H$_{17}$)$_2$], and poly[N-9'-heptadecanyl-2,7-carbazole-alt-5,5-(4',7'-di-2-thienyl-2',1',3'-benzothiadiazole)] [PCDTBT, R ≡ >N-CH-(C$_8$H$_{17}$)$_2$] are shown schematically**.**

In traditional 3D inorganic semiconductors, fourfold (or sixfold, etc.) coordination of each atom to its neighbor through covalent bonds leads to a crystalline structure. Electron excitations may be usually considered in the context of this rigid structure, leading to the conventional conception of generalized electrons or holes as dominant charge carriers. The situation with conjugated polymer semiconductors is quite different: once they form bulk nanocomposites with the dopants embedded, their Q1D structure becomes more susceptible to structural distortion. Therefore, electronic properties of conjugated polymers may be conventionally considered in the frames of bands theory (Singleton 2001) as well as of soliton and polaron one (Lu 1988), based on Peierls instability (Peierls 1996) in Q1D systems. Elementary-charge- and energy-transfer phenomena occurring in such materials are crucial to the structural and conformational diversity of their polymer active matrix. So, in order to construct organic electronic elements based on conjugated polymers, the correlations of their morphology, electronics properties, selectivity, sensitivity, etc. with magnetic, relaxation and dynamics properties of spin charge carriers should be obtained and analyzed.

1.2. Polarons and Bipolarons in Conjugated Polymers

The chains of poly(*p*-phenylene) (PPP) and analogous polymers consist of benzene rings linked via para-position (see Figures 1 and 2). In the solid state two successive benzene rings are tilted with respect to one another by torsion (dihedral) angle θ≈ 23º (Brédas 1986). Such

angle appears as a compromise between the effect of conjugation and crystal-packing energy, which would lead to a planar morphology, and the steric repulsing between ortho-hydrogen atoms, which would lead to a non-planar morphology (Brédas et al. 1982). The globular structures of PPP consist of packed fibrils with a typical diameter of 100 nm.

The band structure of PPP is obtained as a result of the overlapping of π-orbits of the benzene rings (Figure 2). For this polymer a resonance form can also be derived, which corresponds to a quinoid structure. Calculations have indicated that polaron formation is energetically favorable in all the organic conjugated polymers have so far studied (Brédas and Street 1985). The polaron binding energy is of the order of 0.03 eV in PPP and 0.12 eV in PPy. Benzenoid and quinoid forms are characterized by higher and lower energy, respectively. This provokes the formation on polymer chains of topological excitations, namely polaron with spin $S = ½$ whose energy levels ΔE_1 and ΔE_2 of ca. 0.5 eV lie in the gap above the valence band (VB} and below the conduction band (CB) edges as it is shown on Figure 2. At intermediate doping level y a second electron is taken out of the chain, the energetically favorable species, bipolarons, are formed. The energy levels associated with the bipolarons are empty and are located closer to the bandgap than those associated with the polarons (Heeger et al. 1988). The binding energy of bipolarons formed, e.g., in PPy is 0.69 eV (Brédas and Street 1985). The width of the polaron and bipolaron depends on the polymer structure and normally is 3 - 5 and 4 – 5.5 monomer units, respectively (Brédas and Street 1985, Elsenbaumer and Shacklette 1986, Devreux et al. 1987, Lu 1988, Westerling, Osterbacka, and Stubb 2002, Niklas et al. 2013). As a doping level y increases, bipolaron states overlap forming bipolaron bands within the gap. At high doping level, these bands tend
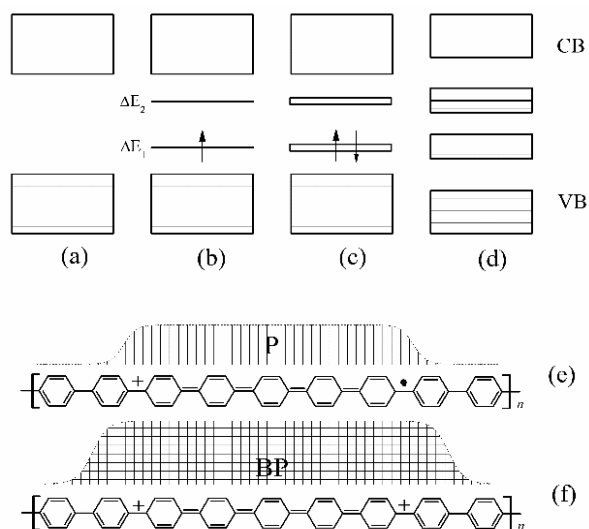
Figure 2. Evolution of an initial band structure of poly(*p*-phenylene) (*a*) during the polymer doping: (*b*) slight doping level with the appearance of polaron states in the mid gap above valence band (VB) and below conducting band (CB) edges, (*c*) intermediate doping level, with the appearance of states of non-interacting diamagnetic bipolarons, (*d*) high doping level, where bipolaron states overlap and form filled and semifilled bands with quasi-metallic behavior; the formation of a spin charged polaron *P* (*e*) and spinless bipolaron *BP* (*f*) on the chain of poly(*p*-phenylene) is shown. The distribution of the spin on the polaron and the double elemental charge on the bipolaron is shown by appropriate filled extended figures.
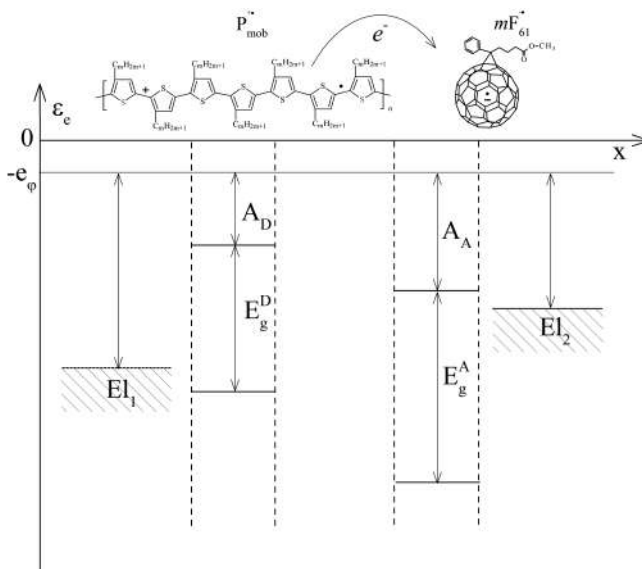
Figure 3. Schematic band diagram of two semiconductors with different electron affinity before making between them the BHJ. The electron donor (A_D) and electron acceptor (A_A) affinities are defined vs. the electron energy in vacuum at the same electrical potential. E_g^D and E_g^A are the band gap energies of the electron donor and electron acceptor, respectively. In the top, the P3AT and PC$_{61}$BM are schematically shown as electron donor and electron acceptor, respectively. The appearance of the polaronic quasi-particle $P_{mob}^{\bullet+}$ with a spin $S = \frac{1}{2}$ and an elemental positive charge in a P3AT chain and ion radical $mF_{61}^{-\bullet}$ with an elemental negative charge and a spin $S = \frac{1}{2}$ on a PC$_{61}$BM is shown as well.

to overlap and create new bandgap energy bands that may merge with the VB and CB allowing freedom for extensive charge transfer. The analogous band structure is formed also in case of other PPP-like polymers (Lu 1988). The energy levels ΔE_1 and ΔE_2 of polarons depend on the polymer structure and the nature of dopant molecule.

Polaron quasi-particles can be also formed on polymer chains, e.g., upon illumination of appropriate polymer:fullerene composites (Sun and Sariciftci 2005, Poortmans and Arkhipov 2006, Pagliaro, Palmisano, and Ciriminna 2008, Krinichnyi 2009, Brabec, Scherf, and Dyakonov 2014, Krinichnyi 2016b, a). Fullerene molecules embedded into polymer matrix of such systems form so called "bulk heterojunctions" (BHJ) with polymer chains. In this case polymer matrix and adduct become as electron donor D (hole transporter, p-type material) and electron acceptor A (electron transporter, n-type material), respectively. Beyond photo induced charge exciting and separation, positive carriers are transported to electrodes by polarons diffusing in the polymer phase and electrons hopping between fullerene domains embedded into polymer matrix. A definitive advantage of BHJ is that it can be made by simply mixing these materials in an organic solvent, and casting with well-known solution deposition techniques, e.g., spin coating (Shaheen et al. 2001). The illumination of such a system by photons with energy hvph higher than the π-π* energy bandgap of polymer matrix leads to the fast formation of spinless excitons in its BHJ. These quasi-particles can geminate ultrafast dissociate forming Coulomb bound electron-hole pairs (charge-transfer states) of electrons on the acceptor moiety and holes on the donor moiety. Then electrons and holes can leave the donor:acceptor interface relaxing into more favorable energy levels (Lupton, McCamey, and Boehme 2010). With increasing distance from the material interface, the

Coulomb attraction becomes less, and finally, the electrons and holes become independent of each other, forming quasi-pairs or charge-separated states. Finally, charge separation is accompanied by the formation of unbound (free) positively charged polarons on polymer chains and negatively charged radical on fullerene globes. After this stage, charge carrier recombination can occur.

Polymer:fullerene BHJ are characterized by efficient light-excited charge generation at the interface between two organic materials with different electron affinity. Figure 3 illustrates the energy diagram of two exemplary intrinsic semiconductors, e.g., regioregular poly(3-alkylthiophene) (P3AT) shown in Figure 1 and fullerene derivative, [6,6]-phenyl-C_{61}-butanoic acid methyl ester ($PC_{61}BM$), widely used in polymer:fullerene photovoltaic devices, before making a contact between them. A heterojunction formed by these materials inserted between a high work-function electrode (El_1) matching the highest occupied molecular orbital level of the donor ($HOMO_D$) and a low work-function electrode (El_2) matching the lowest unoccupied molecular orbital level of the electron acceptor ($LUMO_A$) should in principle act as a diode with rectifying current–voltage characteristics. Under the forward bias (the low work-function electrode is biased negative in respect to the high work-function electrode) the electron injection into the $LUMO_A$ layer from the low work-function electrode as well as the electron extraction out of the $HOMO_D$ by the high work-function electrode is energetically possible and a high current may flow through the heterojunction. Under reverse bias (the low work-function electrode is biased positive in respect to the high work-function electrode), the electron removal from the electron donor and electron injection to the electron acceptor is energetically unfavorable. The formation of the polaron $P^{+\bullet}$ and fullerene $F_{61}^{-\bullet}$ charge carriers is shown in Figure 3 as well. This process occurs in the femtosecond time domain (Banerji et al. 2010), whereas the electron back transfer with charge annihilation is much slower possibly due to dynamics and relative slow structural relaxation in such a system of lowed dimensionality. The separation and recombination of free charge carriers can be considered as concurring opposite directed processes. Recombination of opposite charge carriers can either be geminate, between electrons and holes originating from the same photo-generated exciton, or non-geminate, between separated charge carriers. The geminate recombination of polaron-fullerene pairs is monomolecular and, therefore, a first order process. The non-geminate, bimolecular recombination of separated polaron-fullerene quasi-pairs following Langevin theory of a second order. The formation, separation and recombination of charge carriers are governed also by the energy of initiating photons (Krinichnyi 2016a).

1.3. Resonant Manipulation of Interacting Polarons in Polymer Nanocomposites

The efficiency of energy conversion by organic polymer:fullerene quantum structures is governed partly by charge localization phenomena, which underlie their optical transitions. These molecular systems in which a charge is transferred by weakly spin-orbit coupled carriers are gaining particular interest because the use of spin carriers with additional spin degree of freedom opens an undoubted imperative to develop a remarkable new generation of electronic, "spintronic," devices with spin-assisted and, therefore, handling electronic properties. Because these materials have weak spin-orbit and hyperfine interactions, they can

be used for hosting spin-based classical and quantum information. They exhibit intriguing interfacial effects and can be used to realize flexible multifunctional spintronic devices. Chiral organic systems can also play the role of efficient spin injectors and detectors, which can potentially replace ferromagnetic materials in spin devices. It is well known that the data processing in conventional computers is limited by the transport of elemental charge carriers, electrons, through silicon semiconductors. Exploiting the orientation of electron spin rather than its charge takes a possibility to create spintronic devices which will be smaller, more versatile and more robust than those currently making up silicon chips and circuit elements. This can be also used, e.g., for encoding and transferring information more efficiency then using spinless ones (Dediu et al. 2009). Deposition of isolated tetracyano-*p*-quinodimethane (TCNQ) molecules each possessing a spin to a graphene monolayer leads to formation in the latter of spatially extended spin-split electronic bands (Garnica et al. 2013) that may be used in organic spintronic devices (Shen et al. 2014). The careful controllable preparation, preservation, and manipulation of quantum states should form the backbone of the use of quantum information processing to create organic molecular spin-controlled electronic devices. Orientation of spin in charge carriers survives for a relatively long time (nanoseconds, compared to tens of femtoseconds during which electron momentum decays), which makes spintronic devices particularly attractive for memory storage and magnetic sensors applications, and, potentially for quantum computing where electron spin would represent a bit (called qubit) of information (Lloyd 1993).

Spin feature of charge carriers stabilized or/and induced, e.g., in the above described polymer:fullerene BHJ can also be used for manipulation by electronic properties of such system. Excitons formed in a polymer:fullerene BHJ under illumination at the intermediate step can be conversed into polaron pairs or donor-acceptor complexes which then collapsing into spin pairs of polarons and fullerene anion radicals. Besides, the triplet state of fullerene characterizing by high electron spin polarization can also be easily photoexcited in such a nanocomposite. This can possibly be used as an active media for masers and other molecular devices (Blank, Kastner, and Lebanon 1998). Diffusing and meeting in a system bulk, the above charge carriers recombine. Most organic hydrocarbon materials show only radiative recombination from the singlet state, so that high triplet formation rates form a formidable loss channel in devices with light-emitting recombination (Wohlgenannt et al. 2001). However, this process itself is not a trivial phenomenon which microscopic details still remain unknown. For example, one would not necessarily expect the recombination of a charge carrier with just the first opposite carrier. In this case both the charge carriers exchangeable spin-flip, so that their further recombination become dependent on their dynamics, number, polarization and mutual distinct. For large separations, when the thermal energy exceeds the interaction potential the charges can be considered as non-interacting. However, once the carriers become nearer than the inverted Coulombic interaction potential, their wave functions begin to overlap so that exchange interactions become non-negligible. This can lead to the formation in organic semiconductors of exciton of either singlet or triplet configuration. It is important to note that an electron spin-flip arising from spin-orbit coupling may thus transform the singlet exciton into a triplet one with lower energy level. This process prevails in the most planar structures with particular molecular symmetries (Baunsgaard et al. 1997). So, depending on various conditions, a singlet ($\uparrow\downarrow-\uparrow\downarrow$ or S) and three triplet ($\downarrow\downarrow$, $\uparrow\downarrow+\uparrow\downarrow$, $\uparrow\uparrow$ or T_+, T_0, T_-) spin configurations can be realized in these molecular devices (Lupton, McCamey, and Boehme 2010).

Free charge carriers are generated through dissociation of either singlet or triplet polaron pairs in polymer:fullerene BHJ. The dissociation rates of these carrier pairs are spin dependent, so that sum number of charge carriers should depend on the initial spin state of the polaron pair. A spin configuration of such pairs transforms between singlet and triplet ($S \leftrightarrow T$) either randomly due to irreversible spin-lattice relaxation (with characteristic time T_1) or coherently by an external electromagnetic field which induces electron spin precession and resonant reorientation. Such a coherent manipulation of the spin state requires phase coherence of the initiated spin with the initiating microwave (MW) field. Loss of phase coherence arising, e.g., due to the intrinsic (homogeneous) properties of the spin system, or extrinsic (inhomogeneous) characteristics provoking, e.g., by the system disorder or anisotropic local field distribution is characterizing by spin-spin relaxation time T_2 for homogeneous and T_2^* for inhomogeneous processes. If the charge carriers recombine with higher probability than own dissociation, they form excitons with single or triple multiplicity. This recombination process is strongly spin dependent due to the energetic difference between singlet and triplet states and, therefore, can be characterized by appropriate transition rates. So formed excitons may then decay, radiatively or nonradiatively, to the molecular ground state. This process involves charge transfer through a polymer:fullerene BHJ in which two-step exciton dissociation is accompanied by the transfer of its energy from the donor to the acceptor following by a polaron transfer to the donor (Lloyd, Lim, and Malliaras 2008). In this photovoltaic system, even rarely distributed defects may initiate exciton dissociation and the formation of polaron pairs (Im et al. 2002). Undoubtedly, this process is also spin dependent because in such a system only singlet excitons can be photo induced as well as the triplet excitons are bound stronger than the singlet ones, so that having different energetics. This means that in most photovoltaic systems the triplet exciton dissociation rate can, therefore, be nulled and the contribution of singlet excitons should only be considered.

1.4. Electron Paramagnetic Resonance of Polarons in Polymer Systems

Different methods can be used for the study of charge carriers stabilized or/and exited in polymers and their nanocomposites (Rouxel, Thomas, and Ponnamma 2016). Physics processes carrying out in such objects may be identified and analyzed comparing results obtained by all possible methods at similar experimental conditions, e.g., optical (fluorescence and phosphorescence) and/or electrically detected magnetic resonance (Lupton, McCamey, and Boehme 2010). The former can, in principle, sense singlet and triplet excitons in organic semiconductors (List et al. 2002), however, polaronic charge carriers themselves introduce efficient subgap optical transitions that obstructs unambiguous identification of excitations in such systems. In some cases, incorporation of a heavy-metal atom into an organic complex can increase spin-orbit coupling, effectively mixing singlet and triplet levels. A strong modulation of the phosphorescence signal can occasionally be observed in the presence of an electric field, thus proving the presence of spin triplet polaron pair species, which are much more polarizable than the ultimate triplet exciton (Reufer et al. 2006).

Polaron formed in conjugated polymers possesses a spin $S = 1/2$. So, Electron Paramagnetic Resonance (EPR) was proved (Schlick 2006, Eaton et al. 2010, Lupton, McCamey, and Boehme 2010, Ranby and Rabek 2011, Misra 2011) to be one of the most

widely used and productive physical direct methods for structural and dynamic studies of high-molecular systems with free radicals, ion-radicals, molecules in triplet states, transition metal complexes, other PC. The method is based on resonant absorption of MW radiation by a paramagnetic sample due to the splitting of the energy levels in an external magnetic field. It allowed getting more detailed information on processes carrying out in various solids containing PC. As the original properties of conjugated polymers are related to the existence of PC localized or/and delocalized along and between their chains, a great number of EPR experiments has been performed for the study of their magnetic, relaxation and dynamics properties (Bernier 1986, Mizoguchi and Kuroda 1997, Kuroda 2002). For more than fifty years EPR such investigations are predominantly carried out at convenient X-band (3-cm, 9.7 GHz) EPR, i.e., at registration frequency $\omega_e/2\pi = \nu_e \leq 10$ GHz, and external magnetic fields $B_0 \leq 330$ mT. However, at these wavebands the signals of organic free radicals with *g*-factor lying near *g*-factor of free electron ($g_e = 2.00232$) are registered in a narrow magnetic field range and, therefore, can overlap the lines with close *g*-factors. At this waveband polarons in conjugated polymers demonstrate uninformative single spectra, so the line shape and concentration of these quasi-particles can only be directly measured. Besides, strong cross-relaxation of PC still perceptible at low magnetic fields (Altshuler and Kozirev 1972) additionally complicates the registration and identification of spin packets. EPR spectroscopy was proved also to be powerful method for the study of the exiton collapse into a pair of spin charge carriers, charge separation, transfer and recombination in organic donor:acceptor systems. Indeed, the evidence for a successful charge transfer is based on the fact that excitons generated by light absorption have zero spin and therefore cannot be detected by EPR spectroscopy. If the exciton is split at the interface between donor and acceptor, polaron and anion radical are created which have half integer spin leading to the appropriate EPR signal. The amount of light induced charge carriers can be determined by comparing the EPR spectrum in the dark and after illumination.

Because polarons obtain a spin, this can be used for creation of spintronic devices with spin-assisted electronic properties. Electron spin can be oriented parallel and antiparallel to a direction of the applied magnetic field forming two-level quantum system. To probe resonance spin hopping between these pure quantum states, weak spin-orbit coupling is required, which limits the applicability of the convenient magnetic resonance methods for the study of spin-assisted charge transfer in inorganic spintronic materials (Wolf et al. 2001). In organic semiconductors, however, spin–orbit interaction is very weak due to low atomic order number, so that the information about spin orientation can be easier established by magnetic spectroscopic techniques (Cinchetti et al. 2009). It allows using cutting-edge spectroscopic methods for determination of spin polarization in spin-assisted processes and also for their controlled manipulation. EPR spectroscopy was shown (Lupton, McCamey, and Boehme 2010) to be powerful direct tool able to reveal about the underlying nature of spin carriers excited in quantum systems including multispin polymer systems with weak spin-orbit coupling.

The efficiency of the method increases with spin precession frequency. It was shown that EPR investigation at high spin precession frequencies, $\omega_e/2\pi \geq 100$ GHz corresponding to field strength $B_0 \geq 3$ T, of organic radicals in different solids (Grinberg, Dubinskii, and Lebedev 1983, Krinichnyi 1995), especially polarons stabilized and initiated in conjugated polymers (Krinichnyi 1995, 2006, 2009, 2014b, a, 2016b, a) enables to increase considerably

the precision and descriptiveness of the method. At 2-mm waveband EPR it were investigated in details structure, relaxation, dynamics and other specific characteristics of radical centers and their local environment, elementary charge transfer processes in different solids, biopolymers, conjugated polymers and their nanocomposites. It should, however, be noted that the advantages of the high-frequency/field EPR spectroscopy are limited in practice by a concentration sensitivity that decreases with increasing MW frequency. Nevertheless, multifrequency EPR spectroscopy seems to be powerful direct method for the detailed study of conjugated polymers and their nanocomposites with interacting spin packets.

This chapter summarizes the main results obtained in the investigation of relaxation, magnetic and dynamics parameters of polarons stabilized and initiated in various conjugated polymers and their nanocomposites at wide range of wavebands EPR. It is organized as following. The second part is devoted to an original data obtained in multifrequency EPR study of the nature, relaxation and dynamics of paramagnetic centers delocalized on polaronic charge carriers as well as the mechanisms of charge transfer stabilized and initiated in some widely known conjugated polymers. The use of some conjugated polymers as electron donor in organic composites is described as well. The third part reveals the possibility to handle of charge transport in some multispin polymer composites by using the spin-spin exchange. The fourth part denotes the prospects of the study of organic polymer systems for the further construction of novel elements of molecular electronics. An Appendix containing experimental details of EPR study of the main magnetic resonance, relaxation and dynamics parameters of polaron quasi-particles in organic compounds and short theoretical background finalizes the present chapter.

2. MAGNETIC, RELAXATION AND DYNAMIC PARAMETERS OF POLARONS IN CONJUGATED POLYMERS

Polymer doping and/or illumination leads to the formation of polaron on its chain. It possesses spin, elemental charge and high Q1D mobility along polymer chain. The main properties of such charge carrier are governed by the structure and dynamics of its environment as well as by the external physical effect. The terms of anisotropic *g*-factor and linewidth determined from EPR spectra of polarons stabilized in some conjugated polymers are summarized in Table 1. Below are analyzed the main magnetic, relaxation and dynamics parameters of polaronic charge carriers initiated in various initial and modified conjugated polymers.

2.1. Poly(p-Phenylene)

Poly(*p*-Phenylene) and its nanocomposites are considered as suitable material for constructing of various molecular devices (Brédas and Chance 1990, Nalwa 2001). This is mainly to its simple synthesis and high conductivity. A number of unpaired electrons stabilized in this conjugated polymer reaches $10^{17} - 10^{19}$ cm^{-3}(Bernier 1986) strongly depending on the technique used for its polymerization process. The room temperature (RT) linewidth of PPP increases at doping with the increase of atomic number of an alkali metal

dopant due to a strong interaction between molecule of a dopant and an unpaired electron. Such polymer demonstrates a Korringa spin relaxation mechanism, typical of disordered metals, and the Mott's variable range hopping (VRH) mechanism (Mott and Davis 2012) for carriers localized within weakly conjugated carbonized regions (Matthews et al. 1999). The charge in PPP is transferred mainly by polarons at low doping level and bipolaron at metallic state (Xie, Mei, and Lin 1994), similar to that, as it is observed in analogous highly conjugated polymers (Lu 1988, Lacaze, Aeiyach, and Lacroix 1997).

A series of PPP film-like samples of near 10 μm thickness synthesized electrochemically on a platinum electrode in a BuPyCl-AlCl$_3$ melt were studied at X- and D-bands EPR: as prepared and evacuated PPP: Cl$_3^-$ film (PPP-1), the same film after its storage for forth days (PPP-2), that exposed for a few seconds to air oxygen (PPP-3); after Cl$_3^-$ dopant removal from the PPP-1 sample (PPP-4); and after BF$_4^-$ redoping of the PPP-1 film (PPP-5) (Goldenberg et al. 1990, 1991).

At X-band EPR, PPP-1 – PPP-3 samples demonstrate well-pronounced asymmetric single Dysonian spectrum with effective g = 2.0029 (Figure 4,a). The analogous PPP line shape was also registered at the study of highly lithium-doped PPP (Dubois, Merlin, and Billaud 1999).The line asymmetry factor *A/B* is changed depending on the sample modification. As dopant Cl$_3^-$ is removed, i.e., at the transition from PPP-1 film to PPP-4 one, the above spectrum transforms to a two-component one with $g_\perp$ = 2.0034 and $g_\parallel$ = 2.0020, where $2g_\perp = g_{xx} + g_{yy}$ and $g_\parallel = g_{zz}$ (Figure 4,b). Such a transition is accompanied by a line broadening and by a drastic decrease in the concentration of spin charge carriers from 1.1×10^{19} down to 3.9×10^{17} cm^{-3}. It should be noted that in earlier studies of different PPP samples and other π-conjugated polymers at X-band EPR there was not registered such an axially symmetric EPR spectra (Bernier 1986, Lacaze, Aeiyach, and Lacroix 1997). With PPP doped by BF$_4^-$ anions (PPP-5), the spectrum shape retains, however, a slight decrease in the concentration of polarons, and a change in the sign of its dependency on temperature are observed. Using the difference $g_\perp - g_\parallel = 1.4 \times 10^{-3}$, the minimum excitation energy of unpaired electron $\Delta E_{\sigma\pi*}$ is calculated from Eq.(A.2) to be equal to 5.2 eV. This energy is close to the first ionization potential of polycyclic aromatic hydrocarbons (Traven' 1989). Consequently, PC can be localized in PPP-4 and PPP-5 samples near cross-linkages which appear as polycyclic hydrocarbons as it was predicted earlier (Kuivalainen et al. 1983).

At D-band EPR the bell-like contribution attributed to the manifestation of the fast passage of inhomogeneously broadened line appears at g_{eff} = 2.00319 in sum EPR spectra of the two latter films (Figure 4,c). This effect allows us to evaluate spin-spin relaxation time, T_1 ≈ 10^{-4} s for PC in dedoped and redoped samples.

From the analysis of the X- and D-bands EPR line shape the rate of spin-packets exchange $\nu_{\text{ex}} = 4 \times 10^7$ s^{-1} was estimated for the neutral and redoped films (Goldenberg et al. 1991). This value obtained for doped film increases up to 1.8×10^8 s^{-1} due to the increase in PC concentration and mobility. Effective, isotropic g-factor, $g_{\text{iso}} = 1/3(g_\parallel + 2g_\perp)$ of a neutral sample is equal to g-factor of Cl$_3^-$-doped one. This fact shows that **g**-tensor components of PC are averaged in PPP: Cl$_3^-$ sample due to Q1D spin diffusion with coefficient $D_{1D}^0 \geq$ 4.3×10^7 rad/s. However, Q1D spin diffusion coefficient calculated from relaxation times of

the samples was appeared to be considerably low (Goldenberg et al. 1991) due possible to disordered of polymer matrix. *AC* conductivity calculated for PPP-2, PPP-2 and PPP-3 samples from Eq.(A.35), Eq.(A.38), and Eq.(A.39) changes from 1.5×10^5 S/m up to 1.8×10^5 S/m and then decrease down to 5.3×10^5 S/m, respectively. This parameter obtained for PPP-1 depends on the temperature as $\sigma_{ac} \propto T^{0.23}$. Such a dependency seems to indicate the existence in doped PPP sample of some conductivity mechanisms, namely VRH and isoenergetic tunneling (Kivelson 1980) of charge carriers. The strong decrease in PC concentration as well as the slowdown of spin exchange and spin-spin relaxation processes at the sample dedoping, i.e., at transition from PPP-1 to PPP-4, evidence for the pairing of most polarons into spinless bipolarons, whose Q1D diffusion causes electron relaxation of the whole spin system.

The intrachain spin diffusion coefficients D_{1D} calculated from Eq.(A.25) as well as conductivity σ_{1D} due to Q1D spin diffusion calculated from Eq.(A.34) were appeared to be too small (around $10^5 - 10^6$ rad/s) for the appearing of a Dysonian component in the PPP spectra.

Thus, EPR data analysis allow to conclude that in highly doped PPP-1, the charge is transferred mainly by mobile bipolarons and only small part of mobile polarons take part in this process. In PPP-5 these polarons couple into spinless bipolarons being the predominant charge carriers in this conjugated polymer.

At the electrochemical substitution of Cl_3^- anion by BF_4^- one, the location of the latter may differ from that of the dopant in the initial PPP sample. However, the morphology of the BF_4^--redoped PPP may be close to that of a neutral PPP-4 film.
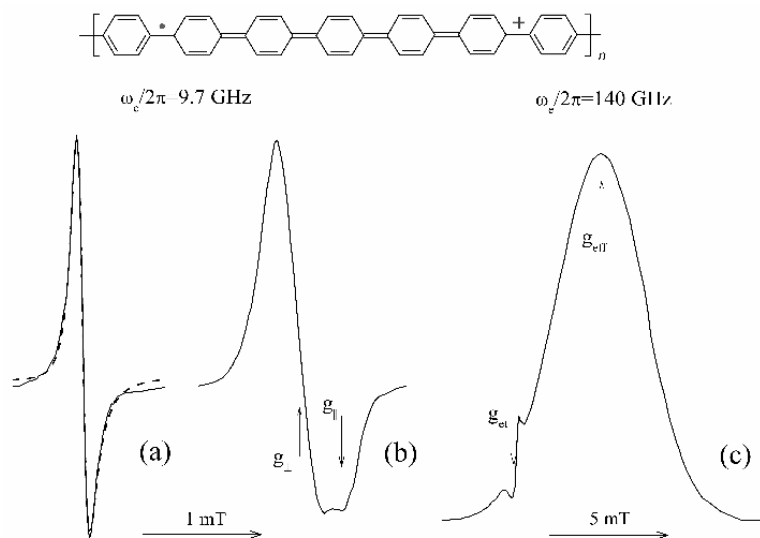
Figure 4. Typical X-band EPR in-phase modulation absorption spectrum of PPP-1 – PPP-3 (*a*) and PPP-4, PPP-5 (*b*) samples; (*c*) typical D-band EPR in-phase modulation dispersion spectrum of PPP-4 and PPP-5 films (see the text) registered at 300 K. The spectrum calculated from Eqs. (A.35), (A.38) and (A.39) with $D/A = 0.39$ and $\Delta B_{pp} = 0.109$ mT is shown at the left by dashed line. A narrow line in the right spectrum is attributed to the lateral standard, single crystal $(DBTTF)_3PtBr_6$ with $g = 2.00411$.

Table 1. The terms and trace of the g-tensor, g_{ii} and g_{iso}, respectively, as well as the linewidth ΔB_{pp}^i of the i-th spectral components (in mT) of polarons stabilized as electron donors in some conjugated polymers and measured at different wavebands (WB) and low (20-80 K) temperatures when all spin motions are considered to be frozen

Sample	g_{xx}	g_{yy}	g_{zz}	g_{iso}	ΔB_{pp}^x	ΔB_{pp}^y	ΔB_{pp}^z	ΔB_{pp}^{iso}	WB[2]	References
PPP	2.0034	2.0034	2.0020	2.0029	0.44	0.44	0.23	0.37	X	(Goldenberg et al. 1990)
PATAC	2.0433	2.00902	2.00243	2.01825	5.66	9.82	5.95	7.14	D	(Krinichnyi, Roth, and Schrödner 2002)
PPy	2.00380	2.00380	2.00235	2.00	0.57	0.57	0.57	0.57	D	(Pelekh, Goldenberg, and Krinichnyi 1991)
PANI-EB	2.00522	2.00401	2.00228	2.00384	1.25	1.25	2.27	1.59	D	(Krinichnyi, Chemerisov, and Lebedev 1997)
PANI-EB	2.00603	2.00382	2.00239	2.00408	0.45	0.45	3.02	1.31	D	(Krinichnyi et al. 2002)
PTTF-CH$_3$-C$_6$H$_4$	2.01191	2.00584	2.00185	2.00652	1.72	1.63	1.79	1.71	D	(Krinichnyi 2006)
PTTF-C$_2$H$_5$-C$_6$H$_4$	2.01405	2.00676	2.00235	2.00772	4.06	4.63	4.43	4.37	D	(Krinichnyi et al. 1993)
PTTF-THA	2.01292	2.00620	2.00251	2.00721	5.53	2.73	1.74	3.33	D	(Krinichnyi, Denisov, et al. 1998)
PT	2.00382	2.00266	2.00266	2.00305	1.45	1.79	1.79	1.68	D	(Krinichnyi et al. 1985)
P3HT	–	–	–	2.0030	–	–	–	0.66	X	(Krinichnyi, Troshin, and Denisov 2008)
P3HT	2.0030	2.0021	2.0011	2.0021	0.16	0.15	0.16	0.16	K	(Konkin et al. 2010)
P3HT	2.0028	2.0019	2.0009	2.0019	1.07	0.53	0.64	0.75	W	(Aguirre et al. 2008)
P3HT	2.00380	2.00230	2.00110	2.00240	0.85	0.88	0.76	0.83	D	(Poluektov et al. 2010)
P3OT	2.00409	2.00332	2.00232	2.00324	0.82	0.78	0.88	0.83	D	(Krinichnyi and Roth 2004)
P3DDT	2.0026	2.0017	2.0006	2.0016	0.25	0.14	0.15	0.18	X	(Krinichnyi, Yudanova, and Spitsina 2010)
PCDTBT	–	–	–	2.0022	–	–	–	0.14	X	(Krinichnyi, Yudanova, and Denisov 2014)
PCDTBT	2.00320	2.00240	2.00180	2.00247	0.44	0.49	0.38	0.44	D	(Niklas et al. 2013)

Notes: [1] the abbreviations mean the following polymers: PPP - poly(p-phenylene), PATAC - poly(*bis*-alkylthioacetylene), PPy - polypyrrole, PANI - polyaniline, PTTF – poly(tetrathiafulvalene), PT - polythiophene, PCDTBT - poly[N-9′-hepta-decanyl-2,7-carbazole-alt-5,5-(4′,7′-di-2-thienyl-2′,1′,3′-benzothiadiazole)].

[2] the wavebands (WB) correspond to spin precession frequency $\omega_e/2\pi$ and resonant magnetic field B_0 of 9.7 GHz and 0.34 T (X), 24 GHz and 0.86 T (K), 38 GHz and 1.2 T (Q), 94 GHz and 3.4 T (W), 140 GHz and 4.9 T (D), respectively.

As it was established by Goldenberg et al. (Goldenberg et al. 1990, 1991), the PPP film synthesized in the BuPyCl-AlCl$_3$ melt is characterized by smaller number of benzoid monomers and by greater number of quinoid units. It leads to a more ordered structure and planar morphology of the polymer that in turn prevents the coupling of spin charge carriers to bipolaron in highly doped polymer. The anions are removed at dedoping, so then the packing density of the polymer chains grows. It can prevent an intrafibrillar implantation of BF_4^- anions and lead to the localization of dopant molecules in the intrafibrillar free volume of the polymer matrix. The change of charge transfer mechanism at the replace of dopants should be a result of such a morphological transition in PPP (Goldenberg et al. 1991).

2.2. Poly(*bis*-Alkylthioacetylene)

The derivative of *trans*-polyacetylene, poly(*bis*-alkylthioacetylene) (Richter et al. 1987) shown in Figure 2, is also an insulator in a neutral form. From the ^{13}C Nuclear Magnetic Resonance (NMR) study (Hempel et al. 1990) the conclusion was made that PATAC has sp^2/sp^3-hybridized carbon atom ratio typical for polyacetylene, however, in the contrast with the latter, pristine polymer has a more twisted backbone. The *dc* conductivity of PATAC increases under chemical doping from $\sigma_{dc} \approx 10^{-12}$ S/m up to $\sigma_{dc} \approx 10^{-8} - 10^{-2}$ S/m depending on the kind and/or concentration of an anion introduced into the polymer in a liquid or gas phase. Upon irradiated by argon laser this parameter increases up to $\sigma_{dc} \approx 1 \times 10^3 - 2 \times 10^4$ S/m depending on the absorbed dose (Roth, Gruber, et al. 1990). Hall coefficient measurement of the laser-modified PATAC (Roth, Gruber, et al. 1990) have shown that the charge carriers are of *p*-type and their mobility μ depends on the temperature as $\mu \propto T^n$ with $0.25 \leq n \leq 0.33$ at $80 \leq T \leq 300$ K. The mobility was obtained at RT to be close to $\mu = 0.1 - 8$ cm^{2}V^{-1}s^{-1} that is close to $\mu = 2$ cm^{2}V^{-1}s^{-1} obtained for *trans*-PA (Bleier et al. 1988).

The X-band EPR study (Roth, Gruber, et al. 1990) has shown that π-like PC with different mobility exist in laser-modified PATAC, however, the conductivity of so treated polymer is mainly determined by the dynamics of diamagnetic bipolarons. It was proposed that as the temperature increases the bipolaron mobility decreases and their concentration in laser-modified PATAC increases, so then these processes should lead to the extremely low (close 10^{-3} K^{-1}) temperature coefficient of the PATAC *dc* conductivity. In laser-treated polymer the RT spin concentration, *g*-factor and peak-to-peak linewidth ΔB_{pp} change from $N \approx 2.7 \times 10^{14}$ cm^{-3}, *g*= 2.0056, and $\Delta B_{pp} = 0.72$ mT to $N \approx 4.7 \times 10^{17}$ cm^{-3}, *g*= 2.0039, and $\Delta B_{pp} = 0.65$ mT, respectively.

An initial, insulating, powder-like PATAC-1 sample and that irradiated by an argon ion laser with dose of 5 J/cm³, PATAC-2, and with the photon energy/wavelength $\lambda_{ph}/h\nu_{ph} = 2.46$ eV/488 nm (here $h = 2\pi\hbar$ is the Planck constant) were studied at both the X- and D-bands EPR at RT (Roth et al. 1999, Krinichnyi, Roth, and Schrödner 2002).

At X-band the PC in the PATAC-2 sample demonstrates a slightly asymmetric Lorentzian spectrum with a weak component at low fields (Figure 5,a). The intensity of the latter component decreases during the PATAC laser modification and/or as the temperature increases. The spectrum simulation has shown that such line asymmetry arises rather due to the anisotropy of *g*-factor. This supposition was confirmed by a more detailed study of the samples at higher registration frequency. D-band EPR spectra of the PATAC-2 sample is also

presented in Figure 5,b. Higher spectral resolution allowed to show the existing in PATAC of two types of PC, namely, polarons localized on the short π-conjugated polymer chain $P_{loc}^{+\bullet}$ with $g_{xx} = 2.04331$, $g_{yy} = 2.00902$, $g_{zz} = 2.00243$, and linewidth $\Delta B_{pp} = 6.1$ mT (D-band), and polarons moving along the main π-conjugated polymer chain $P_{mob}^{+\bullet}$ with $g_{xx} = 2.00551$, $g_{yy} = 2.00380$, $g_{zz} = 2.00232$, $(2g_{\parallel} = g_{xx}+g_{yy}, g_{\perp} = g_{zz})$ and $\Delta B_{pp} = 2.7$ mT (D-band). Simulated spectra of these charge carriers are shown in Figure 5 as well.
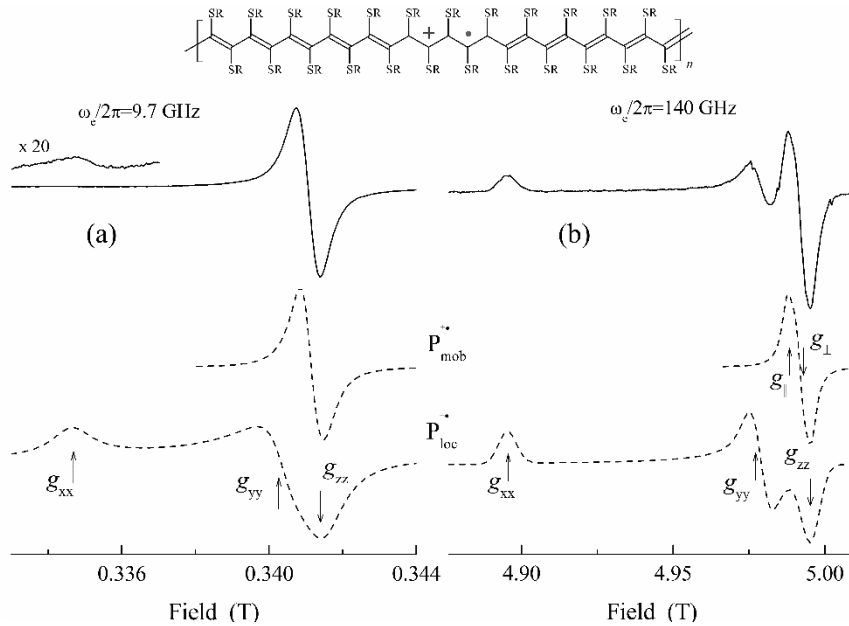
Figure 5. The absorption X- (*a*) and D- (*b*) bands EPR spectra of the laser modified PATAC-2 sample registered at 100 K. Dashed lines show the spectra of radical $P_{loc}^{+\bullet}$ calculated with $g_{xx} = 2.0433$, $g_{yy} = 2.00902$, $g_{zz} = 2.00243$, and radical $P_{mob}^{\bullet+}$ calculated with $g_{xx} = 2.00551$, $g_{yy} = 2.00380$, $g_{zz} = 2.00232$. Polaron initiated in this polymer with $R \equiv -CH_3$ by laser irradiation is shown schematically.

Since the isotropic *g*-factor of the laser-treated PATAC sample is considerably higher than that of most organic conjugated polymers, $g_{iso} \cong 2.003$ (Krinichnyi 1995, Mizoguchi and Kuroda 1997, Krinichnyi 2016b), one can conclude that the unpaired electron in PATAC interacts with sulfur atoms. It is typical for other sulfur-containing compounds, e.g., poly(tetrathiafulvalenes) (Krinichnyi 1996, 2016b) and benzotrithioles (Cameron et al. 1991, 1992, Krinichnyi et al. 1997) in which sulfur atoms are involved into the conjugation. Taking into account that the overlapping integral I_{c-c}^{p} in such organic π-systems depends on the torsion (dihedral) angle θ between *p*-orbits of neighboring C-atoms as $I_{c-c}^{p} \propto \cos\theta$ (Traven' 1989, Masters et al. 1992), the shift of *g*-factor from the *g*-factor for the free electron in Eq.(A.2) should be multiplied by the factor $\lambda_s(1 - \cos\theta)/(1 + k_1\cos\theta)$, where $\lambda_s = 0.047$ eV (Carrington and McLachlan 1967) is the spin-orbit interaction constant for sulfur and k_1 is a constant. The *g*-factor of PC in sulfur-containing solids in which electrons are localized

mainly on the sulfur atom lies in the region of $2.014 \leq g_{iso} \leq 2.020$ (Cameron et al. 1991, 1992, Krinichnyi et al. 1997, Bock et al. 1984). In tetrathiafulvalene (TTF) derivatives an unpaired electron is delocalized on 12 or more carbon atoms and four sulfur atoms leading to the decrease of both $\rho_s(0)$ and, therefore, g_{iso} values (Krinichnyi 2000a). An additional fast spin motion takes place in the PTTF (Krinichnyi 1995, Krinichnyi et al. 1997, Krinichnyi 2000a, 2016b) leading to a further decrease in the $\rho_s(0)$ value, and therefore in g_{iso} down to $2.007 - 2.014$ depending on the structure and effective polarity in PTTF samples. Due to the smaller g-factor in PATAC one can expect a higher spin delocalization in this polymer as compared with the above mentioned organic semi conjugated solids.

Assuming the energy of $n{\to}\pi^*$ transition, $\Delta E_{n\pi^*} \approx 2.6$ eV, typical for benzotrithioles and PTTF (Cameron et al. 1992, Bock et al. 1984), then the g-factor components of PC in the initial PATAC were obtained from Eq.(A.2) to be $\rho_s(0) \approx 1.1$ and $\Delta E_{n\text{-}\sigma^*} = 15.6$ eV. This means that in the initial polymer the spin is localized within one monomer unit.

It was shown (Krinichnyi 1995, Krinichnyi et al. 1997) that the storage of the sample lead to the increase g_{xx} and g_{yy} values of $P_{loc}^{+\bullet}$ up to 2.0451 and 2.00982, respectively. Besides, this originates also the line broadening of this PC up to $\Delta B_{pp} = 12.9$ mT. This means the increase of spin localization on the sulfur nucleus due to the shortness of polymer chains in amorphous regions during the PATAC storage. On the other hand, such destruction does not lead to the change in the magnetic parameters and concentration of mobile polarons.

Supposing the spin delocalization onto approximately five units (Devreux et al. 1987) also in PATAC, then the $\rho_s(0)$ value determined above should decrease down to 0.22. This fits very well the g-factor measured for the PATAC-2 sample. Higher spin delocalization upon laser treatment can be accompanied by the decrease of the θ value down to 21.3°. This should lead to an additional acceleration of spin diffusion along the polymer chains. The latter value is close to the change in θ ($\Delta\theta = 22 - 23^\circ$) at transition from benzoid to quinoid form in PPP (Brédas et al. 1991), from emeraldine base to emeraldine salt form of polyaniline (PANI-EB and PANI-ES, respectively) (Krinichnyi, Chemerisov, and Lebedev 1997), and from the polytertathiafulvalene with phenyl bridges (PTTF-Ph) to that with tetrahydroanthracene (PTTF-THA) ones (Krinichnyi 2000a). This supports the assumption made by Roth et al. (Roth, Gruber, et al. 1990) that laser irradiation leads to a more planar morphology of polymer backbone and therefore to both the higher spin delocalization and conductivity of the sample.

The concentration ratio $[P_{mob}^{+\bullet}]/[P_{loc}^{+\bullet}] \approx 1:2$ obtained for the insulating sample PATAC-1, increases during its modification by laser up to 2:1 determined for the PATAC-2 sample. This means that such the treatment of conjugated polymer leads to a strong increase of the concentration of mobile polarons in laser-treaded system. On the other hand, the concentration of charge carriers determined from Hall and *dc* conductivity studies changes by more than 15 orders of magnitude reaching $N \sim 10^{19}$ cm^{-3} in relatively strong laser-irradiated polymer (Roth, Gruber, et al. 1990). This means that the charge, as in case of some other conjugated polymers, is predominantly transferred by paramagnetic polarons in an initial and slightly modified PATAC. The planarity of chains in highly irradiated polymers increases, so then the most polarons couple into diamagnetic bipolarons.
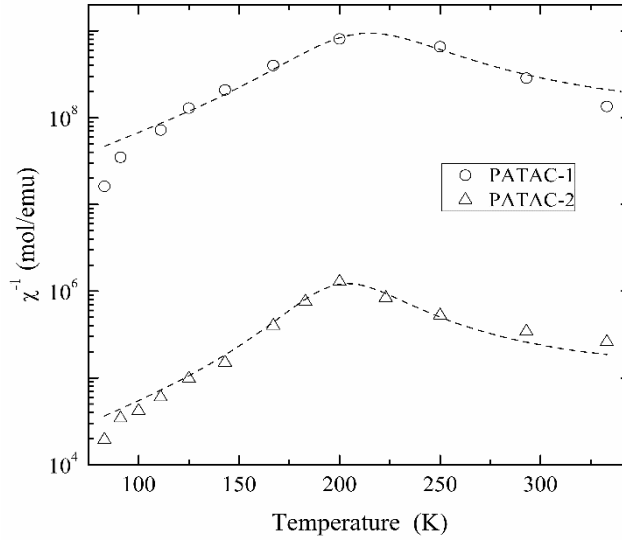
Figure 6. Temperature dependence of spin susceptibility of the PATAC samples. Top-to-bottom dashed lines show the dependencies calculated from Eq.(A.4) with $C = 2.4 \times 10^{-6}$ emu K/mol, $k_1 = 7.2 \times 10^{-4}$ emu K/mol, $J_{af} = 0.069$ eV and $C = 4.6 \times 10^{-3}$ emu K/mol, $k_1 = 0.48$ emu K/mol, $J_{af} = 0.050$ eV.

Spin susceptibility χ of PATAC depends not only on the laser irradiation dose absorbed but also on the temperature. Figure 6 demonstrates inversed temperature dependencies of this value obtained for the PATAC samples. The χ value decreases as the temperature decreases from maximum down to a critical temperature $T_c \approx 200$ - 220 K and then starts to increase at lower temperatures. The observed increase of the magnetic susceptibility at temperatures lower than T_c can result from the formation of clusters with collective localized Curie spins. At higher temperatures, as in case of polyaniline (Iida et al. 1992, Krinichnyi et al. 2002) and poly(3-dodecylthiophenes) (Barta et al. 1994, Cik et al. 1995, Kawai et al. 1996, Cik et al. 2002), the spin susceptibility of PATAC seems also to include a contribution due to singlet-triplet equilibrium described by the second term of Eq.(A.4). The data presented in Figure 6 evidence that $\chi(T)$ dependencies of the PATAC samples are fitted well by Eq.(A.4) with $J_{af} \approx 0.05 - 0.07$ eV.

It is obvious that the above processes should be accompanied by a reversible coupling of polarons into bipolarons and dissociation of bipolarons into polarons. However, Stafström et al. (Stafstrom and Brédas 1988, Stafström and Brédas 1988) have shown that the bipolaron state is not the favorable state in main conjugated polymers.

In order to study the change of spin dynamics in the PATAC backbone under its laser-modification, the temperature dependence of linewidth ΔB_{pp} of mobile polarons $P^{+\bullet}_{mob}$ in both the samples should be analyzed. These dependencies measured at X- and D-bands EPR are shown in Figure 7. It is seen from the Figure that the linewidth measured at X-band EPR is weakly dependent on temperature. However, this value becomes more temperature sensitive at higher spin precession frequency due to the decrease of an exchange interaction between spin packets. The D-band linewidth of the PATAC-1 sample increases with the temperature decrease. At the same time, this value of all laser-modified samples demonstrates the extremal temperature dependence with the critical temperature T_c close to 200 – 220 K. These functions are similar to $\chi(T)$ presented in Figure 6, therefore, such behavior can be associated

with the polaron-bipolaron transition at T_c and can probably not reflect the change of the mobility of charge carriers in the laser-treated sample. At the storage, the linewidth of the PATAC-2 sample becomes linearly dependent on the temperature (Figure 7). The RT linewidth of the sample PATAC-2 was measured at D-band EPR to be 1.45 mT. So, the linewidth of PC $P_{mob}^{+\bullet}$ increases by approximately five times at the transition from the X-band to the D-band mainly due to the effect of spin precession frequency on spin-spin relaxation. The dependences presented are reflect also an exchange spin-spin interaction described by E.(A.17). It is seen from the Figure that the data obtained experimentally are fitted well by this Equation. The energy ΔE_r characterizing the reorganization of polarons decreases more than threefold under the polymer modification by laser irradiation (see Figure 7). This value, however, increases back after the storage of the treated sample. This fact may indicate an increase in the planarity of the sample upon laser irradiation and a decrease in this parameter with time.
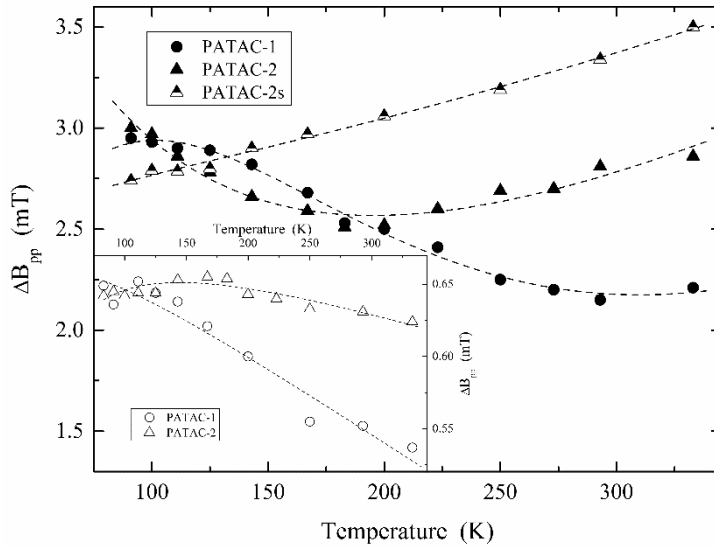
Figure 7. Temperature dependencies of the linewidth of mobile polarons R_2 in the PATAC-1 and PATAC-2 samples determined from their X- (insert) and D-band EPR absorption spectra. Semifilled points show such dependence obtained at D-band EPR for PATAC-2 sample stored for two years. Top-to-bottom dashed lines show the dependencies calculated from Eq.(A.17) with $\omega_{hop}^0 = 9.1 \times 10^8$ s^{-1}, $\Delta E_r = 0.023$ eV, $\omega_{hop}^0 = 7.8 \times 10^6$ s^{-1}, $\Delta E_r = 0.008$ eV, $\omega_{hop}^0 = 5.3 \times 10^7$ s^{-1}, $\Delta E_r = 0.029$ eV, as well as with $\omega_{hop}^0 = 8.7 \times 10^7$ s^{-1}, $\Delta E_r = 0.002$ eV, $\omega_{hop}^0 = 2.1 \times 10^8$ s^{-1}, $\Delta E_r = 0.001$ eV (insert).

As in case of other conjugated polymers, saturation effects were registered in dispersion spectra of the PATAC samples. This allowed investigating anisotropic torsion librations of the pinned polarons near the main *x*-axis of the polymer chains. Such dynamics in the PATAC-1 sample was analyzed within a model of activation motion of immobilized polarons and polymer chains with correlation time of $\tau_c^x = 6.3 \times 10^{-6} \exp(0.043 \text{ eV}/k_B T)$ s (here k_B is the Boltzmann constant) (Roth et al. 1999, Krinichnyi, Roth, and Schrödner 2002). These effects also made it possible to determine also effective spin-lattice and spin-spin relaxation times of the laser-modified PATAC-2 sample. Both relaxation times determined for the initial PATAC-2

polymer and the same sample stored for two years are presented in Figure 8,a as function of temperature. It is seen from the Figure that both relaxation times of polarons initiated in the sample decrease considerably during the storage. Besides, this process leads to the extremal temperature dependence with $T_c \approx 160$ K at which the semiconductor-metal transition occurs. The analogous phenomena was registered in polyaniline (Krinichnyi, Chemerisov, and Lebedev 1997, Krinichnyi et al. 2002), poly(p-phenylene vinylene) (Ahlskog et al. 1997), poly(3,4-ethylene-dioxy-thiophene) (Chang et al. 1999), and other conjugated polymers (Ahlskog, Reghu, and Heeger 1997).
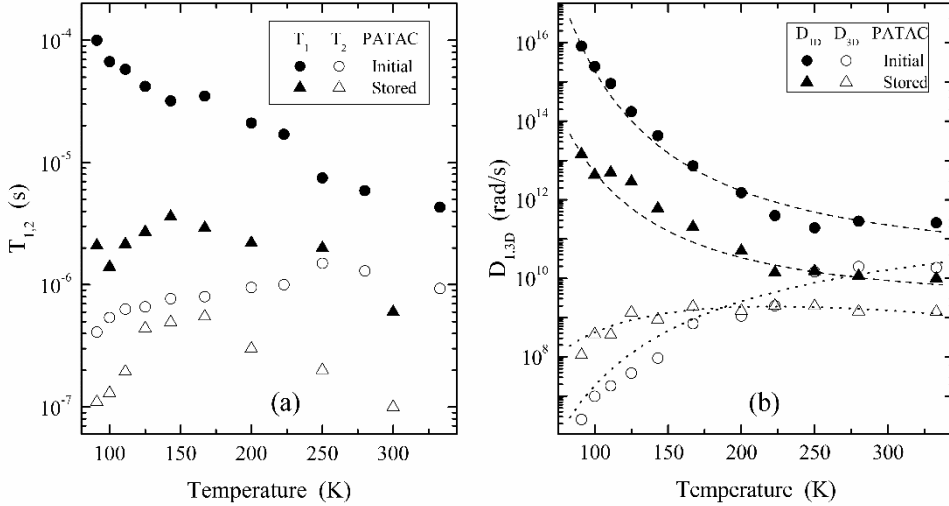
Figure 8. Temperature dependence of the effective spin-lattice T_1 and spin-spin T_2 relaxation times (*a*) intra- D_{1D} and interchain D_{3D} spin diffusion of mobile polarons determined from Eq.(A.25) and Eq.(A.26) (*b*) in as-modified and stored for two years PATAC-2 samples. The dashed lines show dependences calculated from Eq.(A.29) with $E_{ph} = 0.18$ eV and $E_{ph} = 0.15$ eV. The dotted lines depict dependences calculated from Eq.(A.30) with characteristic energy E_a equal to 0.061 and 0.051 eV, respectively.

The involvement of spectral components into the motional exchange and therefore their shift to the spectrum center at the laser modification of PATAC apparently indicates the appearance of polarons moving along the PATAC-2 polymer chains with the rate $D_{1D}^0 \geq 2 \times 10^{10}$ rad/s (Roth et al. 1999, Krinichnyi, Roth, and Schrödner 2002). Assuming the spin situation near sites of cubic backbone, the temperature dependencies of the D_{1D} and D_{3D} values were calculated for the initial and stored for two years PATAC-2 sample from Eq.(A.25) and Eq.(A.26) (see Figure 8,b). It is seen from the Figure that the rate of the spin intrachain diffusion in the samples remains invariable as the temperature decreases down to $T_c \cong 200$ K due probably to the compensation effect of the T_1 increase and the decrease in spin concentration, however, starts to increase at the further temperature decreases. At the same time, D_{3D} decreases monotonically with the temperature decrease of the as-modified PATAC-2 sample. With sample storage this value has a weak fall in temperature (Figure 8,b).

It was shown (Krinichnyi, Roth, and Schrödner 2002) that polaron diffusion along the PATAC chain is governed by the scattering of its spin on the lattice phonons of crystalline domains embedded into an amorphous polymer matrix. The energy of the lattice photons E_{ph}

of the initial and stored PATAC was determined to be 0.18 and 0.15 eV (see Figure 8,b). A difference in energy E_{ph} may indicate a decrease of polymer ordering during its storage. These values is close to that (0.13 eV) obtained for polyaniline doped by hydrochloric acid (Krinichnyi 2000b), however, exceeds by a factor 3 – 4 the activation energy of macromolecular librations in PATAC samples determined by saturation transfer EPR (ST-EPR) method. Spin diffusion between polymer chains of the initial and stored PATAC samples was described within activation mechanism by Eq.(A.30) with characteristic energy E_a equal to 0.061 and 0.051 eV, respectively. These values are close to the typical activation energy of the interchain spin hopping in some other compounds of low dimensionality. The decrease in E_a evidences the decrease of polymer ordering/crystallinity during storage. E_a values are close to those obtained from paramagnetic susceptibility and chain librations data of the samples. This fact leads to the conclusion about the interference of these processes in PATAC. From the average RT mobility $\mu \cong 0.5$ $cm^2V^{-1}s^{-1}$ determined from the Hall study for charge carriers in highly irradiated polymer (Roth, Gruber, et al. 1990) one can evaluate an intrinsic conductivity of the treated PATAC to be close to 3.4×10^2 S/m. This value, however, significantly exceeds respective contributions to *ac* conductivity due to polaron Q1D and Q3D mobility calculated from Eq.(A.34), $\sigma_{1D} = 0.48$ S/m and $\sigma_{3D} = 8.5 \times 10^{-2}$ S/m, respectively. This means that the intrinsic conductivity in highly conjugated PATAC is determined mainly by dynamics of spinless bipolarons with concentration exceeding the number of mobile polarons by approximately two orders of magnitude.

So, multifrequency EPR spectroscopy allowed postulating the existence of two types of paramagnetic centers in laser-modified PATAC – polarons moving along polymer chains in highly ordered crystalline domains and polarons localized by spin traps in amorphous regions of polymer backbone. Assuming that the polaron is covered by electron and excited phonon clouds, one can propose that both spin relaxation and charge transfer should be accompanied by the phonon dispersion. The mobility of the polarons depends strongly on their interaction with other PC and with the lattice phonons. The charge transfer integral and therefore the intrinsic conductivity of the sample is modulated by macromolecular dynamics and such a dynamics reflects the effective crystallinity of PATAC with metal-like domains. The strong spin-spin interaction at high temperatures leads to the stripping of bipolarons into polaron pairs. The number of bipolarons exceeds the number of polarons at least by two orders of magnitude, so the total conductivity of PATAC is determined mainly by dynamics of diamagnetic charge carriers. Magnetic resonance, relaxation and dynamics parameters of PATAC are shown to change during its storage that can be explained by degradation of the polymer.

2.3. Polypyrrole

Polypyrrole is another conjugated polymer widely investigated as perspective molecular system for plastic electronics (Rodriguez, Grande, and Otero 1997, Scotheim and Reynolds 2007). The degree of local order varies for PPy dependent upon the preparation method, with the degree of crystallinity varying from nearly completely disordered up to ~50% crystalline (Epstein 2007). In contrast to polyaniline, the local order in the disordered regions of PPy does not resemble that in the ordered regions.

Neutral PPy exhibits a complex X-band EPR spectrum with a superposition of a narrow (0.04 mT) and a wide (0.28 mT) lines with $g \approx 2.0026$ (Bernier 1986, Saunders, Fleming, and Murray 1995), typical for radicals in polyene and aromatic π-systems (Rodriguez, Grande, and Otero 1997). The intensities of both lines correspond to one spin per a few hundred monomer units. In PPy was also registered single contribution with g_{iso} = 2.0026, ΔB_{pp} = 0.235 mT (Wu, Chang, and Lin 2009) and g_{iso} = 2.0026, ΔB_{pp} = 0.022 mT (Bartle et al. 1993) was also registered.

Paramagnetic susceptibility of the narrow line is thermally activated, while χ parameter of the broad one has a Curie behavior. These features, together with the temperature dependencies of the linewidth, were interpreted in terms of coexistence of two types of PC with different relaxation parameters in neutral PPy. Doped PPy sample exhibits only a strong and narrow (~0.03 mT) X-band EPR spectrum of polarons with g = 2.0028, which follows Curie law from 300 to 30 K (Bernier 1986). However, it was revealed that magnetic susceptibility of polarons in doped PPy is characterized by a Curie-like susceptibility and a weak Pauli contribution; however, the latter does not contribute to the conductivity mechanism (Schmeisser et al. 1998, Kanemoto and Yamauchi 2000b). It was obtained that the charge in PPy is transferred according to the VRH model (Taunk and Chand 2014). The linewidth of PC stabilized in partly stretch-oriented PPy were observed (Sakamoto et al. 1999) to be functions of temperature and the angle between the static magnetic field and the stretched direction. The linewidth of PC becomes higher as the oxygen molecules penetrate into PPy bulk due to the exchange and dipole-dipole interactions of polarons with oxygen biradicals (Kanemoto and Yamauchi 2001). Spin relaxation of PPy was shown (Kanemoto and Yamauchi 2000a, b) to depend on its doping level in relation to several physical properties such as the ratio of the Pauli susceptibility to the total one, the metallic behavior in the conductivity, and the polaron band observed in the optical spectrum. Most of the preceding results imply that EPR signal does not arise from the same species, which carries the charges, because of the absence of correlations of the susceptibility with concentration of charge carriers and the linewidth with the carrier mobility. This was interpreted in favor of the spinless bipolaron formation upon PPy doping (Scott et al. 1983, Chakrabarti et al. 1999). Thus, EPR signal of doped PPy is attributed mainly to neutral radicals and therefore reports little about the intrinsic conjugated processes.

In this case the method of spin probe seems to be more effective for the study of structural and electronic properties of PPy sample. Only a few papers reported the study of conjugated polymers by using spin label and probe at X-band (Audebert et al. 1987, Winter et al. 1990, Shchegolikhin, Yakovleva, and Motyakin 1995, Sersen, Cik, and Veis 2003). It is explained by the fact that main conjugated polymers in conjugated state are insoluble in convenient solvents that prevents an introduction of a stable radical into their bulk. A low spectral resolution at low-frequency wavebands did not allow the registration of all components of **g** and **A** tensors and therefore the separate determination of the magnetic susceptibility of both spin label and PC on the polymer chain, and the measurement of the dipole-dipole interaction between different PC. PPy modified during electrochemical synthesis by nitroxide doping anion, as a label covalently joined to the pyrrole cycle, was studied by Winter et al. (Winter et al. 1990). However, in spite of a high concentration of a spin probe introduced into PPy, effective X-band EPR spectrum of such sample did not contain lines of the probe.

D-band EPR method of spin probe becomes more effective at investigation of PPy synthesized electrochemically on a platinum electrode in an aqueous solution of 0.2 M pyrrole and 0.02 M 2,2,6,6-tetramethyl-1-oxypiperid-4-ylacetic acid (Pelekh, Goldenberg, and Krinichnyi 1991).
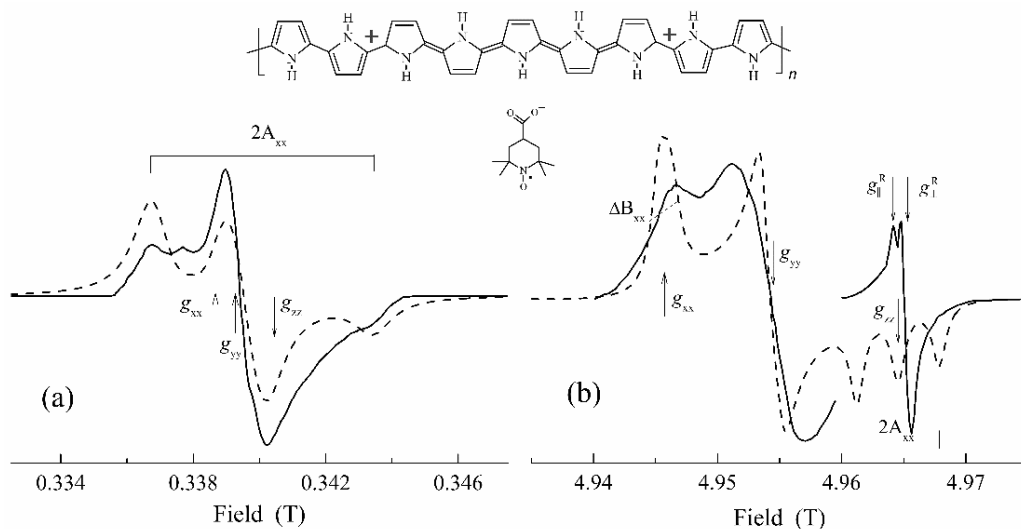
Figure 9. The X-band (*a*) and D-band (*b*) absorption spectra EPR of 4-carboxy-2,2,6,6-tetramethyl-1-oxypiperidiloxyl nitroxide radical introduced into frozen (120 K) toluene (dotted line) and conductive polypyrrole (solid line) as a spin probe. The anisotropic spectrum of localized paramagnetic centers marked by the symbol *R* and taken at a smaller amplification is also shown in the lower part of the Figure. The measured magnetic parameters of the probe and radical *R* are shown. Bipolaron on a PPy chain and nitroxide radical are also shown.

The absorption X- and D-bands EPR spectra of a nitroxide radical, introduced simultaneously as a probe and a counter-ion into PPy as well as a probe into a frozen nonpolar model system are shown in Figure 9. One can see that at X-band EPR the lines of nitroxide radical rotating with correlation time $\tau_c > 10^{-7}$ s overlap with the single line of PC (*R*) stabilized in PPy (Figure 9,a). Such an overlapping stipulated by a low spectral resolution, hinders the separate determination of magnetic resonance parameters of the probe and radical *R* in PPy together with the dipole-dipole broadening of its spectral components.

As it was expected, the spectra of both model and modified polymer systems become more informative at D-band EPR (Figure 9,b). At this waveband all canonic components of EPR spectra of the probe in PPy and toluene are completely resolved so then all the values of **g** and **A** tensors can be measured directly. Nevertheless, the asymmetric spectrum of radicals *R* with magnetic parameters $g_{\parallel}^{R} = 2.00380$, $g_{\perp}^{R} = 2.00235$ and $\Delta B_{pp} = 0.57$ mT is registered on the *z*-component of the probe spectrum. In non-polar toluene the probe is characterized by the following magnetic resonance parameters: $g_{xx} = 2.00987$, $g_{yy} = 2.00637$, $g_{zz} = 2.00233$; $A_{xx} = A_{yy} = 0.60$ mT and $A_{zz} = 3.31$ mT. The difference $\Delta g = g_{\parallel}^{R} - g_{\perp}^{R} = 1.45 \times 10^{-3}$ corresponds to an excited electron configuration in *R* with $\Delta E_{\sigma\pi^*} = 5.1$ eV lying near to an energy of electron excitation in neutral PPP. In conjugated PPy g_{xx} value of the probe decreases down to 2.00906 and the broadening of its *x*- and *y*-components, $\delta(\Delta B_{pp})$ is 4 mT

(Figure 9,b). In addition, the shape of the probe spectrum shows the localization of PC *R* on the polymer pocket of 1 nm size, i.e., the charge is transferred by spinless bipolarons in PPy, as it was proposed in the case of PPP: BF_4^- and PT: BF_4^-.

In neutral PPy the fragments with a considerable dipole moment are *a priori* absent. Besides, the dipole-dipole interactions between the radicals can be neglected due to low concentration of the probe and PC localized on the chain. Therefore, the above change in the probe magnetic resonance parameters taking place at transition from model non-polar system to the conjugated polymer matrix may be caused by Coulombic interaction of the probe active fragment with the extended spinless bipolarons, each carrying double elemental charge (see Figure 9). The effective electric dipole moment of such charge carriers moving near the probe was determined from the shift of g_{xx} component to be equal to dipole moment $\mu_v = 2.3$ D. The shift of **g** tensor component g_{xx} of the probe may be calculated within the frames of the electrostatic interaction of the probe and bipolaron dipoles. The potential of electric field induced by bipolaron in the place of the probe localization is determined by Eq.(A.27) taking μ_u as the dipole moment of the probe, ε is the dielectric constants for PPy, and *r* is the distance between an active fragment of the radical and bipolaron. By using the dependence of the growth of an isotropic hyperfine constant of the probe under microenvironment electrostatic field, $\Delta a = 7.3 e r_{NO} t_{cc}^{-1}$ (here r_{NO} is the distance between N and O atoms of the probe active fragment, t_{cc} is the resonant overlapping integral of C=C bond) and the relation $dg_{xx}/dA_{zz} = 2.3 \times 10^{-2}$ mT^{-1} for hexamerous unit ring nitroxide radical (Krinichnyi 1991b, a), one can write $\Delta g_{xx} = 6 \times 10^{-3} e r_{NO} k_B T(x \coth x - 1)/(t_{cc}\mu_u)$. By using $\mu_u = 2.7$ D (Reddoch and Konishi 1979), $\mu_v = 2.3$ D and $r_{NO} = 0.13$ nm (Buchachenko and Vasserman 1973, Buchachenko, Turton, and Turton 1995), the value of $r = 0.92$ nm is obtained.

The rate of spin-spin relaxation which stipulates the radical spectrum broadening $T_2^{-1} = T_{2(D)}^{-1} + T_{2(0)}^{-1}$ consists of the relaxation rate of the radical non-interacting with the environment $T_{2(0)}^{-1}$ and the growth in the relaxation rate due to dipole-dipole interactions $T_{2(D)}^{-1} = \gamma_e \delta(\Delta B_{x,y})$. The characteristic time τ_c of such an interaction can be calculated from the broadening of the spectral lines using Eq.(A.26) with $J(\omega_e) = 2\tau_c/(1 + \omega_e^2 \tau_c^2)$. The inequality $\omega_e \tau_c \gg 1$ is valid for most condensed systems of high viscosity, so then averaging the lattice sum over angles, $\Sigma\Sigma(1 - 3\cos^2 \vartheta)^2 r_1^{-3} r_2^{-3} = 6.8 r^{-6}$ (Lebedev and Muromtsev 1972), and using $\gamma_e \delta(\Delta B_{pp}) = 7 \times 10^8$ s^{-1} (here γ_e is hyromagnetic ratio for electron) and $r = 0.92$ nm calculated above one can determine $T_{2(D)}^{-1} = 3 \langle \omega^2 \rangle \tau_c$ or $\tau_c = 8.1 \times 10^{-11}$ s. This value lies near to the polaron interchain hopping time, $\tau_{3D} \cong 1.1 \times 10^{-10}$ s estimated for lightly doped PPy (Kanemoto and Yamauchi 2000b). Taking into account, that the average time between the translating jumps of charge carriers is defined by the diffusion coefficient *D* and by the average jump distance equal to a product of lattice constant d_{1D} on half width of charge carrier $N_p/2$, $\tau_c = 1.5 \langle d_{1D}^2 N_p^2 \rangle / D$, and by using then $D = 5 \times 10^{-7}$ m^2/s typical for conjugated polymers, one can determine $\langle d_{1D} N_p \rangle = 3$ nm equal approximately to four pyrrole rings. This value lies near to a width of the polaron in both polypyrrole and polyaniline, but, however, is smaller considerable then N_p obtained for polydithiophene (Devreux et al. 1987).

Thus, the shape of the probe spectrum reports about a very slow motion of the probe due probably to an enough high pack density of polymer chains in PPy. The interaction between spinless charge carriers with an active fragment of the probe results in the redistribution of the spin density between N and O nuclei in the probe and therefore in the change of its magnetic resonance parameters. This makes it possible to determine the distance between the radical and the chain along which the charge is transferred together with a typical bipolaron length in doped conjugated polymers. The method allows also to evaluate characteristic size of a cavity in which the probe is localized and, therefore, the morphology of the sample under study.

2.4. Polyaniline

Figure 10 shows X- and D-band EPR spectra of an initial, emeraldine base form of polyaniline (PANI-EB) (*a*), and X-, Q-, and D-band EPR spectra of emeraldine salt form of polyaniline (PANI-ES) highly doped with 2-acrylamido-2-methyl-1-propanesulphonic acid (AMPSA), PANI:AMPSA$_{0.6}$. At the X-band PANI-EB demonstrates a Lorentzian three-component EPR signal consisting of asymmetric (R_1) and symmetric (R_2) spectra of paramagnetic centers which should be attributed respectively to localized and delocalized PC. R_2PC keep line symmetry at higher doping levels. At the D-band the PANI-EB EPR spectra became Gaussian and broader compared with those obtained at X-band EPR (Figure 10), as is typical of PC in other conducting polymers (Krinichnyi 1996, 2000a, 2016b) At this waveband delocalized PC demonstrate an asymmetric EPR spectrum at all doping levels *y*. The analysis of EPR spectra obtained at both wavebands EPR showed that the line asymmetry of R_2PC in undoped and slightly doped PANI samples can be attributed to anisotropy of the *g*-factor which becomes more evident at the 140 GHz waveband EPR. The linewidth of these PC weakly depends on the temperature. Therefore, the R_1 with strongly asymmetric EPR spectrum can be attributed to a -(Ph- $\overset{\bullet\,+}{\text{NH}}$ -Ph)- radical with $g_{xx}= 2.006032$, $g_{yy} = 2.003815$, $g_{zz} = 2.002390$, $A_{xx}=A_{yy}= 0.45$ mT, and $A_{zz} = 3.02$ mT, localized on a short polymer chain. The magnetic parameters of this radical differ weakly from those of the Ph- $\overset{\bullet\,+}{\text{NH}}$ -Ph radical (Buchachenko and Vasserman 1973, Buchachenko, Turton, and Turton 1995), probably because of a smaller delocalization of an unpaired electron on the nitrogen atom ($\rho_N^\pi = 0.39$) and of the more planar morphology of the sample. Assuming a McConnell proportionality constant for the hyperfine interaction of the spin with nitrogen nucleus $Q = 2.37$ mT (Buchachenko and Vasserman 1973, Buchachenko, Turton, and Turton 1995), a spin density on the heteroatom nucleus of $\rho_N(0) = (A_{xx}+A_{yy}+A_{zz})/(3Q) = 0.55$ is estimated. At the same time another radical R_2 is formed in the system with $g_\perp= 2.004394$ and $g_\parallel = 2.003763$ which can be attributed to PC R_1 delocalized on more polymer units of a longer chain. Indeed, the model spectra presented in Figure 10,a well fit both the PC with different mobility. The lowest excited states of the localized PC were determined from Eq.(A.2) with $\rho_N^\pi = 0.56$ (Long et al. 1994) to be $\Delta E_{n\pi*} = 2.9$ eV and $\Delta E_{\sigma\pi*} = 7.1$ eV.

The shape of EPR spectrum of PANI-ES depends on the nature of counter-ion and doping level *y*. Figure 10,b shows also EPR spectra of the PANI film highly doped with 2-acrylamido-2-methyl-1-propanesulfuric acid, PANI:AMPSA$_{0.6}$, registered at different

frequencies of spin precession ω_e. In order to determine correctly all main magnetic resonance parameters, linewidth, paramagnetic susceptibility, g-factor, of PC with Dysonian contribution, all the effective spectra presented should be calculated using Eq.(A.35), Eq.(A.38) and Eq.(A.39) as described in (Kon'kin et al. 2002). From the analysis it was revealed that EPR spectra of the PANI:AMPSA$_{0.6}$ consist of two contributions due to different PC with Dysonian shape, namely narrow EPR spectrum of PC R_1 with $g = 2.0028$ localized in amorphous polymer backbone and broader EPR spectrum of PC R_2 with $g = 2.0020$ and higher mobility in crystalline phase of the polymer. The RT ΔB_{pp} value of PC R_2 decreases from 54 down to 20 and then down to 5.3 G at the increase of registration frequency $\omega_e/2\pi$ from 9.7 up to 36.7 and then up to 140 GHz (Figure 11), so one can express this value as $\Delta B_{pp}(\omega_e) = 0.15 + 2.2 \cdot 10^8 \omega_e^{-0.84}$ mT. Such extrapolation reveals the dependence of spin-spin relaxation time on the registration frequency and allows estimating correct linewidth at $\omega_e \to 0$ limit to be 0.15 mT. The cooling of the sample leads to the decrease in the relative concentration of PC R_2 and to the monotonous increase in its linewidth, as it is seen in Figure 11. In the same time, the linewidth of PC R_1 decreases monotonously and the sum spin concentration increases at the temperature decrease. Main magnetic resonance parameters of polarons stabilized in PANI are summarized in Table 1.
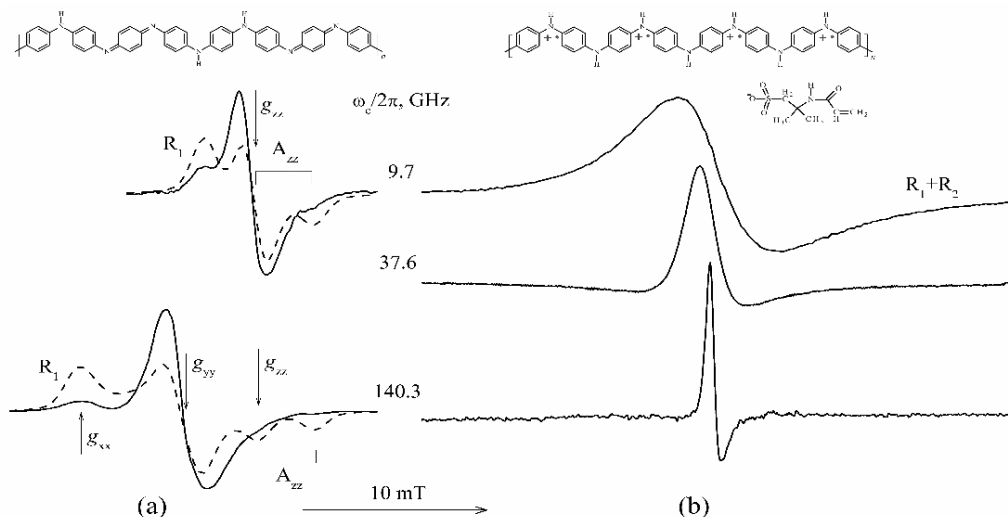
Figure 10. (*a*) Room temperature X- (9.7 GHz) and D- (140.3 GHz) bands EPR absorption spectra of emeraldine base form of polyaniline (PANI-EB) and these calculated with $g_{xx} = 2.006032$, g_{yy} 2.003815, $g_{zz} = 2.002390$, $A_{xx} = A_{yy} = 0.45$ mT, $A_{zz} = 3.02$ mT (R_1), and with $g_\perp = 2.004394$ and $g_\parallel = 2.003763$ (R_2) are shown by dashed lines. (*b*) Room temperature X- (9.7 GHz), Q- (37.6 GHz), and D- (140.3 GHz) bands EPR effective absorption spectra of emeraldine salt form of polyaniline (PANI-ES) highly doped by 2-acrylamido-2-methyl-1-propanesulphonic acid (AMPSA), PANI:AMPSA$_{0.6}$. Structures of PANI-EB, PaNI-ES and AMPSA are shown schematically.
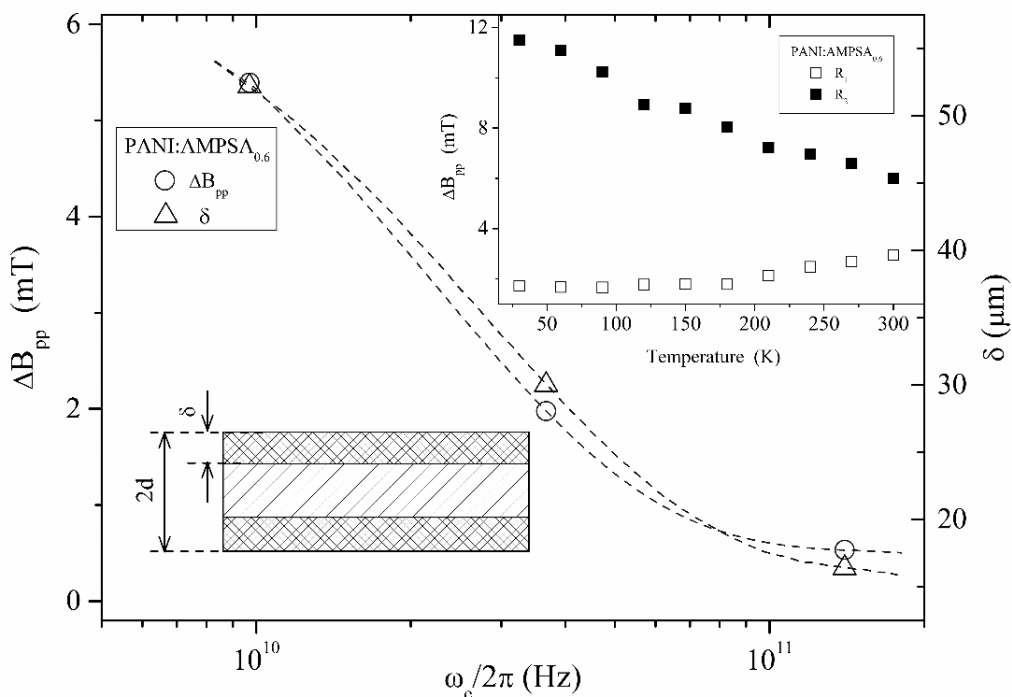
Figure 11. The peak-to peak linewidth ΔB_{pp} of the PANI:AMPSA$_{0.6}$ film as well as the thickness of skin-layer δ formed on its surface as function of spin precession frequency $\omega_e/2\pi$. In the inset is shown temperature dependence of the ΔB_{pp} value of the R_1 (open points) and R_2 (filled points) PC stabilized in this sample determined from its X-band EPR spectra with the Dyson contribution.

The narrowing of the line on raising the PANI temperature can be explained by averaging of the local magnetic field caused by hyperfine interaction between the localized spins whose energy levels lie near the Fermi level. The EPR line of the sample may also be broadened to some extent by relaxation due to the spin-orbital interaction responsible for linear dependence of T_1^{-1} on temperature (Sariciftci, Heeger, and Cao 1994), however, this such interaction can be neglected in case of PANI:AMPSA. It is significant that the linewidth of both types of PC is appreciably larger than that obtained previously for the fully oxidized powder-like and analogous films (Sariciftci, Heeger, and Cao 1994) which indicates a higher intrinsic conductivity of the PANI:AMPSA sample. Comparison of the ΔB_{pp} values suggested that a crystalline phase is formed in the amorphous phase of this PANI-ES beginning with the oxidation level $y = 0.3$, and that the PC in such phase exhibit a broader EPR spectrum. In the amorphous phase of the polymer, the PC R_1 are characterized by less temperature-dependent linewidth and are likely not involved in the charge transfer being, however, as probes for whole conductivity of the sample. At the same time, the magnetic resonance parameters of radicals of the R_2 type should reflect the charge transport in the crystalline domains of PANI:AMPSA.

Figure 12 depicts the inversed effective paramagnetic susceptibility χ and χT product (insert) of the R_1 and R_2 PC stabilized in the PANI:AMPSA$_{0.6}$ sample as function of temperature. It is seen that at low temperatures when $T \leq T_c \approx 100$ K the Pauli and Curie terms prevail in the total paramagnetic susceptibility χ of both type PC in this sample. At $T \geq T_c$,

when the energy of phonons becomes comparable with the value $k_B T_c \approx 0.01$ eV, the spins start to interact that causes the increase in the third term of Eq.(A.4) of sum susceptibility as result of the equilibrium between the spins with triplet and singlet states in the system. It is evident that the R_1 signal susceptibility obeys mainly the Curie law typical for localized isolated PC, whereas the R_2 susceptibility consists of the Curie-like and Pauli-like contributions. The dependences calculated from Eq.(A.4) with respective $\chi_P = 2.2 \cdot 10^{-5}$ emu/mol, $C = 1.7 \cdot 10^{-2}$ emu K/mol, $J_{af} = 4$ meV and $\chi_P = 5.3 \cdot 10^{-3}$ emu/mol, $C = 6.5 \cdot 10^{-1}$ emu K/mol, $J_{af} = 6$ meV are fitted well experimental data obtained for PC R_1 and R_2, respectively. The J_{af} values obtained are much lower of the corresponding energy (0.078 eV) obtained for ammonia-doped PANI-ES (Iida et al. 1993).
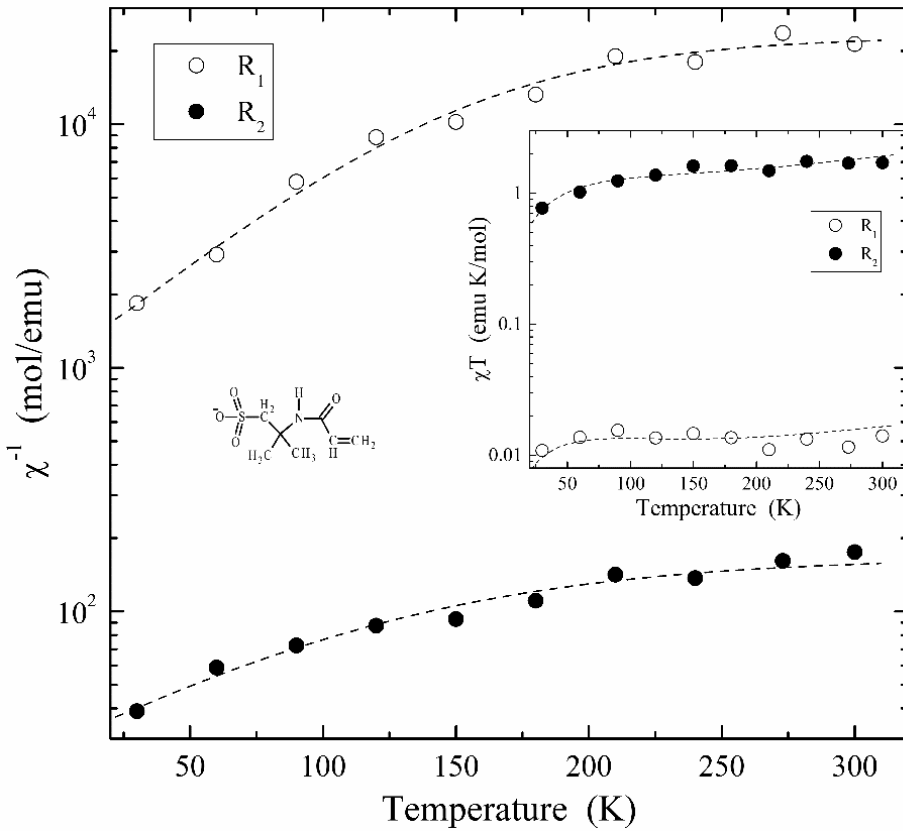
Figure 12. Temperature dependence of inversed effective paramagnetic susceptibility χ and χT product (insert) of the R_1 (open points) and R_2 (filled points) PC stabilized in the PANI:AMPSA$_{0.6}$ sample with different doping levels y. Dashed lines show the dependences calculated from Eq.(A.4) with respective $\chi_P = 2.2 \cdot 10^{-5}$ emu/mol, $C = 1.7 \cdot 10^{-2}$ emu K/mol, $k_1 = 1.7 \cdot 10^{-2}$ emu K/mol, $J_{af} = 4$ meV and $\chi_P = 5.3 \cdot 10^{-3}$ emu/mol, $C = 6.5 \cdot 10^{-1}$ emu K/mol, $k_1 = 1.2 \cdot 10^{-2}$ emu K/mol, $J_{af} = 6$ meV.

The density of states at the Fermi level ε_F, $n(\varepsilon_F) = 3.5$ states/eV Ph obtained for the charge carriers in the PANI:AMPSA$_{0.6}$ is in agreement with that determined in the optical (Lee, Heeger, and Cao 1995) and EPR (Sariciftci, Heeger, and Cao 1994) study of structurally close

polymer system. The Fermi energy of the Pauli-spins, $\varepsilon_F \approx 0.2$ eV, is lower than that (0.4 - 0.5 eV) obtained for other highly doped PANI-ES (Lee, Heeger, and Cao 1993, Krinichnyi 2000b, Krinichnyi et al. 2002). Assuming that the mass of charge carrier in heavily doped polymer is equal to the mass of free electron ($m_c = m_e$), the number of charge carriers in such a quasi-metal (Blakemore 1985), $N_c \approx 4.3 \cdot 10^{21}$ cm^{-3}, can be determined. This is close to the spin concentration in this polymer; therefore, one can conclude that all delocalized PC are involved in the charge transfer in the PANI:AMPSA$_{0.6}$ sample. The velocity of charge carriers near the Fermi v_F level was calculated for PANI:AMPSA$_{0.6}$ to be $6.2 \cdot 10^5$ m/s that slightly excesses that, $(2.8 - 4.0) \times 10^5$ m/s, evaluated for other PANI-ES samples from their EPR magnetic susceptibility data (Beau, Travers, and Banka 1999, Beau et al. 1999, Krinichnyi, Konkin, and Monkman 2012).

AC conductivity of the highly doped PANI:AMPSA$_{0.6}$ film determined from Dysonian spectra of the R_2 PC and also *dc* conductivity of this polymer determined by the *dc* conductometry method (Kon'kin et al. 2002) are given in Figure 13 as function of temperature (Krinichnyi, Konkin, and Monkman 2012). The analysis of these data evidenced on the complex charge transfer in the sample. Charge carriers were shown to hop through amorphous part of the sample and then to diffuse through its crystalline domain, so then the *dc* term of the total conductivity of the samples should be determined by 1D VDH between metal-like domains and their scattering on the lattice phonons in these domains (Krinichnyi 2014a). These processes occur in parallel, so the effective conductivity should be explained in terms of both models. Indeed, Figure 13 shows that the $\sigma_{ac}(T)$ dependences obtained experimentally for charge carriers R_1 and R_2 can be fitted by Eq.(A.28), Eq.(A.29) with $h\nu_{ph} = 0.039$ and 0.020 eV, respectively, and Eq.(A.34) (Krinichnyi 2014a). The energy determined for phonons in this PANI-ES sample lies near that obtained for other conductive polymers (Krinichnyi 2016b) and evaluated (0.066 eV) from the data determined by Wang et al. for HCl-doped PANI (Wang, Li, et al. 1991, Wang et al. 1992). It is evident that E_a determined for the PANI:CSA$_{0.6}$ sample lie near. This means that protons situated in crystalline domains sense electron spin dynamics. The data obtained can be evidence of the contribution of the R_1 and R_2 PC in the charge transfer through respectively amorphous and crystalline parts of the polymer. RT σ_{ac} values determined from Dysonian spectra of R_2 PC lies near respective σ_{dc} values that is characteristic for classic metals. Besides, RT σ_{ac} values determined from Dysonian spectra of R_2 PC lies near respective σ_{dc} values that is characteristic for classic metals. The data obtained can be evidence of indirect contribution of the R_1 PC and direct contribution of the R_2 PC in the charge transfer through respectively amorphous and crystalline parts of the polymer matrix.

Thus, both pinned and delocalized PC are formed simultaneously in the PANI regions with different crystallinity. An anti-ferromagnetic interaction in crystalline domains is stronger than that in amorphous regions of PANI-ES. Charge transport between crystalline metal-like domains occurs through the disordered amorphous regions with more localized charge/spin carriers. The change of conductivity with temperature is consistent with a disordered metal close to the critical regime of the metal-insulator transition with the Fermi energy close to the mobility edge (Sariciftci, Heeger, and Cao 1994, Sariciftci et al. 1995).
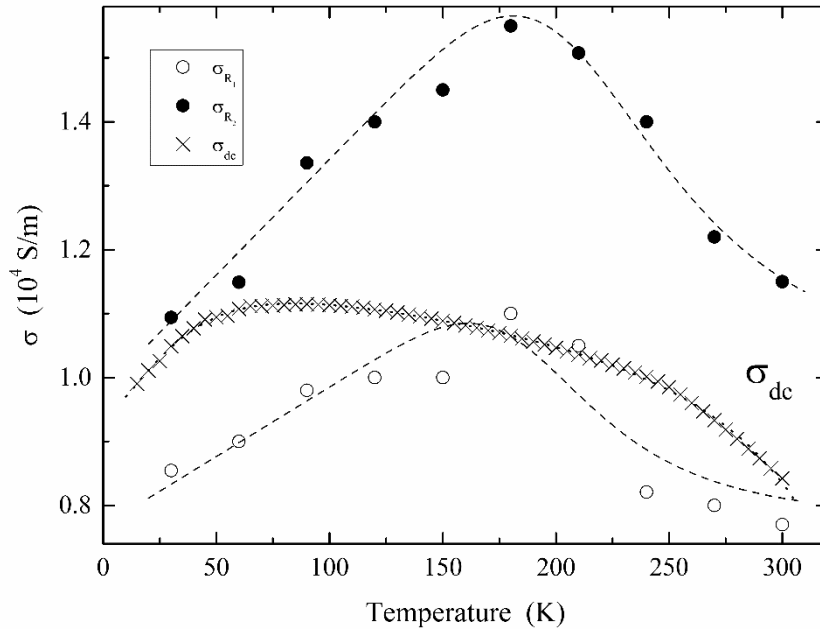
Figure 13. Temperature dependence of *ac* and *dc* conductivity of the PANI:AMPSA$_{0.6}$ film. Dashed lines show the dependences theoretically calculated in framework of VRH and polaron scattering on the lattice phonons from Eq.(A.28), Eq.(A.29) with $h\nu_{ph}$ = 0.039 and 0.020 eV, respectively, and Eq.(A.34).

The main polarons are localized in the highly doped PANI:AMPSA sample at $T \leq T_c$. This is the reason for the Curie type of susceptibility of the sample and should lead to the VRH charge transfer between the polymer chains. The spin-spin exchange appears at $T \geq T_c$ due likely to the activation librations of the polymer chains (Krinichnyi 2014a). The energy required for such dynamics lies within the energy range characteristic of other PANI-ES (Pratt et al. 1997, Krinichnyi, Chemerisov, and Lebedev 1997, Krinichnyi 2014a) and poly(tetrathiafulvalenes) (Krinichnyi 1996, Krinichnyi, Denisov, et al. 1998, Krinichnyi 2016b).This energy is governed by the effective rigidity and planarity of the polymer chains that are eventually responsible for the electronics properties of such polymer system. The results of the EPR study of other PANI-ES with various structure and number of dopants are described in (Krinichnyi 1995, 2014b, a, 2016b).

2.5. Poly(Tetrathiafulvalenes)

In recent decades, the electron donor TTF and its derivatives have been a subject of chemical and physical studies, due to the fact that many compounds of this group can form electrically conjugated charge transfer salts (Williams et al. 1992). In order to design TTF-based elements of molecular electronics, e.g., chemical sensors (Faridbod et al. 2008), powder-like PTTF matrices were synthesized in which TTF units with hydrogen, methyle and ethyle side substitutes *R* are linked *via* phenyl bridges (PTTF-R-C$_6$H$_4$) (Hinh, Schukat, and

Fanghänel 1979, Trinh et al. 1989) and *via* tetrahydroanthracene bridges (PTTF-THA) (Quang 1987) (Figure 1).

Iodine doped PTTF is a *p*-semiconductor with highest *dc* conductivity on the order of σ_{dc} ≈ 0.1 − 0.01 S/m depending on the structure of monomer unit (Roth et al. 1988). The temperature dependency of *dc* conductivity was obtained to be explained in terms of a VRH and a thermally activated hopping at low and high temperature ranges, respectively (Gruber et al. 1990). EPR and Mössbauer measurements of doped PTTF indicate a polaron-bipolaron charge transfer mechanism governed by the doping level and temperature (Roth et al. 1989, Roth, Brunner, et al. 1990, Patzsch and Gruber 1992).

PTTF-CH$_3$-C$_6$H$_4$, PTTF-C$_2$H$_5$-C$_6$H$_4$ and PTTF-THA samples schematically shown in Figure 1 were studied at X-band EPR (Roth et al. 1988, Roth, Brunner, et al. 1990). EPR spectrum of a simplest PTTF-H-C$_6$H$_4$ sample was analyzed to be a superposition of a strongly asymmetric spectrum of immobilized PC with g_{xx} = 2.0147, g_{yy} = 2.0067, g_{zz} = 2.0028 and a symmetric spectrum caused by mobile polarons with g = 2.0071. A relatively high value of **g** tensor evidences for the interaction of an unpaired electron with sulfur atom having large spin-orbit coupling constant. Roth et al. shown (Roth et al. 1988, Roth, Brunner, et al. 1990) that the spin-lattice relaxation time T_1 of an undoped PTTF-C$_2$H$_5$-C$_6$H$_4$ sample depends on the temperature as $T_1 \propto T^{-\alpha}$ with α decreases from two at 100 <*T* < 150 K temperature range down to one at higher temperatures. The addition of a dopant causes the change of a line shape of this sample due to the appearance of a larger number of mobile PC. Such a change in the magnetic and relaxation parameters was attributed to the conversion of spinless bipolarons into the paramagnetic polarons induced by the doping or/and heating of the polymer. In neutral and slightly doped polymers the charge is transferred by small polarons (Patzsch and Gruber 1992) whom dynamics is described by Eq.(A.32). However, it is difficult to carry out at X-band EPR the detailed investigation of doped PTTF samples with low concentration of the immobilized PC for the further analysis of spin effect in electron relaxation and dynamics.

The nature, composition and dynamics of PC in initial and iodine-doped PTTF samples above mentioned were studied by multifrequency EPR method more completely (Krinichnyi et al. 1993, Krinichnyi, Denisov, et al. 1998, Krinichnyi 2000a, 2006, 2016b).

Multifrequency EPR spectra of exemplary PTTF-CH$_3$-C$_6$H$_4$ sample iodine-doped up to y = 0.08 are presented in Figure 14. They allow one to determine more correctly all terms of the anisotropic **g**-tensor and to separate the lines attributed to polarons with different mobility. Computer simulation shows that the anisotropic EPR spectrum of the sample consists of localized PC $P_{loc}^{+\bullet}$ with slowly temperature dependent magnetic parameters g_{xx} = 2.01191, g_{yy} = 2.00584, g_{zz} = 2.00185, and more mobile PC $P_{mob}^{+\bullet}$ with g_{iso} = 2.00655 and ΔB_{pp}^{iso} = 5.6 mT. The analogous spectrum of $P_{loc}^{+\bullet}$ in PTTF-C$_2$H$_5$-C$_6$H$_4$ is characterized by the magnetic parameters g_{xx} = 2.01405, g_{yy} = 2.00676, g_{zz} = 2.00235, whereas PC with nearly symmetric spectrum are registered at g^p = 2.00774 with ΔB_{pp}^{iso} = 13.4 mT. The canonic components of **g**-tensor of PC localized in PTTF-THA are g_{xx} = 2.01292, g_{yy} = 2.00620, g_{zz} = 2.00251, whereas more mobile PC with weakly asymmetric spectrum are characterized by the parameters $g_{\parallel}^{P}$ = 2.00961 and $g_{\perp}^{P}$ = 2.00585. These *g*-factors exceed the corresponding magnetic parameters of the polarons in PATAC evidencing of the larger interaction of an unpaired electron with sulfur nuclear in PTTF. The ratio of concentrations of the localized and mobile PC is 1:4.5 in

neutral PTTF-CH$_3$-C$_6$H$_4$, 1:21 in PTTF-C$_2$H$_5$-C$_6$H$_4$, and 1:15.8 in neutral PTTF-THA. The existing in these systems of two polaron ensemble with different mobility was confirmed by their ^{1}H NMR study (Krinichnyi 2016b).

As effective $g^p = 1/3(g_{\parallel}^P + 2 g_{\perp}^P)$ is close to the average g-factor of immobilized polarons, PC of two types with approximately equal magnetic parameters exist in PTTF, namely polarons moving along the polymer main axis with minimum rate of $D_{1D}^0 \geq 3 \times 10^{10}$ rad/s and polarons pinned on traps or/and on short polymer chains. The comparatively large iodine ions soften the polymer matrix at the doping of a polymer, so then the mobility of its chains increases. It seems just a reason for the growth in a polymer of a number of delocalized polarons (Figure 14). The main terms of **g**-tensor of some PC in PTTF-C$_2$H$_5$-C$_6$H$_4$ are averaged completely due to their mobility, whereas such an averaging takes place only partially in the case of other PTTF samples. This fact can be explained by a different structure and morphology of the polymers' matrix.
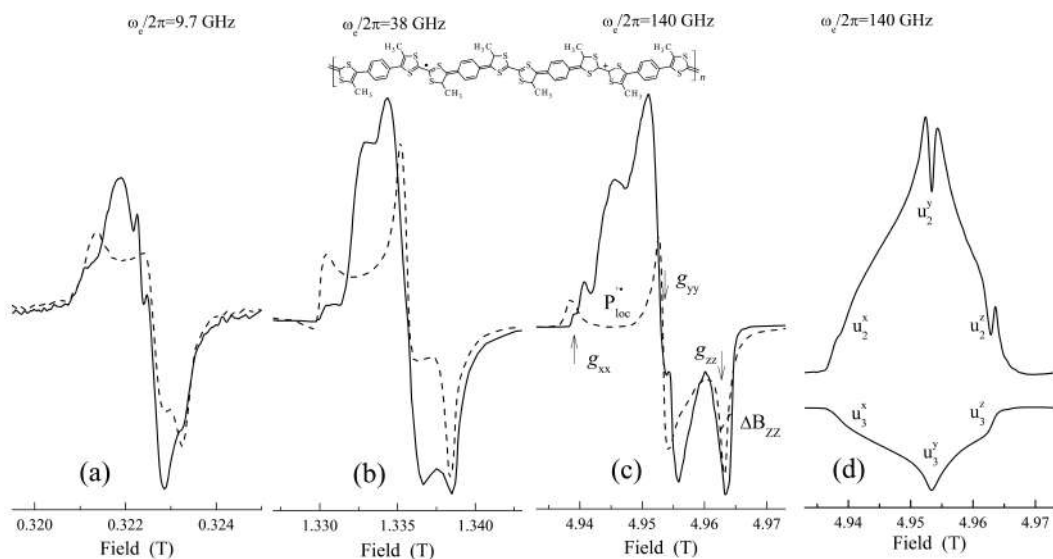
Figure 14. In-phase X- (*a*), Q- (*b*) and D- (*c*) bands absorption spectra EPR of the initial (dashed lines) and iodine-doped (solid lines) PTTF-CH$_3$-C$_6$H$_4$ samples registered at room temperature. (*d*) Typical in-phase (u_2) and $\pi/2$-out-of-phase (u_3) terms of D-band dispersion spectra of the samples are shown. The formation of the polaron on PTTF chain and measured magnetic parameters are shown as well.

So, the high spectral resolution at D-band EPR allows to determine separately all components of spectra of the polarons with different mobility and then to analyze their temperature dependence. Figure 15 shows the linewidth of polarons stabilized in the initial and iodine-doped PTTF-CH$_3$-C$_6$H$_4$ and PTTF-THA samples as function of temperature. It is seen from the Figure that the linewidth of localized polarons changes slightly in PTTF-CH$_3$-C$_6$H$_4$, however, this parameter doubles under doping of PTTF-THA. The increase of the spectrum linewidth of the mobile polarons in PTTF-CH$_3$-C$_6$H$_4$ sample indicates the acceleration of polaron diffusion in this system. Such a change in ΔB_{pp}^P of mobile polaron is analogous to the line narrowing of spin charge carriers in the PANI:AMPSA organic metal described above. Polaron motion along the polymer chain initiates interactions between

electron spins and also between electron and proton spins. Such interactions depend also on the spin precession frequency. RT linewidth ΔB_{pp} of the EPR spectral components of polarons immobilized, e.g., in PTTF-C_2H_5-C_6H_4 increases from 0.28 to 0.38 and then to 3.9 mT while electron spin precession frequency $\omega_e/2\pi$ increases from 9.5 to 37 and then to 140 GHz, respectively. On the other hand, linewidth of mobile polarons increases from 1.02 to 1.15 and then to 17.5 mT, respectively at such a transition. The width of all NMR lines also increase by factor $1.5 - 2$ with the increase of $\omega_p/2\pi$ from 300 MHz to 400 MHz (Krinichnyi 2016b). The fact, that the mobile PC has a broader line than the pinned ones, can be explained by the higher probability of its interaction with other electron and nuclear spins and with the dopant ions due mobility. This feature is typical for conjugated polymers (Krinichnyi 2000a, 2016b), however, disagrees with that obtained earlier for such system at X-band EPR (Roth et al. 1988, Roth, Brunner, et al. 1990).
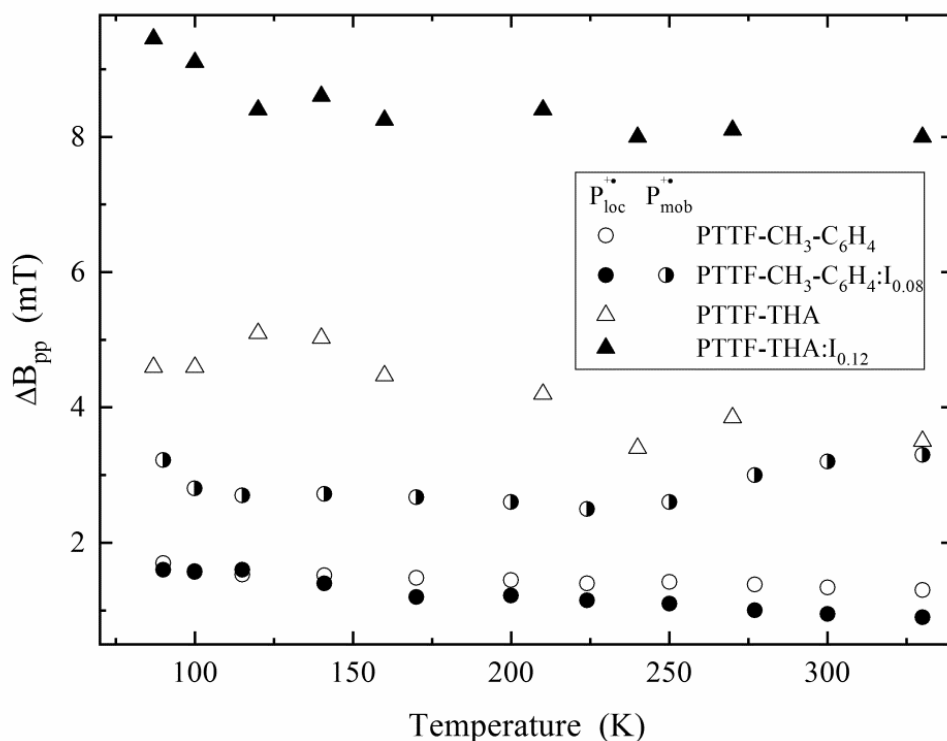
Figure 15. Temperature dependence of the linewidth of localized $P_{loc}^{+\bullet}$ and mobile $P_{mob}^{\bullet+}$ polarons in the initial (open points) and iodine-doped (filled points) PTTF-CH_3-C_6H_4 and PTTF-THA samples up to y = 0.08 and 0.12, respectively, determined from their D-band EPR spectra.

The concentration of PC in PTTF-CH_3-C_6H_4 slightly increases from 2×10^{17} cm^{-3} up to 3×10^{17} cm^{-3} at the polymer doping. Such process of PTTF-THA also changes slightly this parameter, from 3×10^{18} cm^{-3} up to 4×10^{18} cm^{-3}. PC concentration in doped PTTF-C_2H_5-C_6H_4 is 5×10^{17} cm^{-3}.

Paramagnetic susceptibility of the initial PTTF-CH$_3$-C$_6$H$_4$ and PTTF-THA samples as well as that reached upon their iodine doping up to $y = 0.08$ and 0.12, respectively, is presented in Figure 16 as function of temperature. This value changes monotonically within all temperature region The analysis of the data obtained shown that the susceptibility of the initial and iodine-doped (up to $y = 0.08$) PTTF-CH$_3$-C$_6$H$_4$ samples is determined mainly by the second term of Eq.(A.4) with $C = 1.9 \times 10^{-4}$ and 5.7×10^{-4} emu K/mol, respectively. This parameter of the initial and slightly iodine doped (up to $y = 0.12$) PTTF-THA samples is also governed by the Curie term of Eq.(A.4) with $C = 1.1 \times 10^{-2}$ and 4.2×10^{-3} emu K/mol, respectively. The results presented evidence that spin susceptibility of the PTTF-CH$_3$-C$_6$H$_4$ system increases with the doping, whereas such parameter of the PTTF-THA polymer decreases. This can indicates the charge transfer mainly by spinless bipolarons in the latter.

The increase of spectral linewidth within the $37 \leq \omega_e/2\pi \leq 140$ GHz registration range confirms a weak interaction between spin packets in this polymer. This provokes MW saturation of PC in PTTF at comparatively small B_1 values at D-band EPR. It causes the appearance of bell-like terms in both the in-phase and $\pi/2$-out-of-phase components of its dispersion signal due to manifestation of fast passage effects (see Figure 14,d). The u_i^x, u_i^y, and u_i^z terms of the dispersion signal U in Figure 14,d are attributed to PC with a strongly asymmetric distribution of spin density which are differently oriented in an external magnetic field. The simulation of the PTTF dispersion spectra allowed to identify them as a superposition of a spectrum, attributed to mobile polarons and a predominant asymmetric spectrum with $g_{xx} = 2.01189$, $g_{yy} = 2.00564$, $g_{zz} = 2.00185$ in undoped PTTF-CH$_3$-C$_6$H$_4$, $g_{xx} = 2.01356$, $g_{yy} = 2.00603$, $g_{zz} = 2.00215$ in undoped PTTF-C$_2$H$_5$-C$_6$H$_4$, and $g_{xx} = 2.01188$, $g_{yy} = 2.00571$, $g_{zz} = 2.00231$ in undoped PTTF-THA of immobile polarons.

The temperature dependencies of effective relaxation times of polarons in PTTF samples determined from their D-band EPR dispersion spectra using the method described earlier (Krinichnyi et al. 1993) are summarized in Figure 17. T_1 value of such charge carriers in all PTTF samples with phenyl bridges and in undoped PTTF with THA bridges was shown to change monotonically with temperature as $T^{-\alpha}$ with exponent α lying near 3 and 5 for mobile and pinned polarons, respectively. This value determined for PTTF at D-band EPR is larger than that measured for immobile radicals by using spin echo technique at X-band EPR (Roth et al. 1988). A difference between T_1^{mob} and T_1^{loc} can be caused, e.g., by a strong interaction between different PC.

Analyzing MW saturated spins stabilized on polymer chains one can use the ST-EPR method (Hyde and Dalton 1979) to determine super slow macromolecular librations in conjugated polymer systems (Krinichnyi 2006). Such dynamics in PTTF-CH$_3$-C$_6$H$_4$ and PTTF-THA systems was studied at D-band EPR (Krinichnyi et al. 1993, Krinichnyi, Denisov, et al. 1998, Krinichnyi 2006). The energy E_a required for activation of such dynamics in the first initial and doped system was determined from Eq.(A.30) to be 0.11 and 0.14 eV, respectively. This parameter determined for the in initial and doped latter sample is 0.19 and 0.07 eV, respectively. E_a values obtained at D-band EPR are comparable with that determined at lower registration frequency for interchain charge transfer in doped PTTF (Roth et al. 1988, Roth, Brunner, et al. 1990) that indicates the interaction of pinned and mobile polarons in this polymer matrix.
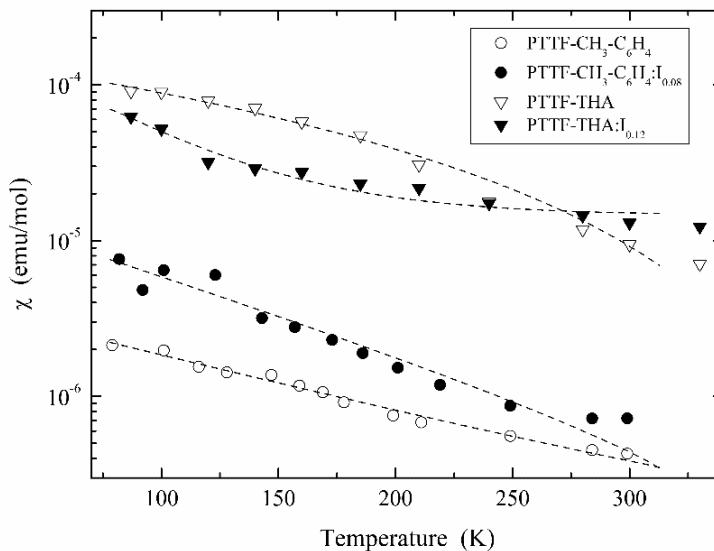
Figure 16. Temperature dependence of paramagnetic susceptibility of polarons stabilized on the initial PTTF-CH$_3$-C$_6$H$_4$ and PTTF-THA samples as well as on those iodine doped up to $y = 0.08$ and 0.12, respectively. Top-to-bottom dashed lines show dependences calculated from Eq.(A.4) with $C = 1.1 \times 10^{-2}$, 4.2×10^{-3}, 5.7×10^{-4} and 1.9×10^{-4} emu K/mol, respectively.
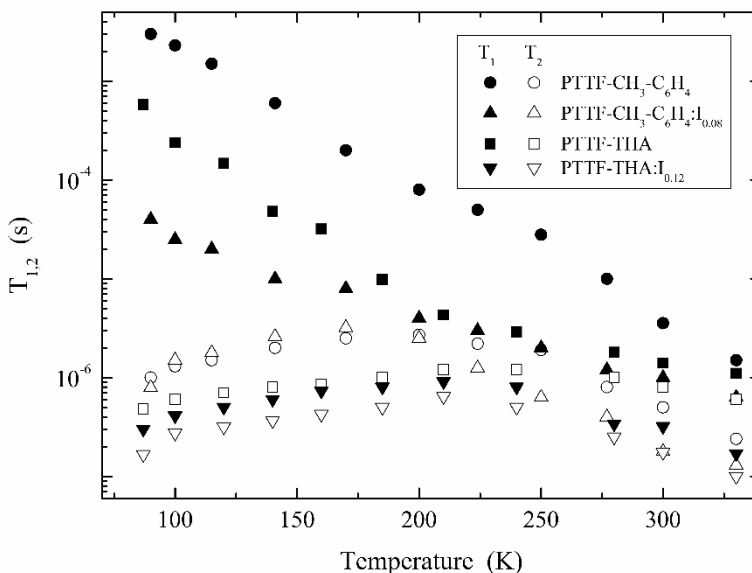
Figure 17. Spin-lattice T_1 (points) and spin-spin T_2 (points) relaxation times determined for polarons stabilized in the initial PTTF-CH$_3$-C$_6$H$_4$ and PTTF-THA samples as well as on those iodine doped up to $y = 0.08$ and 0.12, respectively, as function of temperature.

In order to compare experimental results with the polaron theory, Q1D diffusion motion of PC diffusing along and between PTTF's chains with the diffusion coefficients D_{1D} and D_{3D}, respectively, was also assumed. The temperature dependencies of effective D_{1D} and D_{3D} calculated for PC in different PTTF samples by using Eq.(A.25), Eq.(A.26) and the data presented in Figure 17 are shown in Figure 18. Assuming that the spin delocalization over the

polaron in PTTF occupies approximately five monomer units (Devreux et al. 1987) the maximum value of D_{1D} does not exceed 2×10^{12} rad/s for PTTF samples at room temperature. This value is at least two orders of magnitude lower than that determined earlier by low-frequency magnetic resonance methods for polarons in polypyrrole (Devreux and Lecavelier 1987) and polyaniline (Devreux et al. 1987), but higher then D_{1D}^0 evaluated above. RT anisotropy of spin dynamics in PTTF is $A = D_{1D}/D_{3D} \geq 10$. Figure 18 shows that D_{3D} value increases at RT by ca. an order of magnitude at transition from PTTF-CH$_3$-C$_6$H$_4$ to PTTF-THA sample due probably to more intensive interaction between spins in the latter. The variation of g_{xx} value is $\Delta g_{xx} = 1.0\times10^{-3}$ at such a transition. Assuming, that the overlapping integral t_{cc} of macromolecules depends on dihedral angle θ (i.e., the angle between p-orbits of neighboring C-atoms) as $t_{cc}\propto \cos\theta$, and that spin density on sulfur atom ρ_s depends as $\rho_s \propto \sin\theta$(Traven' 1989), one can calculate from Eq.(A.2) the difference $\Delta\theta$ at such a transition to be $\Delta\theta = 22^0$. Note, that analogous change in θ takes place at transition from benzoid to quinoid form of PPP (Brédas 1986), at transition from EB to ES form of PANI (Krinichnyi, Nazarova, et al. 1998, Krinichnyi et al. 2002) and laser treatment of PATAC.
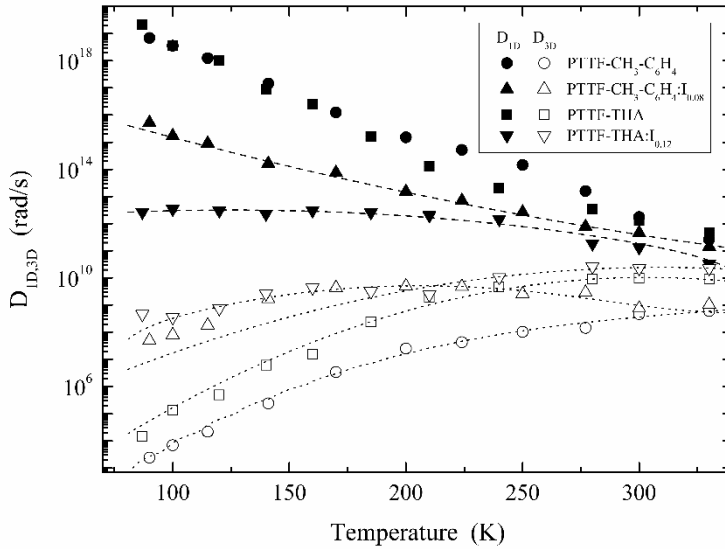
Figure 18. Temperature dependencies of the effective rates of polaron intrachain D_{1D} and interchain D_{3D} diffusion in the PTTF samples with phenyl and THA bridges determined from Eq.(A.25), Eq.(A.26) and the data presented in Figure 17. Top-to-bottom dashed lines show dependences calculated from Eq.(A.29) with $E_{ph} = 0.11$ and 0.025 eV, respectively. Top-to-bottom dotted lines show dependences calculated from Eq.(A.30) with $E_a = 0.14$, 0.07, 0.19, and 0.11 eV, respectively.

The D_{1D} and D_{3D} values of the PTTF samples calculated using Eq.(A.25) and Eq.(A.26) are presented in Figure 18 as function of temperature. It is seen that the D_{1D} values of the initial PTTF samples demonstrate stronger temperature dependence. Such dependencies cannot be described by tunnel charge transfer mechanisms. The most acceptable charge dynamic process can be suggested in terms the Kivelson-Heeger theory of polaron interaction with the lattice phonons. The data presented in Figure 18 evidence that the D_{1D} parameter of the iodine-doped PTTF-CH$_3$-C$_6$H$_4$ and PTTF-THA can indeed be fitted by Eq.(A.29) with $E_{ph} = 0.11$ and 0.025 eV, respectively. The interchain diffusion coefficient $D_{3D}$of the samples

monotonically increase with the temperature (Figure 18). The data presented can be suggested within the thermally activated interchain polaron hopping in conduction band tails with activation energy E_a. Temperature dependencies of conductivity due to such spin motion calculated from Eq.(A.30) are also shown by dotted lines on Figure 18. The energy required for activation of charge hopping between the chains of the iodine-doped PTTF-CH$_3$-C$_6$H$_4$ systems was determines to be $E_a = 0.11$ and 0.14 eV, respectively. The respective values were obtained for PTTF-THA, $E_a = 0.19$ and 0.07 eV, respectively.

It is seen from Figure 18, that D_{3D} value increases at the replacement of phenyl bridges by tetrahydroanthracene ones in PTTF. This fact allows concluding that this parameter and therefore the anisotropy of charge carrier transfer is governed by the polymer structure. Indeed, the structure of a polymer becomes more planar at such transition, so then the polymer chains are situated closer in PTTF-THA and the probability of interchain transfer increases due to the increase of appropriate transfer integral. This obviously leads to the decrease in the anisotropy of charge transport in this polymer. In other words, such a transition increases the dimensionality (crystallinity) of the system, which is typical for highly ordered metal-like organic systems.

The Fermi velocity v_F was determined for polaron diffusion in PTTF samples to be near to 1.9×10^7 cm/s (Krinichnyi 2000a). So the mean free path l_i of a charge was determined to be $l_i = v_{1D} c_{1D}^2 v_F^{-1} = 10^{-2} - 10^{-4}$ nm for the PTTF samples. The l_i is less then lattice constant d (Patzsch 1991) therefore the charge transfer is incoherent in this polymer which cannot be considered as Q1D metal. For such case the interchain charge transfer integral can be determined as (Wang et al. 1992) $t_\perp = v_F \hbar /2d = 0.05$ eV. This value lies near activation energy of chain librations and also near normalized activation energy of interchain polaron hopping in doped PTTF-CH$_3$-C$_6$H$_4$ and PTTF-THA samples. These facts allow us to conclude that charge transfer in PTTF is determined mainly by interchain phonon-assisted hopping of polarons which is stimulated by super slow macromolecular dynamics. This evidences for the correlation of molecular and charge dynamics in such polymer system. It confirms also the supposition (Madhukar and Post 1977), that the fluctuations of lattice oscillations, librations among them, can modulate the electron interchain transfer integral in conjugated compounds.

The rise of libron-exciton interactions at the polymer doping evidences for the formation of a complex quasi-particle, namely molecular-lattice polaron (Silinsh, Kurik, and Chapek 1988) in doped PTTF. According to this phenomenological model, molecular polaron is additionally covered by lattice polarization so then its mobility becomes as sum of mobilities of molecular and lattice polarons. The energy of formation of such molecular-lattice polaron E_p in PTTF was determined to be 0.19 eV (Krinichnyi et al. 1993). This value is smaller than that (0.1 eV) obtained for other disordered conjugated polymers (Zuppiroli, Paschen, and Bussac 1995). Therefore, the characteristic time, necessary for polarization of both atomic and molecular orbits of polymer, can be determined as $\tau_p \approx \hbar E_p = 3.5 \times 10^{-15}$ s. This value is sufficiently smaller than intra- and interchain hopping times for charge carriers in PTTF (Figure 18). This allow to conclude that the time τ_h required for the hopping of charge carriers in PTTF sufficiently exceeds the polarization time for charge carriers' microenvironment in the polymer, i.e., $\tau_h \gg \tau_p$. This inequality is a necessary and sufficient condition for electronic polarization of polymer chains by a charge carrier.

Thus, both the Q1D and Q3D spin dynamics are realized in PTTF affecting the charge transfer process. Q3D polaron diffusion dominates in the polymer conductivity; however,

Q1D diffusion of spin and spinless charge carriers also plays an important role in effective conductivity of the polymer.

2.6. Polythiophene

Polythiophene, its alkyl derivatives and their nanocomposites shown in Figure 1 and Figure 3 are also considered as perspective systems for design of various molecular devices (Samuelsen and Mardalen 1997, Zanardi et al. 2009, Zaumseil 2014). Pristine PT demonstrates at X-band EPR a single symmetric line with $g = 2.0026$ and $\Delta B_{pp} = 0.8$ mT, showing that the spins do not belong to a sulfur-containing moiety and are localized on the polymer chains (Bernier 1986, Mizoguchi and Kuroda 1997). The low concentration of PC ($n \cong 66$ ppm or 6.6×10^{-5} spin per a monomer unit) is consistent with a relatively high-purity of material, containing few chain defects. The doping of polymer leads to the formation on its chains of polarons which spins are delocalized along eight thiophene units (Springborg 1992). This process also provokes the appearance in the gap of asymmetric states with $\Delta E_1 = 0.32$ eV and $\Delta E_2 = 0.47$ eV (Stafström and Brédas 1988) (Figure 2). Stafström and Brédas (Stafström and Brédas 1988) found that these energies increase up to 0.57 and 0.73 eV, respectively, as pairs of polarons pair into diamagnetic bipolarons. Kaneto et al. (Kaneto et al. 1985) obtained from EPR study a maximum number of spins in PT doped with BF_4^- up to $y \approx 0.03$, suggesting a cross-over from polaron to bipolaron at this doping level. On the other hand, a fairly small number of spins in iodine-doped PT were reported (Moraes et al. 1985, Hayashi et al. 1986). Chen *et al*. (Chen, Heeger, and Wudl 1986) found only a vanishingly small EPR signal in PT electrochemically doped with ClO_4^- up to $y = 0.14$, suggesting a bipolaron ground state.

Spin dynamics in PT electrochemically doped with ClO_4^- was studied at RT by EPR (Mizoguchi et al. 1994). It was shown that highly doped sample reveals temperature dependence of linewidth due to the Elliott mechanism (Elliott 1954), characteristic of metals. RT coefficients of spin diffusion along and between polymer chains as well as the conductivity terms due to such spin diffusion were obtained to be respectively $D_{1D} = 1.9 \times 10^{15}$ rad/s, $D_{3D} = 5.5 \times 10^9$ rad/s and $\sigma_{1D} = 1.2 \times 10^5$ S/m, $\sigma_{3D} = 3.7$ S/m at $n(\varepsilon_F) = 0.12$ states per eV per C atom. The conductivity of PT:ClO_4^- changes as T^{-2} at high temperatures, whereas a metal-insulator (or semiconductor) transition takes place in this sample at 30 K (Masubuchi et al. 1993). The temperature dependence of conductivity of PT:BF_4^- supports the Mott's VRH mechanism (Demirboga and Onal 2000). Temperature dependence of activation energy indicated that the charge carrier hopping is the dominating mechanism of charge transport in this sample.

Powder-like nanocomposites of polythiophene synthesized electrochemically from monothiophene (PT) and dithiophene (PdT) and BF_4^-, ClO_4^-, and I_3^- counter-ions as a dopant were studied at both the X- and D-bands EPR (Krinichnyi et al. 1985).

At the X- band EPR these samples demonstrate a symmetric single line with effective $g \cong g_e$ and the width, slightly changing in a wide temperature range. However, the spectrum of the PT:I_3^- sample is broadened significantly with the temperature increase. At this waveband

EPR spectrum of PdT:ClO_4^- appears as a single symmetric line, which width decreases smoothly monotonically from 0.70 down to 0.25 mT with the temperature decrease from RT down to 77 K. So, magnetic resonance parameters of polarons are expectable governed by the structure of counter-ions.

D-band EPR spectra of these conjugated polymers demonstrate a greater variety of line shape (Figure 19). The Figure shows that PC stabilized in PT:BF_4^- and PT:ClO_4^- samples are characterized by an axially symmetric spectrum typical for PC localized on a polymer backbone. The analogous situation seems to be realized also for PT:I_3^-, for which the broadening and overlapping of canonic components of EPR spectrum can take place due to a stronger spin-orbit interaction of PC with counter-ions. PdT:ClO_4^- sample also demonstrates a single EPR line at this waveband EPR in a wide temperature range, thus indicating the domination of delocalized PC in this polymer.
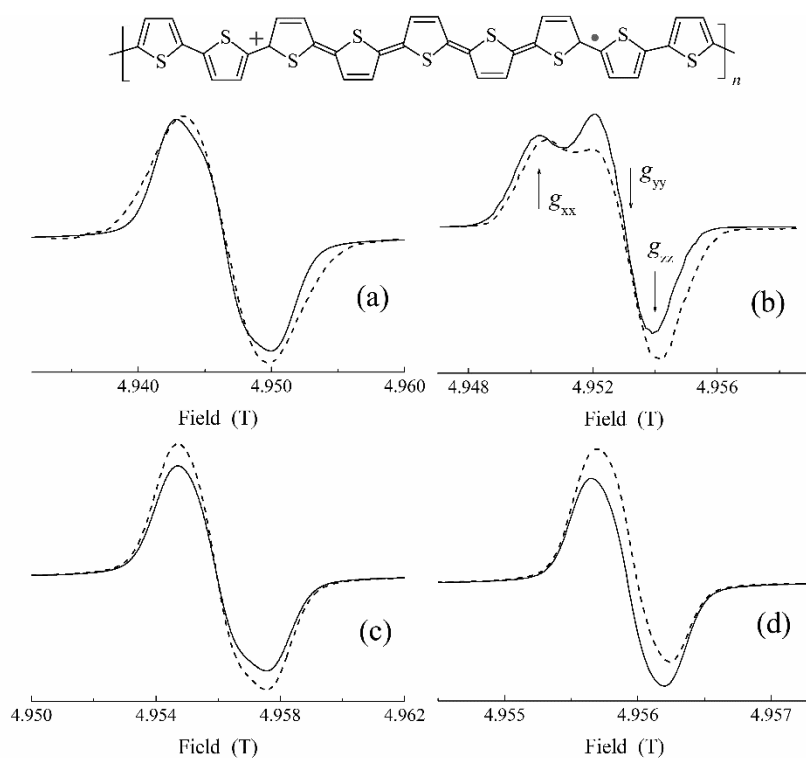
Figure 19. D-band absorption EPR spectra of electrochemically synthesized polythiophene modified by I_3^- (*a*), BF_4^- (*b*), ClO_4^- (*c*), (*d*) counter-ions and poly(di)thiophene (PdT) doped with ClO_4^- counter-ions (*d*) and registered at *T* = 300 (solid line) and 200 K (dashed line). The components of **g** tensor are shown. At the top the PT-based nanocomposite with polaron charge carrier is shown schematically.

Main magnetic resonance parameters, evaluated, e.g., for PT:BF_4^- sample from its D-band EPR spectra are also presented in Table 1. The terms of *g*-factor of PT doped with I_3^-, BF_4^-, ClO_4^- as well as of PdT doped with ClO_4^- were measured to be $g_\parallel$ = 2.00679 and $g_\perp$ = 2.00232, $g_\parallel$ = 2.00412 and $g_\perp$ = 2.00266, $g_\parallel$ = 2.00230 and $g_\perp$ = 2.00239, $g_\parallel$ = 2.00232 and

$g_\perp$= 2.00364, respectively. It derives from the analysis of the data, that the energy of an excited configuration $\Delta E_{\sigma\pi} \propto \Delta g^{-1}$ determined from Eq.(A.2), increases more than four times at the transition from I_3^- to BF_4^- and to ClO_4^- anions. The width of EPR spectral components of PT increase by factor of seven with the increase of registration frequency from 9.7 up to 140 GHz (Krinichnyi et al. 1985, Krinichnyi 2000a), indicating a strong spin-spin exchange in this system. Spin susceptibility of these nanocomposites changes within the series from 2.7×10^{-5} up to 6.8×10^{-5} down to 4.4×10^{-5} and up to 8.7×10^{-5} emu/mol, respectively. Such a transition leads also to the acceleration of spin dynamics and the growth of film conductivity. As the temperature decreases, a Dyson-like line is displayed in the region of a perpendicular component of the PT: BF_4^- EPR spectrum without a noticeable change of signal intensity (Figure 19,b). The further temperature decrease results in the increase of the line asymmetry factor *A/B* without reaching the extreme in the 100 – 300 K temperature range, thus being the evidence for the growth of *ac* conductivity as it occurs in case of other semiconductors of lower dimensionality. Therefore, an intrinsic conductivity of PT samples can be determined from Eq.(A.35), Eq.(A.36) and Eq.(A.37) using the characteristic size of sample particles. The *ac* conductivity of these samples was estimated to change from 3.2×10^2 up to 1.2×10^3 then down to 6.8×10^2 S/m (Krinichnyi et al. 1985, Krinichnyi 2000a). Then applying relationship (A.34), one can determine the rate of Q1D diffusion D_{1D} of charge carriers in the samples. This value calculated for the above series changes from 1.2×10^{13} down to 1.1×10^{13} and then up to 1.0×10^{14} rad/s. This may be the evidence for the realization of charge transfer in PT both by polarons and bipolarons, whose concentrations depend on the origin of anion, introduced into a polymer.

With the temperature growth a linewidth of the PdT: ClO_4^- sample first increases and starts to decrease as *T* becomes lower than $T_c \approx$ 170 K (Figure 20). This is accompanied by the resembling change in an inverted paramagnetic susceptibility χ^{-1} (Figure 20). Such a fact is evidence that the $\Delta B_{pp}(T)$ and $\chi(T)$ dependencies obtained for this sample are not symbasys. An extremal change in $\Delta B_{pp}(T)$ can be interpreted in terms of the Houzé-Nechtschein model (Houze and Nechtschein 1996) of the exchange interaction of spins localized on neighboring polymer chains in Q1D polymer system. Figure 20 shows the adaptability of this model for the PdT: ClO_4^- sample and evidences for the strong and weak interaction between spins below and above T_c, respectively. The energy of activation of such interaction obtained from Eq.(A.19), E_r = 0.040 eV, lies near that determined for macromolecular librations in other conjugated polymers (Krinichnyi 1995, 2000a, 2006). This leads to reversible pairing of polarons into bipolarons at $T \leq T_c$ and to bipolaron dissociation to polarons at higher temperatures. Figure 20 also shows that the temperature dependence of an effective magnetic susceptibility of the sample follows Eq.(A.4) with χ_P = 8.2×10^{-5} emu/mol, *C* = 2.1×10^{-2} emu K/mol, and J_{af} = 0.071 eV. Assuming a linear dependency for the bipolaron decay rate and frequency of polymer chain librations, the activation energy of the latter process can be evaluated from $\chi(T)$ dependency to be equal to E_a= 0.025 eV at $T \geq$ 200 K. Such a complex character of polaron-bipolaron transformation and spin-spin interaction seems to explain the above mentioned narrowing of X-band EPR spectrum of this sample with temperature.

RT intrinsic conductivity of the samples was also evaluated for the PdT:ClO_4^- sample from their Dysonian D-band EPR spectra to be 5.5×10^3 S/m. The rate of Q1D diffusion of charge

carrier, $D_{1D} = 4.1 \times 10^{13}$ rad/s, obtained for this system is less considerably than $D_{1D} = 1.1 \times 10^{13}$ rad/s obtained above and 1.9×10^{15} rad/s determined by Mizoguchi et al. (Mizoguchi et al. 1994) for PT:ClO_4^- sample, but close on the order of value to that evaluated for polarons in doped PANI-ES, in which interchain charge transfer dominates. The conductivity of PdT:ClO_4^- sample reveals an extremal character with bending point $T_c \approx 170$ K characteristic for the $\Delta B_{pp}(T)$ dependence (Figure 20). The charge transfer in the PdT:ClO_4^- sample, as in case of other conjugated polymers, was analyzed in terms of Q1D Mott's hopping and electron scattering on the lattice phonons. As Figure 20 evidences, $\sigma_{ac}(T)$ is approximated well by Eq.(A.29) with $E_{ph} = 0.13$ eV. The addtivity of the ΔB_{pp} and σ_{ac} values supports the Houzé-Nechtschein model (Houze and Nechtschein 1996) predicted linear dependence of these values.
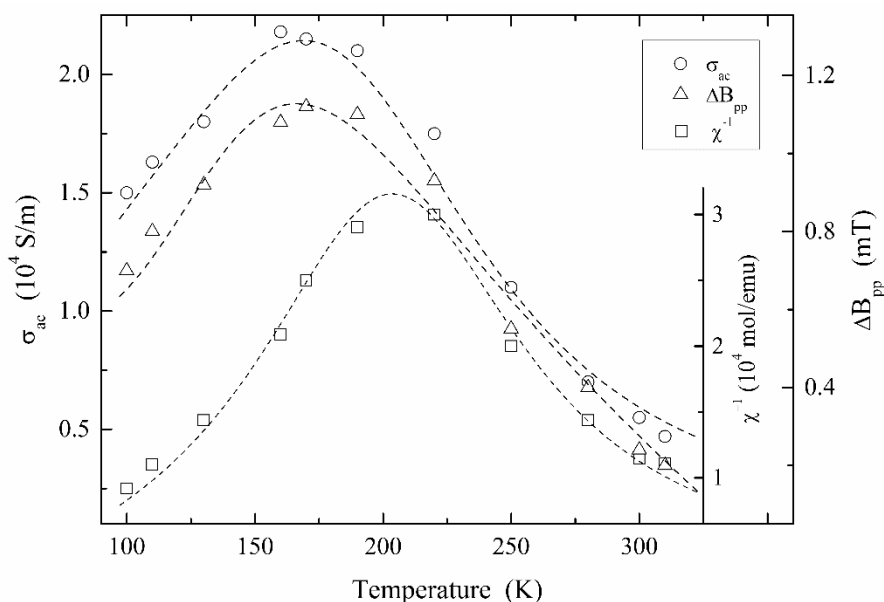
Figure 20. Temperature dependence of the intrinsic conductivity σ_{ac}, linewidth ΔB_{pp}, and inverted magnetic susceptibility χ of PdT:ClO_4^- determined from its Dysonian D-band EPR spectra. Top-to-bottom dashed lines present the dependencies calculated from Eq.(A.29) with $E_{ph} = 0.13$ eV, Eq.(A.19) with $E_r = 0.040$ eV, and Eq.(A.4) with $\chi_P = 8.2 \times 10^{-5}$ emu/mol, $C = 2.1 \times 10^{-2}$ emu K/mol, $c_{af} = 10.2$ emu K/mol, $J_{af} = 0.071$ eV.

2.7. Poly(3-Alkylthiophenes)

Poly(3-alkylthiophenes) (Figure 1) were shown (Kaeriyama 1997, Hotta 1997) to be suitable model system for understanding the electronic and optical properties of sulphur-based Q1D conjugated polymers with non-degenerate ground states (Gronowitz 1991, Kaeriyama 1997, Hotta 1997). Later, these polymers were appeared to be most effective active matrix for organic electronic and photonics devices (Sun and Sariciftci 2005, Poortmans and Arkhipov 2006, Jeffries-El and McCullough 2007, Pagliaro, Palmisano, and Ciriminna 2008, Brabec, Scherf, and Dyakonov 2014, Zaumseil 2014).

P3AT in undoped state are semiconductors, whom energy bandgap is determined by the presence of the π-orbital conjugation along the main polymer axis. For P3AT the gap amounts ca. 2 eV at ambient temperatures giving rise to its characteristic red color. This parameter, however, demonstrates temperature dependency, so that this color transforms to yellow at the temperature change ("thermochromism"). McCullough et al. (McCullough et al. 1993) have reported the maximum RT σ_{dc} of I_2-doped P3AT to be 6×10^3 S/m for poly(3-hexylthiophene) (P3HT, $m = 6$ in Figure 1), 2×10^4 S/m for poly(3-octylthiophene) (P3OT, $m = 8$ in Figure 1), and 1×10^5 S/m for poly(3-dodecylthiophene) (P3DDT, $m = 12$ in Figure 1). This shows the correlation of the P3AT *dc* conductivity with the alkyl group length and the morphology of the sample. It is well known that the transport properties of this class of materials are mainly governed by the presence of positively charged mobile polarons originating from the synthesis and the adsorption of oxygen from ambient atmosphere (spontaneous *p*-type doping) (Conwell 1997, Menon 1997). These charge carriers are subsequently partly trapped by the impurities, as opposed to inorganic semiconductors where, in the case of *p*-type doping, the hole is transferred from the impurity to the valence band. The presence of polaron in polythiophene and its derivatives was revealed by optical absorption measurements and EPR (Mizoguchi and Kuroda 1997). When the concentration of dopant *y* (oxygen, iodine, etc.) increases, the number of polarons also increases and, starting from some doping level, polarons combine into diamagnetic bipolarons. Kunugi et al. (Kunugi et al. 2000) have shown by the electrochemical study of charge transport that the RT carrier mobility μ in a regioregular P3OT film is 5×10^{-7} m^2 V^{-1}s^{-1} at $y = 1.4\times10^{-4}$. This value decreases down to $\mu = 5\times10^{-8}$ m^2 V^{-1}s^{-1} at $y = 1.0\times10^{-2}$ due to the scattering of polarons by ionized dopants and the formation of immobile π-dimers. Then it increases up to $\mu = 0.5$ cm^{2}V^{-1}s^{-1} at $y = 0.23$ due to the formation of bipolarons, followed by the evolution of the metal-like conduction.

Polarons can also be initiated by light illumination of P3AT with an electron acceptor introduced into its bulk as it is seen in Figure 3. This process is reversible, so both the spins photo induced in a polymer:fullerene BHJ tend to recombine after the light off.

Polarons stabilized in P3AT possess spin $S = \frac{1}{2}$ as well that also stipulates their wide investigation by different magnetic resonance methods. ^{1}H NMR proton spin-lattice relaxation time study of an initial and ClO$_4$-doped P3OT samples have shown (Masubuchi et al. 1999) that the molecular motion of the chains and side octyl groups occurs at different temperatures. At X-band EPR the spectrum of polaron in P3AT is characterized by a single line with the linewidth $\Delta B_{pp}\approx 0.6 - 0.8$ mT and the *g*-factor close to the *g*-factor of a free electron (Mizoguchi and Kuroda 1997). EPR signal of a slightly BF$_4$-doped poly(3-methylthiophene) (P3MT, $n = 1$ in Figure 1) was found to be a superposition of Gaussian line with $g_1 = 2.0035$ and $\Delta B_{pp} \cong 0.7$ mT attributed to the presence of localized PC and a Lorentzian one with $g_2 = 2.0029$ and $\Delta B_{pp} = 0.15$ mT due to delocalized PC (Scharli et al. 1987). In this sample the total concentration of PC amounts to about 3×10^{19} cm^{-3}, *i.e.*, about one spin per 300 thiophene rings. After doping, only one symmetric Lorentzian component of the former spectrum is observed. This line is symmetric at $y \leq 0.25$ and demonstrates a Dyson-like line at higher *y* (Tourillon et al. 1984). This process is accompanied by a sufficient decrease of electron both spin-lattice and spin-spin relaxation times (Scharli et al. 1987), which may indicate the growth of system dimensionality upon doping process. The analysis of χ(*y*) dependency shows that polarons are formed predominantly at low doping

level and then start to combine into bipolarons at higher *y*. Main magnetic resonance parameters, determined at various wavebands EPR for polarons stabilized or initiated in some P3AT are presented in Table 1.

Below are presented experimental data obtained in the study of polarons stabilized and initiated in some P3AT.

2.7.1. Poly(3-Hexylthiophene)

Detached regioregular P3HT modified by *bis*-PC$_{62}$BM shown in Figure 21 are characterized by the absence of both "dark" and light induced EPR (LEPR) signals over the entire range of temperatures studied. Their composite irradiated by visible light directly in a cavity of the EPR spectrometer, two overlapping LEPR lines appear reversibly at $T \leq 200$ K (Figure 21). Low- and high-field lines were attributed to positively charged polarons P$^{+\bullet}$ with isotropic *g*-factor, g_{iso}^P, and negatively charged methanofullerene ion radical with effective g_{iso}^F background photo induced in the P3HT:*bis*-PC$_{62}$BM BHJ. The effective values $g_{iso}^P = 2.0023$ and $g_{iso}^F = 2.0007$ are close to those obtained for charge carriers photo induced in other polymer:fullerene composites (Marumoto et al. 2003, Janssen, Moses, and Sariciftci 1994, Krinichnyi 2009), however, exceed those, $g_{iso}^P = 2.0017$ and $g_{iso}^F = 1.9996$, obtained for P3HT:PC$_{61}$BM (Krinichnyi, Yudanova, and Spitsina 2010). Note, that the g_{iso}^P value of the latter measured more accurately at W-band (94 GHz) EPR is equal to 2.00187 (Aguirre et al. 2008). These parameters were appeared to become weakly temperature dependent than those of the P3HT:PC$_{61}$BM composite (Krinichnyi, Yudanova, and Spitsina 2010). As in case of other polymer:fullerene systems (Krinichnyi and Balakai 2010, Krinichnyi, Yudanova, and Spitsina 2010, Krinichnyi 2016a), LEPR spectra of the P3HT:*bis*-PC$_{62}$BM BHJ consists of two Lorentzian contributions of mobile polarons and *bis*-methanofullerene anion radicals in quasi-pairs P$_{mob}^{+\bullet} \leftrightarrow bm$F$_{mob}^{-\bullet}$ as well as a contribution of localized polarons, P$_{loc}^{+\bullet}$, pinned in polymer traps (shown by dashed lines in Figure 21). It should be to note that, as compared with the P3HT:PC$_{61}$BM system, there is absent contribution of pinned fullerene radicals, bmF$_{loc}^{+\bullet}$. This implies that the number of deep traps able to capture a anion radical in the P3HT:*bis*-PC$_{62}$BM composite is sufficiently lower than that in the P3HT:PC$_{61}$BM one due to the better ordinary of the former. The best fit of the LEPR spectra of the sample was achieved using a convolution of Gaussian and Lorentzian line shapes, which means that electron excitation leads to inhomogeneous and homogeneous line broadening, respectively, due to unresolved hyperfine interaction of unpaired spin with neighboring protons and also to its different mobility.

Effective *g*-factor of polarons is strongly governed by the structure and conformation of a conjugated π-electron system. Our D-band EPR study of P3OT showed (Krinichnyi and Roth 2004) that an unpaired electron delocalized on polaron and extended over *L* lattice units weakly interacts with sulfur heteroatoms involved in the polymer backbone (see below). This provokes rhombic symmetry of spin density and, therefore, anisotropic *g*-factor and linewidth. Since the backbone of this and other P3AT polymers can be expected to lie preferably parallel to the film substrate (Kim et al. 2006), the lowest principal *g*-value is associated with the polymer backbone. The macromolecule can take any orientation relative to the *z*-axis, i.e., the polymer backbone direction as is derives from the presence of both the

g_{xx} and g_{yy} components in the spectra for all orientations of the film. Thus, the *g*-factor anisotropy is a result of inhomogeneous distribution of additional fields along the *x* and *y* directions within the plane of the polymer σ-skeleton rather than along its perpendicular *z* direction. This was confirmed later at millimeter waveband LEPR study of the P3HT:PC$_{61}$BM composite. Thus, it was shown that the spin of polarons photo induced in the P3HT chains is also characterized by rhombic symmetry originating anisotropic *g*-factor (see Table 1). Spin distribution in the $m\text{C}_{61}^{-\bullet}$ anion radical embedded into P3HT matrix is also characterized by rhombic symmetry that leads to respective anisotropy of its *g*-factor with g_{xx} = 2.00058, g_{yy} = 2.00045, g_{zz} = 1.99845 (Poluektov et al. 2010).
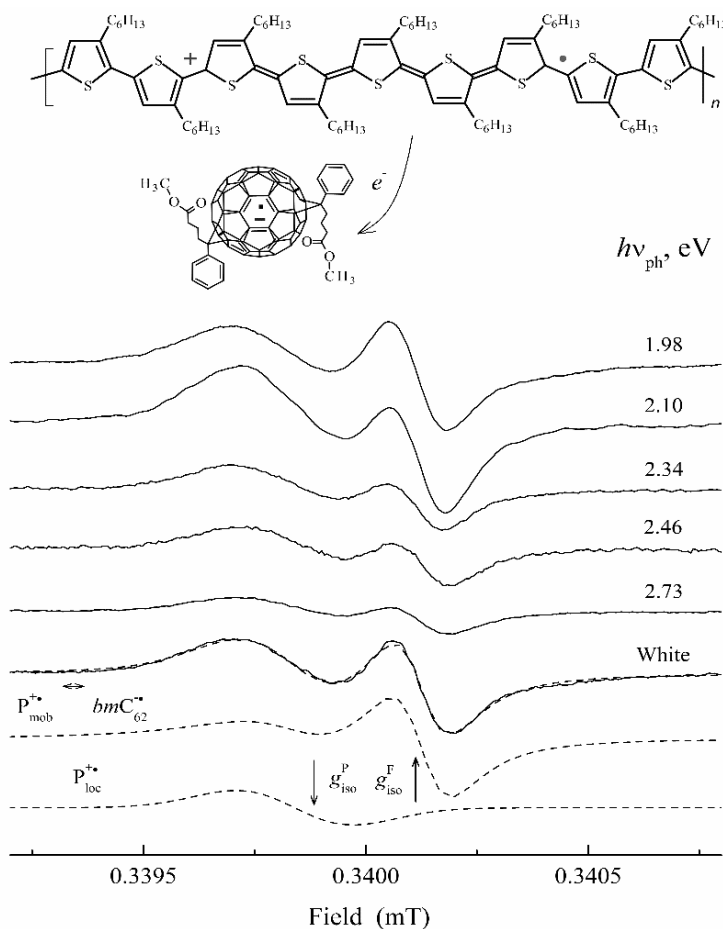
Figure 21. X-band LEPR spectra of charge carriers background photo induced at 77 K in BHJ formed by macromolecules of regioregular P3HT with globes of *bis*-PC$_{62}$BM by monochromic light with different photon energy $h\nu_{ph}$ and by polychomatic white light at *T* = 77 K. Sum spectrum as well as its Lorentzian contributions caused by mobile radical quasi-pairs, $\text{P}_{mob}^{+\bullet} \leftrightarrow bm\text{F}_{mob}^{-\bullet}$, and localized polarons, $\text{P}_{loc}^{+\bullet}$, are shown by dashed lines. The positions of LEPR spectra of localized and mobile charge carries are shown as well. At the top are schematically depicted P3HT with a polaron and *bis*-PC$_{62}$BM.

P3HT HOMO energy level E_{HOMO} depends on the overlap of adjacent thiophene MOs and, therefore, is expected to shift with ring angle (Conwell et al. 1988) similarly to the valence band involved in the π-π* transition. The band gap, $E_{LUMO} − E_{HOMO}$, should depend on torsion angle θ between the planes of the neighboring thiophene rings (Harigaya 1998), being near 30º in regioregular P3HT (Łużny, Trznadel, and Proń 1996). A decrease in g_{iso}^{P} occurs at electron excitation from the unoccupied shell to the antibonding orbit, π → σ* (Buchachenko, Turton, and Turton 1995), so one may conclude that the energy of antibonding orbits decreases as $PC_{61}BM$ globes is replaced by *bis*-$PC_{62}BM$ ones in this composite. This increases g_{iso}^{P} of the P3HT:*bis*-$PC_{62}BM$ composite and decreases the slope of its temperature dependency which is characteristic of more ordered system. Indeed, the changes in total energy with the torsion angle θ appear as effective steric potential energy. The angular dependence of this energy is an harmonic, with larger angles becoming more probable with the temperature increase. In this case the decrease of molecular regioregularity or a greater distortion of the thiophene rings out of coplanarity reduces charge mobility along the polymer chains (Lan and Huang 2008). This is usually attributed to a decrease in the effective conjugation lengths of the chain segments. The intrachain transfer integral t_{1D} is primarily governed by the degree of overlap between the p_z atomic orbitals of the carbon atoms forming polymer units and, therefore, should evolve a square-cosine function of the torsion angle θ (Van Vooren, Kim, and Cornil 2008). This allows one to evaluate the decrease in the θ value by ~10º at the replacement of the $PC_{61}BM$ by *bis*-$PC_{62}BM$ in the P3HT:methanofullerene system. This fact and the weaker temperature dependence of *g*-factors of both charge carriers in the P3HT:*bis*-$PC_{62}BM$ composite indicate the growing in planarity and ordering of polymer matrix occurring at such replacement.

The limiting number of polarons n_p and fullerene anion radicals n_f simultaneously formed per each polymer unit in the P3HT:*bis*-$PC_{62}BM$ BHJ can be determined, as in the case of analogous systems (Krinichnyi, Yudanova, and Spitsina 2010), by I_2-doping of the sample. Limiting paramagnetic susceptibility χ of iodine-treated composite was determined at 310 and 77 K to be $8.7×10^{-6}$ and $9.9×10^{-5}$ emu/mole, respectively. The analysis showed that the cooling of the sample leads to the appearance in its sum EPR spectra of anisotropic contribution attributed to trapped polarons. The ratio of a number of mobile to trapped polarons at 77 K is appeared to be near 7:1. Mobile polarons initiated in the sample by the I_2-doping demonstrate at 310 K single Lorentzian EPR spectra with peak-to-peak linewidth ΔB_{pp} of 0.56 mT, which are broader than that obtained for polarons stabilized in the P3HT:$PC_{61}BM$ (Krinichnyi, Yudanova, and Spitsina 2010) and other conjugated polymer matrices (Krinichnyi 2000a) Such broadening of the EPR line becomes most likely due to stronger dipole-dipole interaction between charged polarons. The contribution to linewidth due to such interaction can be estimated as $\Delta B_{dd} = \mu_B R_0^{-3} = 4/3 \, \pi\mu_B n_p$, where μ_B is Bohr magneton, R_0 is distance between polarons proportional to their concentration n_p on the polymer chain. At 77 K, the ΔB_{pp} values of mobile and trapped polarons are equal to 0.18 and 0.19 mT and characterized by Lorentzian and Gaussian distribution of spin packets, respectively. Assuming intrinsic linewidth of polarons $\Delta B_{pp}^{0} = 0.15$ mT in regioregular P3HT (Breiby et al. 2003), one can obtain $R_0 \approx 1.3$ nm from the line broadening due to dipole-dipole interaction in P3HT:*bis*-$PC_{62}BM$. The maximum density of polaron transport states was estimated (Westerling, Osterbacka, and Stubb 2002), e.g., for regioregular P3HT to be near 10^{21} cm^{-3}

assuming that one polaron occupies approximately five monomer units. Intrinsic concentration of doping-initiated polarons counting only upon polymer fraction in the P3HT:*bis*-PC$_{62}$BM composite was determined at 77 K to be 2.2×10^{19} cm^{-3}. This value lies near 2×10^{19} cm^{-3} obtained for concentration of acceptors in ZnO-treated P3HT (Marchant and Foot 1995). Effective concentration calculated for both the polymer and fullerene phases is 2.1×10^{18} cm^{-3} in this composite. This allows one to evaluate an effective number of both types of charge carriers per each polymer unit initiated in the polymer:fullerene composites by light irradiation (see Figure 22) and I$_2$-initiated polarons, $n_p = 3.8\times10^{-3}$. The n_P values obtained are considerably lower than that, $n_p \approx 0.05$, estimated for polarons excited in doped polyaniline (Houze and Nechtschein 1996).
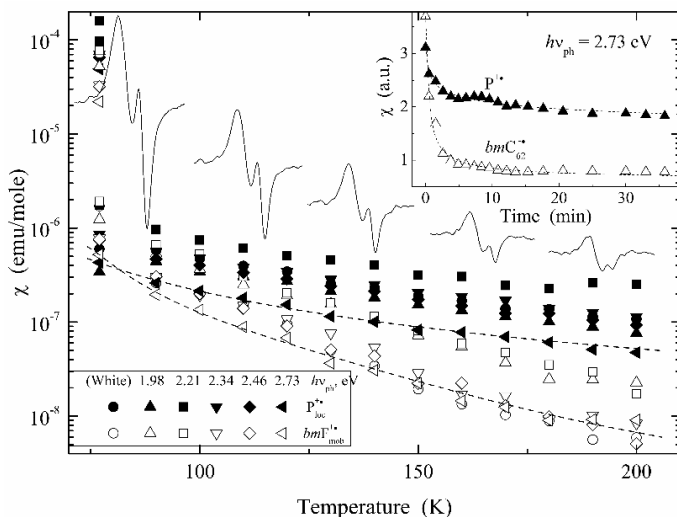
Figure 22. Temperature dependence of paramagnetic susceptibility of the $P_{loc}^{+\bullet}$ and $bmF_{mob}^{-\bullet}$ charge carriers photo induced in BHJ P3HT:*bis*-PC$_{62}$BM by polychromatic white and monochromatic light with different photon energy $h\nu_{ph}$. Respective limiting values evaluated for these carriers at 77 K by using iodine doping of the composite are shown as well. Exemplary dashed lines show dependences calculated from Eq.(A.12) with $E_r = 0.018$ and 0.041 eV. LEPR spectra of the sample registered at respective temperatures are shown at the top. In the insert are shown the decay of spin susceptibilities of pinned polarons $P_{loc}^{+\bullet}$ (filled points) and methanofullerene anion radicals $bmF_{mob}^{-\bullet}$ (open points) photo induced in the BHJ of P3HT:*bis*-PC$_{62}$BM composite by photons with $h\nu_{ph} = 2.73$ eV at 77 K. Dashed lines show the dependences calculated from Eq.(A.10) with $E_0 = 0.011$ and 0.023 eV.

The deconvolution of LEPR spectra of the P3HT:*bis*-PC$_{62}$BM composite allowed us to obtain separately all terms of its effective paramagnetic susceptibility χ as contributions of mobile and localized polarons χ_P and methanofullerene anion radicals χ_F. Figure 22 illustrates the changes in LEPR spectra of the P3HT:*bis*-PC$_{62}$BM composite with its heating and temperature dependences of all contributions into sum χ. Since concentration of main charge carriers decreases dramatically at $T > 200$ K, the precision of determination of their spin susceptibility falls significantly.

Fast initiation and consequent slow recombination of spin charge carriers in polymer:fullerene BHJ at background illumination allow one to register spin susceptibility as a differential result of these processes. The probability of the latter is mainly governed by

polaron multistage diffusion along a polymer chain through an energetic barrier and further electron tunneling from a fullerene anion to a polymer chain (Yan et al. 2000). Motion of polarons is assumed to be described by the a multiple trapping in sites with respective energy E_t (Nelson 2003, Tachiya and Seki 2010). Since crystalline subsystems in a composite are characterized by different band gaps, their E_t energies are also different and distributed exponentially. If energy of a trapped polaron exceeds E_t, it is occasionally thermally detrapped to the free state. A positive charge of polaron is not required to be recombined with negative charge on first fullerene. Diffusing along polymer backbone with positive elemental charge it may collide with the nearest fullerene anion radical located between polymer chains and then to recombine with a charge on a subsequent counter-anion. Assuming that polaron motion is not disturbed by the presence of fullerene molecules, we can conclude that the collision duration is governed by polaron diffusion. As it walks randomly along the chain, it passes a given fullerene molecule with the frequency $\nu_c \approx \omega_{hop}/L^2$. The polaron that diffuses between initial i and final j sites spatially separated by distance R_{ij} spends the energy equal to the difference of their depths, ΔE_{ij}. Thus, spin susceptibility of the sample should become energy-dependent and follow Eq.(A.6). A positive charge of polaron is not required to be recombined with negative charge on first fullerene; it can to recombine with a charge on a subsequent counter-ion. The fullerene molecules can be considered as fast relaxing impurities, so the susceptibility of polarons in the composite should follow Eq.(A.12) with the spin flip-flop probability p expressed Eq.(A.11). As it is seen from Figure 22, the net electronic processes in the composites can be described in terms of the spin exchange mechanism. The energy barrier tunneling by polaron was determined from Eq.(A.12) at irradiation of the composite by photons with $h\nu_{ph} = 1.98, 2.10, 2.34, 2.46, 2.73$ eV and by the white light to be $\Delta E_{ij} = 0.001, 0.029, 0.014, 0.016, 0.018$, and 0.003 eV, respectively.

It is evident that the energy required for polaron trapping in the polymer matrix is lower than that obtained for other charge carriers. ΔE_{ij} evaluated from $\chi(T)$ for these charge carriers increases considerably indicating higher energy required for their trapping in the system. The data presented evidence additionally that all spin-assisted processes are governed mainly by the structure of anion radicals as well as by the nature and dynamics of charge carriers photo induced in BHJ. It is seen that the χ value of both charge carriers becomes distinctly higher at characteristic energy $h\nu_{ph} \approx 2.1$ eV lying near the band gap of P3AT (Al Ibrahim et al. 2005). Such a dependence of spin concentration on photon energy can be explained either by the formation of spin pairs with different properties in homogeneous (higher ordered) composite fragments or by the excitation of identical charge carriers in heterogeneous domains (lower ordered) of the system under study. Different spin pairs can be photo induced as a result of the photon-assisted appearance of traps with different energy depths in a polymer matrix. However, the revealed difference in the parameters of radicals seems to be a result of their interaction with their microenvironment in domains in homogeneously distributed in polymer:fullerene composite. Different ordering of these domains can be a reason for variation in their band gap energy leading, hence, to their sensitivity to photons with definite but different energies. This can give rise to the change in the interaction of charge carriers with a lattice and other spins. Effective spin susceptibility of the sample discussed somewhat exceeds that obtained for P3HT:PC$_{61}$BM (Krinichnyi, Yudanova, and Spitsina 2010). This effect and the absence of trapped anion radicals in the former allowed to conclude additionally more ordered BHJ in the P3HT:*bis*-PC$_{62}$BM composite which interfere in the formation of traps.

If one includes Coulomb interactions, this should affect the activation energy for either defrosting or thermally assisted tunneling by an amount $U_c = e^2/4\pi\varepsilon\varepsilon_0 r$, where e is elemental charge, ε is a dielectric constant, and r is charge pair separation. Assuming $\varepsilon = 3.4$ for P3HT (Deibel et al. 2010), minimum separation of charge carriers is equal to the radius a of π electrons on the C atoms which two times longer than the Bohr radius, i.e., 0.106 nm, r equal to interchain separation, 0.38 nm (Chen, Wu, and Rieke 1995), one obtains the decrease in U_c from ~0.4 eV down to 0.02 eV during dissociation of an initial radical pair. Therefore, both the photo induced polaron and anion radical should indeed be considered as noninteracting that prolongs their life.

When initiating background illumination is switched off, photo initiation of charge carriers in BHJ stops and the concentration of spin charge carriers excited starts to decrease as shown in the insert of Figure 22. Live time of charge carriers seems to be much longer than $t \sim 0.1$ µs obtained by optical absorption spectroscopy for relevant recombination times of mobile photoexcitations in organic solar cells (So, Kido, and Burrows 2008, Sharma 2010). So, the data presented are mainly pertinent to carriers trapped in polymer matrix. Generally, charge recombination is described as a thermally activated bimolecular recombination (Brabec et al. 2003) which consists of temperature-independent fast and exponentially temperature-dependent slow steps (Westerling, Osterbacka, and Stubb 2002). At the latter step, polaronic charge carrier can either be retrapped by vacant trap sites or recombine with electron on fullerene anion radical. Trapping and retrapping of a polaron reduces its energy that results in its localization into deeper trap and in the increase in number of localized polarons with time. So, the decay curves presented can be interpreted in terms of bulk recombination of holes and electrons during their repeated trapping into and detrapping from trap sites with different depths in energetically disordered semiconductor (Tachiya and Seki 2010). The traps in such a system are characterized by different energy depths and energy distribution E_0. Polarons fast translative diffuse along a polymer backbone, and fullerene anion radicals can be considered to be immobilized between polymer chains. The dependences calculated in frames of this approach are shown in Figure 22. Trap energy distribution in the composite was determined upon its irradiation by photons with $h\nu_{ph} = 1.98$, 2.10, 2.34, 2.46, 2.73 eV and by the white light to be $E_0 = 0.041, 0.027, 0.018, 0.014, 0.011$, and 0.031 eV, respectively. Therefore, the decay of long-lived polaron excitations originated from initial excitons and spin quasi-pairs photo induced in the polymer:fullerene composite can be described in terms of the above model in which the low-temperature recombination rate is strongly governed by temperature and the width of energy distribution of trap sites. Non-linear change $E_0(h\nu_{ph})$ dependence should indicate that the local structure and ordering govern the depth of spin traps and their distribution in this composite. This allows one to conclude the crucial role of the photon energy on the formation and energy properties of the traps in a BHJ of disordered systems.

Effective EPR linewidth of both charge carriers photo induced in the P3HT:*bis*-PC$_{62}$BM composite is presented in Figure 23 as a function of temperature and photon energy. It is seen that this value obtained for polarons changes extremely with the temperature with characteristic temperature $T_c \approx 130$ K, whereas linewidth of the methanofullerene anion radicals demonstrates monotonic temperature dependence and decreases with the system heating. This indicates echange interaction of polaron spins which broadens their lines. Besides, sulphur and hydrogen atoms in the composite possess a nuclear magnetic moment

initiating the hyperfine interaction between the electrons and the nuclei. Polaron translational and fullerene pseudorotational diffusion in a polymer:fullerene composite should also be taken into account. In this case a polaron should interact with the other PC with the collision probability p expressed by Eq.(A.10), so then its absorption line should additionally be broaden by the value expressed by Eq.(A.19). Successful fitting of experimental data with t_{1D} = 1.18 eV (Cheung, McMahon, and Troisi 2009) are presented in Figure 23 should evidence the applicability of such approach for interpretation of electronic processes realized in the P3HT:*bis*-PC$_{62}$BM composite. The energy E_r obtained lies near that evaluated for regioregular P3HT from *ac* conductometric (0.080 eV) (Obrzut and Page 2009) and ^{13}C NMR (0.067 – 0.085 eV at T< 250 K) (Yazawa et al. 2010) data.
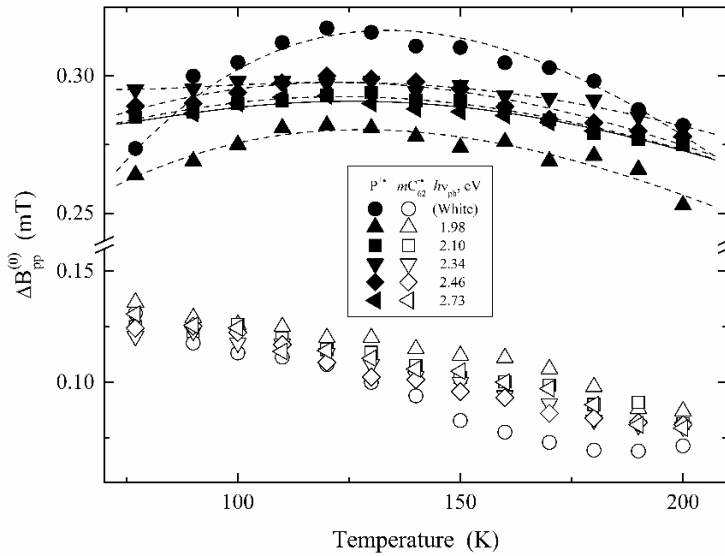
Figure 23. Linewidth of charge carriers photo induced in the P3HT:*bis*-PC$_{62}$BM composite as a function of temperature and photon energy $h\nu_{ph}$. Top-to-bottom dashed lines show the dependences calculated from Eq.(A.19) with E_r = 0.045, 0.047, 0.051, 0.050, 0.050, 0.048 eV. The symbol (0) in $\Delta B_{pp}^{(0)}$ implies that the LEPR spectra were measured far from MW saturation, when $B_1 \rightarrow 0$.

The main relaxation parameters of the pined and mobile polarons determined using steady-state saturation method are presented in Figure 24,a as a function of temperature and photon energy. It is seen from the Figure that the interaction of most charge carriers with the lattice is characterized by monotonic temperature dependence. All relaxation parameters are governed by structure and morphology of the polymer:fullerene composite as well as by the energy of initiating phonons. Polarons induce an additional magnetic field in the BHJ accelerating electron relaxation of all spin ensembles. As their relaxation in conjugated polymers are defined mainly by their dipole-dipole interaction (Krinichnyi et al. 1992, Krinichnyi 2000a) the respective coefficients of spin intrachain D_{1D} and interchain D_{3D} diffusion can be calculated from Eq.(A.25), Eq.(A.26) and the data presented in Figure 24,a. Figure 24,b depicts both these parameters obtained for polarons in the composite as a function of the energy of initiating phonons and temperature. The Figure shows that both the coefficients of polaron diffusion are governed sufficiently by the energy of initiated photons $h\nu_{ph}$. To account for the LEPR mobility data obtained, different theoretical models can be

used. Intrachain polaron dynamics in the P3HT:*bis*-PC$_{62}$BM composite is characterized by strong temperature dependence (Figure 24,b). Typically, such a behavior can be associated with the scattering of polarons on the lattice phonons of crystalline domains immersed into an amorphous polymer matrix. It is seen from Figure 24,b that the experimental polaron intrachain dynamics data obtained at irradiation of the composite by photons with $h\nu_{ph} = 1.98$, 2.10, 2.34, 2.46, 2.73 eV and by the white light can successfully be fitted by Eq.(A.31) with $E_{ph} = 0.077$, 0.075, 0.091, 0.088, 0.065, and 0.062 eV, respectively. This parameter lies near that determined for PANI-ES (0.09 – 0.32 eV) (Krinichnyi 2000b) and laser modified PATAC (0.15 – 0.18 eV) (Krinichnyi, Roth, and Schrödner 2002).
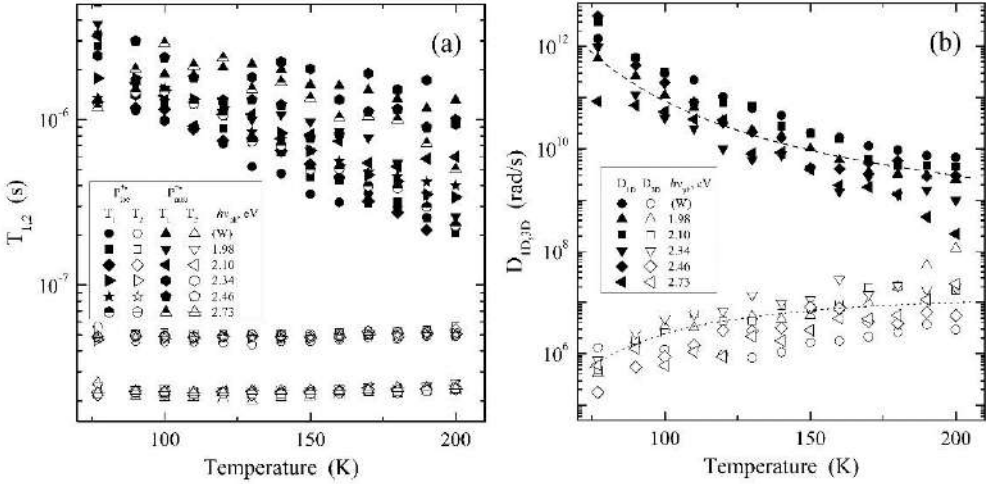
Figure 24. Temperature dependence of spin-lattice T_1 (filled points) and spin-spin T_2 (open points) relaxation times (*a*) as well as intrachain (D_{1D}, filled points) and interchain (D_{3D}, open points) diffusion coefficients of localized $P_{loc}^{+\bullet}$ and mobile $P_{mob}^{+\bullet}$ polarons photo induced in the P3HT:*bis*-PC$_{62}$BM composite by the polychromatic white and monochromatic light with different photon energy $h\nu_{ph}$. Above and below exemplary dashed lines show dependences calculated from Eq.(A.29) with $E_{ph} = 0.077$ eV and from Eq.(A.31) with $E_t = 0.128$eV, respectively.

The interchain spin hopping dynamics can be analyzed in terms of the Hoesterey-Letson formalism modified for amorphous low-dimensional systems (Fishchuk et al. 2002). According to this model, spin hoping between polymer chains should be controlled by the traps with concentration n_t and depth E_t. Figure 24,b shows also the temperature dependences calculated from Eq.(A.31) with $T_{cr} = 127 – 140$ K. The Figure evidences that interchain polaron dynamics in the composite irradiated by photons with $h\nu_{ph} = 1.98$, 2.10, 2.34, 2.46, 2.73 eV and by the white light can be described in the frames of the above mentioned theory with $E_t = 0.128$, 0.129, 0.128, 0.119, 0.125, and 0.123 eV, respectively.It should be noted that the E_t values obtained for P3HT:PC$_{61}$BM composite prevail those characteristic of P3HT:*bis*-PC$_{62}$BM (Krinichnyi 2016a) that is additional evidence of deeper traps formed in the former polymer matrix. This fact, probably, indicates the decrease in trap concentration due the increase in effective crystallinity of the polymer matrix.

So, the main magnetic resonance, relaxation and dynamic parameters of polarons photo initiated in the P3HT:*bis*-PC$_{62}$BM composite are governed by the structure, conformation and ordering of BHJ as well as by the energy of excited photons. This can be partly as a result of structural inhomogeneity of the polymer:fullerene composite, conditioning reversible photon-initiated traps with different depth and distribution. The data obtained allowed us to suggest the importance of the ring-torsion and ring-librative motions on the charge initiation, separation and diffusion in this disordered organic system. It was shown that a polaron diffusing along a polymer backbone exchanges with the spin of a counter methanofullerene anion radical in terms of the modified Marcus theory. Charge recombination occurs in terms of spin multitrapping in energetically disordered semiconductor whose local structure and ordering govern the number, depth and distribution of charge traps. The interaction of most charge carriers with the lattice is characterized by monotonic temperature dependence. Electron relaxation of charge carriers was shown to be also governed by dynamics, structure and conformation of their microenvironment as well as by photon energy. Selectivity to photon energy is governed by properties of donor and acceptor forming BHJ and can be used, for example, in plastic sensoric photovoltaics. The energetic barrier required for polaron interchain hopping predominantly prevails that of its intrachain diffusion in the composite.

2.7.2. Poly(3-Octylthiophene)

P3OT is also expected to be a suitable and perspective material for molecular electronics (Carter 1982, Brédas and Chance 1990, Salaneck, Clark, and Samuelsen 1991, Ashwell 1992, Scrosati 1993, Wong 1993), e.g., polymer sensors (Bobacka, Ivaska, and Lewenstam 1999) and polymer:fullerene solar cells (Sariciftci and Heeger 1995, Lee et al. 1993, Lee et al. 1994, Gebeyehu et al. 2000, Gebeyehu et al. 2001). The piezoelectric effect has been also registered in P3OT (Taka et al. 1993). DC conductivity of an as synthesized P3OT is about 10^{-4} S/m (Chen, Wu, and Rieke 1995). A constriction of the P3OT bandgap was observed (Kaniowski et al. 1998) due to the decrease of the torsion angle between its adjacent thiophene rings and the enhancement of interchain interactions between parallel polymer planes. More detail information on the magnetic and electronic properties of the initial P3OT sample and treated by an annealing (P3OT-A) and by both recrystallization and annealing (P3OT-R) was obtained at X- and D-bands EPR (Roth and Krinichnyi 2003, Krinichnyi and Roth 2004). The transition temperature of P3OT is close to 450 K, so respective treatment was made at this temperature.

Figure 25 shows EPR spectra of polarons stabilized in the initial and treated P3OT samples obtained at both wavebands EPR. At the X-band the samples show a single nearly Lorentzian EPR line with $g_{iso} = 2.0019$. The asymmetry factor of the lines is $A/B =1.1$, and their peak-to-peak linewidth was determined to be $\Delta B_{pp} = 0.27$ (P3OT), 0.27 (P3OT-A), and 0.26 mT (P3OT-R). The latter value is smaller than $\Delta B_{pp} \approx 0.6 - 0.8$ mT obtained for PT and P3MT (Mizoguchi and Kuroda 1997), however, is close to 0.32 mT registered for polarons in regioregular P3OT (Marumoto et al. 2002). The X-band EPR spectrum of the P3OT sample stored for two years is also drawn in Figure 25,a by the dotted line. Its computer modeling has shown that it consists of anisotropic and isotropic spectra. The effective *g*-factors obtained from these spectra are close; therefore one can conclude that localized PC with more anisotropic magnetic parameters appear at the polymer storage.

The RT total spin concentration of P3OT increases during the polymer treating from 3.9×10^{19} cm^{-3} in P3OT up to 3.1×10^{20} cm^{-3} in P3OT-A and 3.5×10^{20} cm^{-3} in P3OT-R or from 0.013 to 0.11 and to 0.11 spin per a monomer unit, respectively. Their effective paramagnetic susceptibility χ and the χT value are presented in Figure 26 as function of temperature.
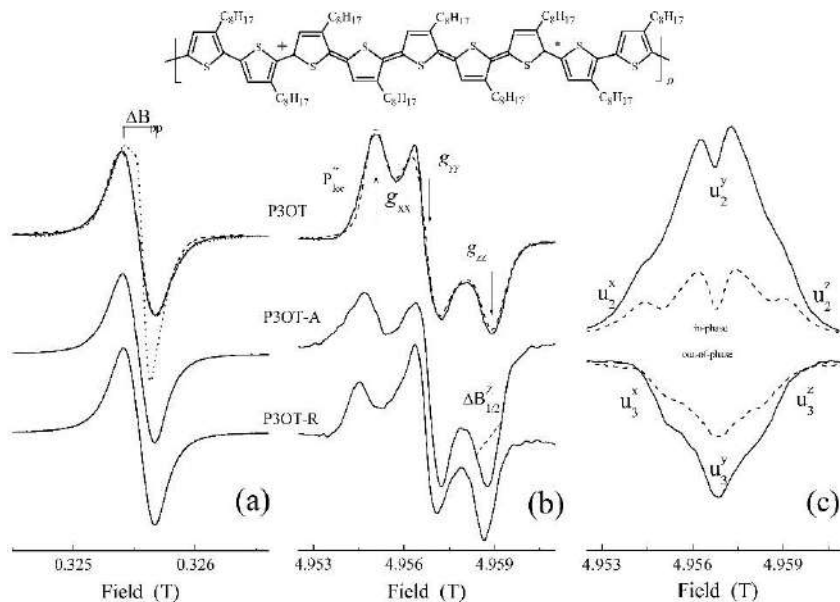
Figure 25. RT X-band (*a*) and D-band (*b*) absorption EPR spectra of the P3OT, P3OT-A, and P3OT-R samples. The X-band EPR spectrum of the P3OT stored for two years is shown on the left by the dotted line. The magnetic resonance parameters measured are shown. The spectra calculated using $g_{xx} = 2.004089$, $g_{yy} = 2.003322$, $g_{zz} = 2.002322$, $\Delta B_{pp}^{x} = \Delta B_{pp}^{y} = \Delta B_{pp}^{z} = 0.25$ mT, and Lorentzian/Gaussian = 0.9 line shape ratio (*a*), and $\Delta B_{pp}^{x} = 0.82$ mT, $\Delta B_{pp}^{y} = 0.78$ mT, $\Delta B_{pp}^{z} = 0.88$ mT, and Lorentzian/Gaussian = 0.4 line shape ratio (*b*) are shown by the dashed lines. The sum spectrum of the lines calculated with $g_{\parallel} = 2.00387$, $g_{\perp} = 2.00275$, $\Delta B_{pp} = 0.11$ mT and $g_{iso} = 2.00312$ and $\Delta B_{pp} = 0.35$ mT with amplitude ratio of 2.5:1 is shown by dotted line on the right as well. (*c*) In-phase (u_2) and $\pi/2$-out-of-phase (u_3) terms of D-band dispersion spectra of the samples registered at $T = 100$ K (solid lines) and 145 K (dashed lines) are shown. The formation of the polaron on P3OT chain and measured magnetic parameters are shown as well.

In the high-temperature region the spin susceptibility of the P3OT and P3OT-R samples seems to include a contribution due to a strong spin-spin interaction as it was revealed in PANI (Iida et al. 1992, Krinichnyi et al. 2002), PATAC (Krinichnyi, Roth, and Schrödner 2002) and P3DDT (Barta et al. 1994, Cik et al. 1995, Kawai et al. 1996, Cik et al. 2002). This contribution disappears at low temperatures due to the phase transition opening an energy gap at the Fermi level (Mizoguchi and Kuroda 1997), so then the susceptibility demonstrates the Curie behavior. Figure 26 shows that the total spin susceptibility of all P3OT samples follows Eq.(A.4). As in the case of sulfonated polyaniline (Kahol et al. 1999), these results evidence that the annealing of the P3OT polymer affects an effective exchange coupling between spins which results in the change of an effective number of the Bohr magnetons per a monomer unit, however, the recrystallization neglects this effect.
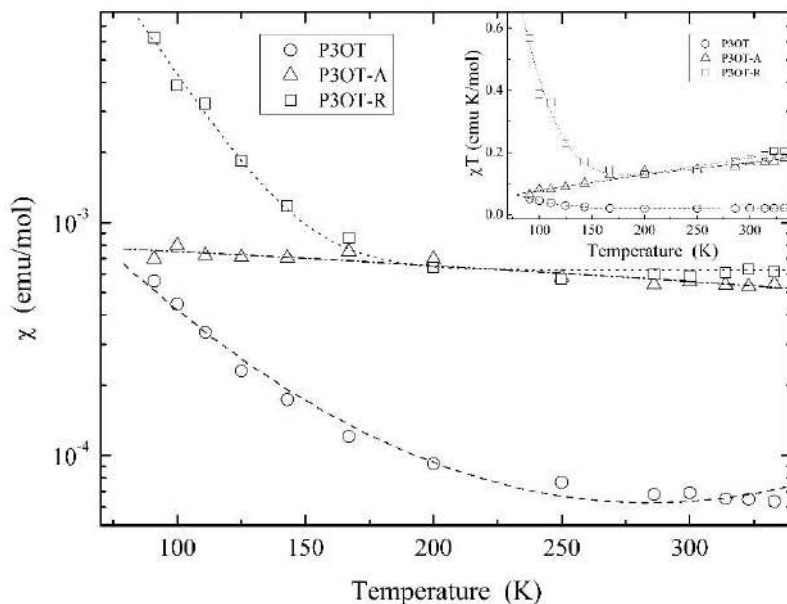
Figure 26. The $\chi(T)$ and $\chi T(T)$ (insert) dependencies of paramagnetic susceptibility of the P3OT, P3OT-A, and P3OT-R samples. The dependencies calculated from Eq.(A.4) with $\chi_P = 4.5 \times 10^{-4}$ emu/mol, $C = 0.044$ emu K/mol, $c_{af} = 0$ (dotted line), $\chi_P = 0$, $C = 4.1$ emu K/mol, $c_{af} = 52.1$ emu K/mol, and $J_{af} = 0.011$ eV (dash-dotted line), and $\chi_P = 0$, $C = 0.72$ emu K/mol, $c_{af} = 10.6$ emu K/mol, and $J_{af} = 0.0062$ eV (dashed line) are shown as well.

At the D-band EPR the samples demonstrate the superposition of more broadened convoluted Gaussian and Lorentzian lines (with the Lorentzian/Gaussian line shape ratio ca. 0.4) with the anisotropic *g*-factor (Figure 25,b) as it is typical for PC in some other conjugated polymers with heteroatoms above described. The linewidth of the spectra increases by a factor of ca. 3 at the increase of the registration frequency (Figure 27). It is seen that the linewidths of the PC in the samples depend on the polymer treatment and temperature. The treatment leads to the decrease in the averaged linewidth $\langle \Delta B_{pp} \rangle$ from 0.82 mT in P3OT down to 0.78 mT in P3OT-A and then to 0.67 mT in P3OT-R confirming the above supposition of the growth of the system crystallinity. The linewidth of the P3OT increases with the temperature increase from 90 K up to the phase transition characteristic temperature $T_c = 200$ K and then decreases at the further temperature growth. The analogous tendency demonstrates P3OT-R, however, its T_c value decreases down to ca. 170 K (Figure 27). This effect of the linewidth decrease below T_c was detected also in the study of doped polyaniline (Krinichnyi, Chemerisov, and Lebedev 1997, Krinichnyi et al. 2002) and was not registered in other conjugated polymers; it can be interpreted, e.g., as the manifestation of defrosting of molecular motion and/or acceleration of relaxation processes at low temperatures. On the other hand, the ΔB_{pp}^{x} value of P3OT-A decreases with the temperature increase of up to $T_c = 200 - 250$ K and starts to increase at $T \geq T_c$, whereas the other spectral components are broadened linearly with the temperature growth from 100 K (Figure 27). If one supposes that molecular dynamics and/or electron relaxation should stimulate activated broadening of the *i*-th line, $\Delta B_{pp}^{i} = \Delta B_{pp}^{i(0)} \exp(E_a/k_B T)$, from the slopes of these dependencies it is possible to

determine separately the parameters of electron relaxation and molecular dynamics near the principal macromolecular axes. The energies E_a^x, E_a^y, and E_a^z required for activation of molecular motion near the principal *x*-, *y*- and *z*-axes in the samples P3OT, P3OT-A, and P3OT-R were determined to be 3.6, 4.9, 4.3 meV, 7.2, 2.0, 2.1 meV, and 2.4, 1.9, 1.8 meV, respectively.
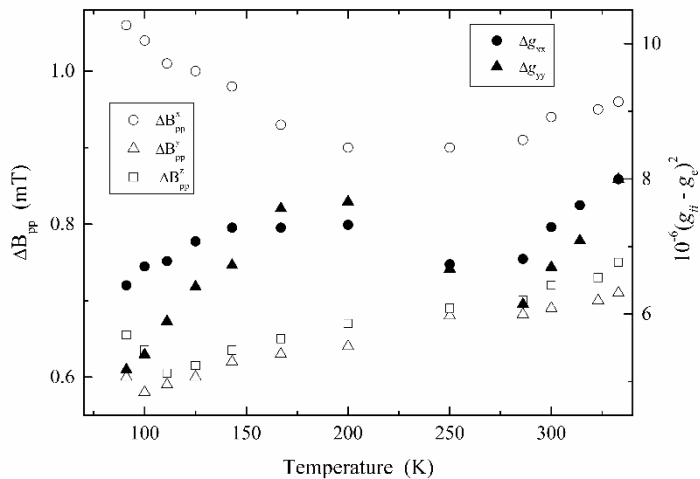
Figure 27. The D-band spectral component linewidth (*a*) and squared shifts of the g_{xx} and g_{yy} values from g_e = 2.00232 (*b*) of the P3OT as function of temperature.

From the RT spectra of P3OT the main components of its **g** tensor were also determined to be g_{xx} = 2.00409, g_{yy} = 2.00332, and g_{zz} = 2.00235. The treatment of the samples leads to the change of these parameters to g_{xx} = 2.00404, g_{yy}= 2.00315, and g_{zz} = 2.00231 for P3OT-A and to g_{xx} = 2.00402, g_{yy} = 2.00313, and g_{zz} = 2.00234 for P3OT-R. The structure of a polymer should affect the distribution of an unpaired electron in polaron changing the principal values of its PC **g**-tensor and hyperfine structure. The shift of the g_{xx} and g_{yy} values from the g_e-factor for a free electron can be compared with that calculated from Eq.(A.2) with the constant of spin-orbit interaction of the electron spin with the sulfur nuclear λ_s equal to 0.047 eV.

The effective *g*-factor of the P3AT is higher than that of most hydrocarbonic conjugated polymers, therefore one can conclude that in P3AT the unpaired electron interacts with sulfur atoms. This is typical for other sulfur-containing compounds, e.g., PTTF (Krinichnyi 2000a), PATAC (Krinichnyi, Roth, and Schrödner 2002) and benzo-trithioles (Krinichnyi et al. 1997) in which sulfur atoms are involved into the conjugation. In such organic solids an unpaired electron is localized mainly on the sulfur atom so its an effective *g*-factor is 2.014 <g_{iso}< 2.020 (Williams et al. 1992, Cameron et al. 1991, 1992, Krinichnyi et al. 1997, Bock et al. 1984). The *g*-factor of PC in P3OT is much smaller so one can expect a higher spin delocalization in the monomer units. Indeed, assuming $\Delta E_{n\pi*}\approx$ 2.6 eV as typical for sulfuric solids, then the *g*-factor components of the initial P3OT yields the decrease in $\rho_s(0)$ by a factor of 1.8 as compared with PATAC (Krinichnyi, Roth, and Schrödner 2002) and by a factor of 2.6 – 3.9 as compared with poly(tetrathiafulvalenes) (Krinichnyi 2000a). One can evaluate the lower limit of RT probability (in frequency units) for the duration of the stay of

spin at the sulfur site in the P3OT samples by the total shift of the spectral components registered at the above mentioned positions g_{ii}^{P3OT} relative to the g_{ii}^{S} value typical for the sulfuric radical to be $D_{1D}^0 \geq 3.4 \times 10^9$ rad/s.

As in the case of other organic radicals, the g_{zz} values of the P3OT samples are close to the g-factor for a free electron so they feel the change in the system properties weakly. In contrast to X-band EPR, high spectral resolution achieved at D-band EPR allows one to register separately the structure and/or dynamic changes in all spectral components. Figure 27 evidences that the g_{xx} and g_{yy} values reflect more efficiently the properties of the radical microenvironment. These values of the initial P3OT decrease with the temperature decrease from 333 down to 280 K possibly due to the transition to the more planar morphology of the polymer chains. Below 280 K, these values increase at the sample freezing down to 160 – 220 K and then also decrease at the further temperature decrease. The decrease of g_{xx} and g_{yy} values at low temperatures can be explain by a harmonic vibration of macromolecules which evokes the crystal field modulation and is characterized by the $g(T) \propto T$ dependence (Owens 1977). The temperature polymer treatment weakly affects these parameters. This fact can be interpreted by the growth of the system crystallinity due to the higher chain packing in the treated polymers. The analysis of the data presented in Figure 27 shows that the linewidth can also correlate with the spin-orbit coupling in the framework of the Elliott mechanism playing an important role in the charge transfer in organic ion-radical salts (Williams et al. 1992) and conductive polymers with pentamerous unit rings (Mizoguchi and Kuroda 1997). Indeed, $\Delta B_{pp}^x \propto \Delta g_{xx}^2$ and $\Delta B_{pp}^y \propto \Delta g_{yy}^2$ dependencies are valid for, e.g., P3OT at least at $T \leq T_c$. This means that different mechanisms can affect the individual components of the P3OT spectrum and that the scattering of charge carriers should be governed by the potential of the polymer backbone.

Figure 25,c exhibits also in-phase and $\pi/2$-out-of-phase terms of D-band EPR dispersion spectra of P3OT registered at different temperatures. It is seen that the bell-like contribution with Gaussian spin packet distributions appears in both dispersion terms. This is attributed to the adiabatically fast passage of saturated spin packets by a modulating magnetic field at this waveband EPR, as in case of PTTF (see Figure 14,d) and other conjugated polymers (Krinichnyi 2006). The intensities of the $\pi/2$-out-of-phase spectral components change with the temperature. This effect evidences the appearance of the saturation transfer over the quadrature spectrum term due to super slow macromolecular dynamics (Krinichnyi 2008b, a). The analysis of spectral u_3^i components allowed determining the correlation time τ_c^x of libration motion of the chain macromolecular segments near the principal molecular x axis in the initial and treated P3OT samples. The energy required for activation of such libration dynamics in the P3OT, P3OT-A and P3OT-R samples was also determined to be $E_a = 0.069$, 0.054 and 0.073 eV, respectively.

The linear compressibility of an initial P3OT with planar chains is strongly anisotropic, being 2.5 times higher for the direction along molecular a-axis than along the b-axis (Mardalen et al. 1998). It was proved that the low- and high-frequency modes exist in polythiophenes (Sauvajol et al. 1997). These modes differently superposed in P3OT originating "successive" macromolecular dynamics in P3OT and P3OT-A and "parallel" molecular librations in P3OT-R (Krinichnyi 2008b, a). Osterbacka et al. (Österbacka et al. 2001) have found that the interchain coupling existing in self-assembled lamellae in P3AT

drastically changes the properties of polaron excitations. So that the polaron, normally Q1D delocalized in conjugated polymers, can be delocalized in two dimensions in P3OT that results in a much reduced relaxation energy and multiple absorption bands. The upper limit for the correlation time of anisotropic molecular motion in the P3OT registered by the ST-EPR method is $\tau_c^x \leq 4.4 \times 10^{-4}$ s at 66 K.

It is evident that the polymer structure and the polymer treatment should influence on spin charge relaxation and dynamics. At $T \geq 200$ K the inequality $\omega_m T_1 < 1$ holds for polarons in all P3OT samples. The opposite inequality is fulfilled at lower temperatures when the dispersion spectrum is determined by the two last terms presented in Figure 25,c. The semilogarithmic temperature dependence of the relaxation times determined from these saturated EPR dispersion spectra terms are shown in Figure 28,a. One can conclude from these data that the polymer treatment leads to the acceleration of the PC effective relaxation possibly due to the increase of the interaction of polaron charge carriers with the lattice phonons. The relaxation times of the samples increase simultaneously at the temperature decreases from 333 down to ca. 250 K (P3OT, P3OT-R) and 150 K (P3OT-A) (Figure 28,a). The spin-spin relaxation is accelerated below this point leading to the appropriate change of the spectral component linewidth (Figure 27).

The spin-spin relaxation time of the P3OT samples determined from their X-band EPR absorption and D-band EPR dispersion spectra increases approximately by a factor of six. This means that the experimental data can rather be explained in terms of a modulation of spin relaxation by the polaron intra- and interchain motion in the polymers. In the framework of such approach, the relaxation time of the electron or proton spins in the sample should vary as $T_{1,2} \propto \omega_e^{1/2}$ (Butler, Walker, and Soos 1976, Nechtschein 1997) that increase relaxation times approximately by a factor of four. Note, that Q2D spin motion should lead to $T_{1,2} \propto \ln(\omega_e)$ dependency (Butler, Walker, and Soos 1976, Nechtschein 1997) that increase these parameters by factor of about two at the same change in spin precession frequency.

In Figure 28,b are shown the temperature dependencies of the effective dynamic parameters D_{1D} and D_{3D} calculated for PC in the initial and treated P3OT samples from the data presented in Figure 28,a with Eq.(A.25) and Eq.(A.26) at $L \approx 5$ (Devreux et al. 1987). The RT D_{3D} value obtained is about $D \approx 2.1 \times 10^{10}$ s^{-1} evaluated from the charge carrier mobility in slightly doped P3OT (Kunugi et al. 2000) and the D_{1D} value exceeds by $1 - 2$ orders of magnitude the lower limit of the spin motion D_{1D}^0. The RT anisotropy of spin dynamics D_{1D}/D_{3D} increases from 6 in P3OT up to 18 in P3OT-A and decreases down to 2 in P3OT-R. At the temperature decreases down to 200 K this value increases up to 2.5×10^3, 1.4×10^2, and 3.9×10^2, respectively, and then up to 3.8×10^8, 6.5×10^7, and 3.4×10^{10}, respectively, as the temperature decreases down to 100 K (Figure 28,b).

The $D_{1D}(T)$ dependence calculated from the ^{1}H 50 MHz spin-lattice relaxation data obtained by Masubuchi et al. (Masubuchi et al. 1999) for the initial P3OT with the respective equation and spectral density function is also presented in Figure 28,b. It is seen from the Figure that the D_{1D} value calculated from the NMR data is changed weaker with temperature. Besides, this value considerably exceeds the D_{1D} value obtained by EPR at high temperatures and is close to that determined for the low-temperature region. Such discrepancy occurs probably because NMR is not a direct method for studying electron spin dynamics in this and other conjugated polymers.
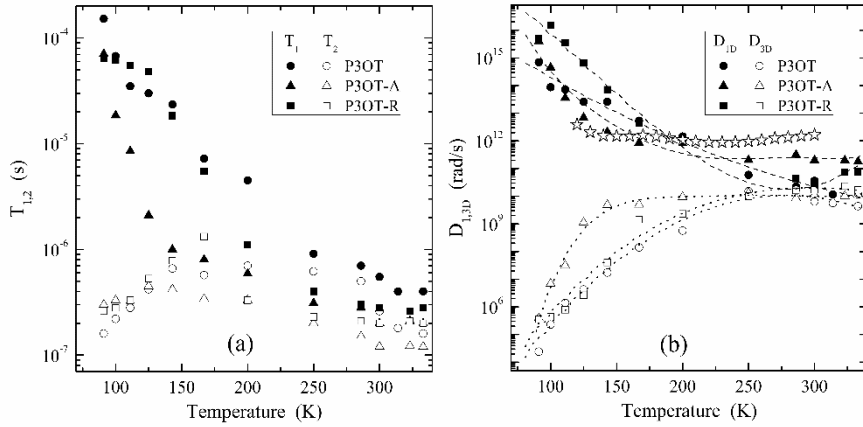
Figure 28. Temperature dependencies of the relaxation times T_1 (filled symbols), T_2 (open symbols) (*a*) and spin diffusion coefficients D_{1D} (filled symbols), D_{3D} (open symbols) (*b*) of the P3OT, P3OT-A, and P3OT-R samples. Open stars show the $D_{1D}(T)$ dependence calculated from the data obtained from ^{1}H NMR study of P3OT (Masubuchi et al. 1999). The dependencies calculated from Eq.(A.29) with $E_{ph} =$ 0.18, 0.20, 0.13 eV (dashed lines), and Eq.(A.30) with $E_a = 0.18, 0.19, 0.19$ eV (dotted lines) are shown.

The temperature dependencies calculated from Eq.(A.29) are also presented in Figure 28,b. The Figure evidences that the intramolecular spin dynamics follows well Eq.(A.29) with the energy of optical phonons of 0.13 eV for P3OT, 0.20 eV for P3OT-A, and 0.18 eV for P3OT-R samples. This value is close to the respective energy determined for PANI-ES and laser-modified PATAC (see above).

The polaron-phonon interaction seems play an important role also in the interchain charge transfer at $T \geq T_c$. However, another mechanism should prevail at lower temperatures. Figure 28,b shows that spin interchain dynamics increases with the temperature increase at the low-temperature region and then slightly decreases at $T \geq T_c$. Such dependence is typical for the systems with a strong coupling of the charge with the lattice phonons. The analogous dependence with the characteristic temperature $T_c \approx 150$ K was obtained, e.g., for *dc* conductivity of P3HT (Yamauchi et al. 1997). In this case the strong temperature dependence of the hopping conductivity is more evidently displayed in spin interchain dynamics. This interaction should lead to the narrow energy gap E_a much higher than the RT thermal energy ($k_B T \approx 0.026$ eV). The strong temperature dependence for D_{3D} at low temperatures can be due to the thermal activation of spin charge carriers from widely separated localized states in the gap to closely localized states in the tails of the polymer VB and CB. Indeed, the data obtained experimentally for the spin interchain dynamics can be approximated by Eq.(A.30) with respective E_a values. The increase of the dimensionality of the polymer system should lead to the decrease in E_a. Charge transfer through bulk of P3MT was analyzed by Parneix, et al. (Parneix and El Kadiri 1987) in terms of such approach with $E_a = 0.18$ eV. So, we can also to explain the data obtained for Q3D spin dynamics in the P3OT samples in terms of this theory. The temperature dependencies calculated from Eq.(A.30) for the P3OT samples are also shown in Figure 28,b for comparison. The activation energies required for spin interchain diffusion in the P3OT, P3OT-A, and P3OT-R samples were obtained to be $E_a = 0.18, 0.19,$ 0.19 eV, respectively. These values are close to those determined for the charge transfer in

nanomodified PATAC, PTTF-C_2H_5-C_6H_4, PANI, P3HT, and poly[N-9′-hepta-decanyl-2,7-carbazole-alt-5,5-(4′,7′-di-2-thienyl-2′,1′,3′-benzothiadiazole)]   (PCDTBT)   conjugated polymers (Krinichnyi 2016b). *DC* conductivity of P3OT is close to 10^{-4} S/m and is determined mainly by the activation hopping of a charge carrier between high-conductive crystalline domains (Chen, Wu, and Rieke 1995). Because an intrinsic conductivity of this polymer is defined by the σ_{1D} and σ_{3D} values determined from Eq.A.34), so the $\sigma_{1,3D} \gg \sigma_{dc}$ relation should hold for all the samples.

Thus, the interaction of the spin charge carrier with the heteroatom in sulfurous organic polymer semiconductors P3OT leads to the appearance of the *g*-factor anisotropy in their D-band EPR spectra. Spin relaxation and dynamics are determined by the interaction of the mobile polaron with optical phonons of the polymer lattice. Polymer modification leads to a distinct change in magnetic, relaxation and dynamics properties of the polaron and its microenvironment. The close values of the energies of spin interchain transport, dipole-dipole interaction and the optical lattice phonons indicates the correlation of charge transport and macromolecular dynamics in P3OT. These energies increase at the polymer treatment indicating the increase of its effective crystallinity. It can be concluded that the two types of charge transport mechanism can be associated with change in the lattice geometry at the characteristic (the polymer-glass transition) temperature T_c, e.g., with its thermochromic effect.

3. SPIN-ASSISTED POLARON DYNAMICS IN POLYMER:DOPANT/POLYMER:FULLERENE NANOCOMPOSITES

An unique capability of spin orientation in external magnetic field and its very weak interaction with own environment in semiconductors open an undoubted imperative to developing new spin electronic (magneto-electronic, spintronic) devices simultaneously exploiting both charge and spin of electrons in the same device and appropriate cutting-edge spectroscopic methods suitable for registration of spin polarization and its controlled manipulation (Maekawa 2006, Dediu et al. 2009). EPR spectroscopy was proved to be the most effective direct tool able to register spin excitations, study their nature, properties and manipulate in such systems (Lupton, McCamey, and Boehme 2010).

The interaction between spin charge carriers should also affect electronic properties of organic polymers with spin charge carriers. PANI-ES seems to be one of the most suitable systems for the study of spin-assisted charge transfer in organic semiconductors. Above it was demonstrated the existence in PANI-ES of polarons trapped on chains in amorphous polymer phase and polarons diffusing along and between polymer chains. Polarons diffusing along polymer chains appeared to be accessible for triplet excitations injected into the polymer bulk. Spin exchange interaction leads to collision of domestic and guest spins dramatically changing their magnetic, relaxation and electron dynamics parameters. Such effect was registered only in PANI-ES highly doped with *para*-toluenesulfuric acid (PANI:*p*TSA) (Krinichnyi, Roth, et al. 2006, Krinichnyi, Tokarev, et al. 2006). PANI:*p*TSA becomes Fermi glass with high density of states near the Fermi energy level ε_F (Kahol 2000, Wessling et al. 2000), *dc* conductivity of PANI-ES follows the Q3D Mott's VRH model (Kapil, Taunk, and Chand 2010). Other PANI-ES doped with, e.g., sulfuric acid (PANI:SA) can also be

characterized as Fermi glass but with localized electronic states at the Fermi level ε_F due to disorder. This predestined the use of both these PANI-ES as reservoir of stabilized spins. P3DDT:PC$_{61}$BM was used as a second spin reservoir in comparative experiments (Krinichnyi, Yudanova, and Wessling 2013, Yudanova, Bogatyrenko, and Krinichnyi 2016). EPR study of PANI-ES/P3DDT:PC$_{61}$BM composites and their ingredients is expected to provide a good framework for understanding the underlying nature of exchange interactions between different spins in multispin system. Below are presented the first results of the LEPR study of main magnetic resonance parameters of polarons stabilized in highly doped PANI:pTSA, polarons and fullerene radical anions photo induced in the P3DDT:PC$_{61}$BM composite under background illumination by white light, as well as these charge carriers stabilized in the PANI:pTSA/P3DDT:PC$_{61}$BM composite in a wide temperature range. To emphasize these results, the analogous investigation with PANI:SA and PANI:SA/P3DDT:PC$_{61}$BM composite was also made.

To analyze the nature of all paramagnetic centers in both the PANI:SA/P3DDT:PC$_{61}$BM and PANI:pTSA/P3DDT:PC$_{61}$BM composites, first related study of spin properties of their ingredients was done (Krinichnyi, Yudanova, and Wessling 2013, Krinichnyi 2014b, a, 2016a).

Initial PANI:SA and PANI:pTSA samples exhibit single X-band EPR spectra presented in Figure 29,a and Figure 29,b attributed to polarons $P_1^{+\bullet}$ with effective g-factor equal to 2.0031 and 2.0028 stabilized in backbone of PANI-SA and PANI:pTSA, respectively. These values remain almost unchanged within all temperature range used during long time that is characteristic of paramagnetic centers in crystalline high-conductive solids (Krinichnyi 1996, 2000b, a). As-prepared P3DDT:PC$_{61}$BM sample does not demonstrate any EPR spectrum without light irradiation (Figure 29,c). When illuminated by visible light, positively charged polaron is formed on a polymer backbone due to electron transfer to methanofullerene (see Figure 3). Thus, two partly overlapping LEPR lines are observed at low temperatures (Figure 29,c). As in case of other polymer nanocomposites (Krinichnyi et al. 2007, Krinichnyi, Yudanova, and Spitsina 2010, Krinichnyi and Balakai 2010, Krinichnyi 2016a), this spectrum was attributed to radical pairs of positively charged diffusing polarons $P_2^{\bullet+}$ with isotropic (effective) $g_{iso} = 2.0018$ and negatively charged radical anions $C_{61}^{-\bullet}$ with effective $g_{iso} = 1.9997$ rotating about the main axis. These values are close to those obtained for spin charge carriers photo induced in other polymer/fullerene BHJ (Janssen, Moses, and Sariciftci 1994, Marumoto et al. 2003, Krinichnyi 2016a). The EPR line shape due to dipole or hyperfine broadening is normally Gaussian. For spin Q3D motion in metal-like crystallites of PANI-ES or exchange of different spin packets, the line shape becomes close to Lorentzian shape, corresponding to an exponential decay of transverse magnetization. The effective LEPR spectrum presented in Figure 29,c exhibits mainly a Lorentzian doublet of mobile radical pairs $P_2^{+\bullet} - mC_{61}^{-\bullet}$, shown in Figure 29,d as a sum of equally contributed mobile polarons $P_2^{+\bullet}$ and methanofullerene radical anions $mC_{61}^{-\bullet}$ as well as a Gaussian contribution of the former charge carriers pinned by deep traps appeared in a polymer matrix under its illumination (shown in Figure 2,e). Both mobile charge carriers recombine with the probability increasing with temperature, and their effective spectrum shown in Figure 29,d becomes too weak to be registered at $T \geq 200$ K at a reasonable signal-to-noise ratio. Captured polarons $P_2^{+\bullet}$ are characterized by higher stability, and their spectrum can be observed for several hours even at

high temperatures. Nevertheless, these carriers indirectly participate in collective charge transfer through BHJ.

It is evident that LEPR spectra of both PANI:SA/P3DDT:PC$_{61}$BM and PANI:pTSA/P3DDT:PC$_{61}$BM composites presented in Figure 29,f and Figure 29,g, respectively, can be considered as a sum of P3DDT:PC$_{61}$BM and appropriate PANI-ES contributions. As an illumination is turned off, the spectra originated from the polarons P$_1^{+\bullet}$ stabilized in PANI-ES (shown in Figure 29,a and Figure 29,b) and polarons P$_2^{+\bullet}$ pinned in P3DDT:PC$_{61}$BM (shown in Figure 2,e) can only be registered (see Figure 29,f and Figure 29,g). In order to study charge-separated states and spin-spin interactions in these systems more precisely, their spectra should be tentatively deconvoluted, as it was successfully done for analogous spin-modified systems (Takeda et al. 1998, Yanilkin et al. 2007, Poluektov et al. 2010, Krinichnyi 2016a). This allowed to obtain separately magnetic resonance parameters of all paramagnetic centers stabilizing in initial polymers and appropriate composites and analyze their interaction in BHJ.
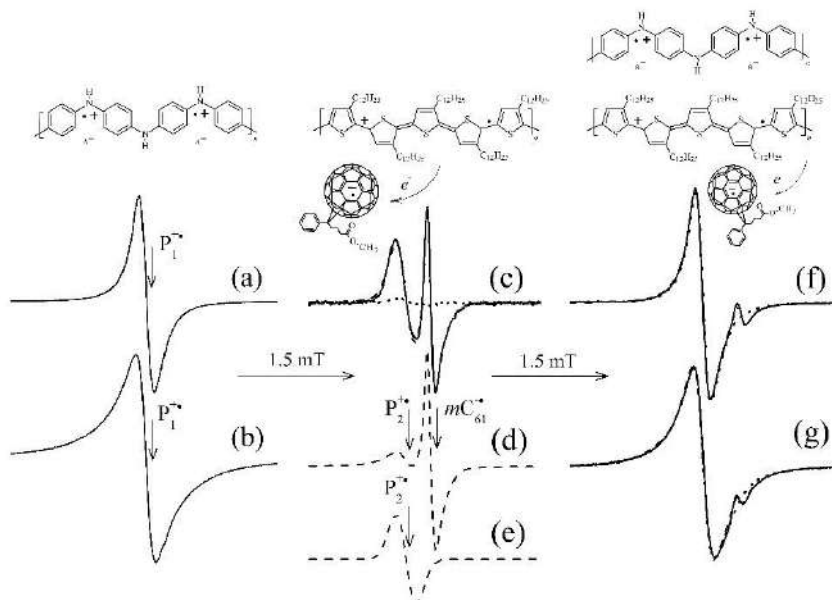
Figure 29. X-Band EPR spectra of polarons P$_1^{\bullet+}$ stabilized in fully doped with sulfuric acid, PANI:SA (*a*) and *para*-toluenesulfuric acid, PANI:pTSA (*b*), P3DDT:PC$_{61}$BM BHJ illuminated by achromatic white light with color temperature 5500 K at $T = 77$ K (*c*) with contributions due to mobile polaron-methanofullerene radical quasi-pairs P$_2^{+\bullet}$— mC$_{61}^{-\bullet}$ (*d*) and localized polarons P$_2^{+\bullet}$ pinned by deep traps (*e*) as well as PANI:SA/P3DDT:PC$_{61}$BM (*f*) and PANI:pTSA/P3DDT:PC$_{61}$BM (*g*) composites illuminated by achromatic white light with color temperature 5500 K at $T = 77$ K. Dashed line show sum EPR spectrum (*c*) and deconvoluted its contributions (*d*, *e*) calculated using $\Delta B_{pp}^{P} = 0.27$ mT, ΔB_{pp}^{F} = 0.12 mT, and [P$_2^{+\bullet}$]/[mC$_{61}^{-\bullet}$] = 2.0. In (*c*, *f*, *g*), dotted lines exhibit "dark" EPR spectra of PC stabilized in appropriate composites, whereas the spectra calculated at their illumination by white light at 77 K are shown by dashed lines. The positions of paramagnetic centers are shown as well. Structure of PANI-ES fully doped with sulfuric (A$^-$ ≡ SA, *a*) and (A$^-$ ≡ pTSA, *b*) acids, regioregular P3DDT (*c*), and PC$_{61}$BM (*d*). The appearance of positive charged polaron in the P3DDT backbone due to photo initiated charge separation and transfer to the fullerene globe is shown schematically.
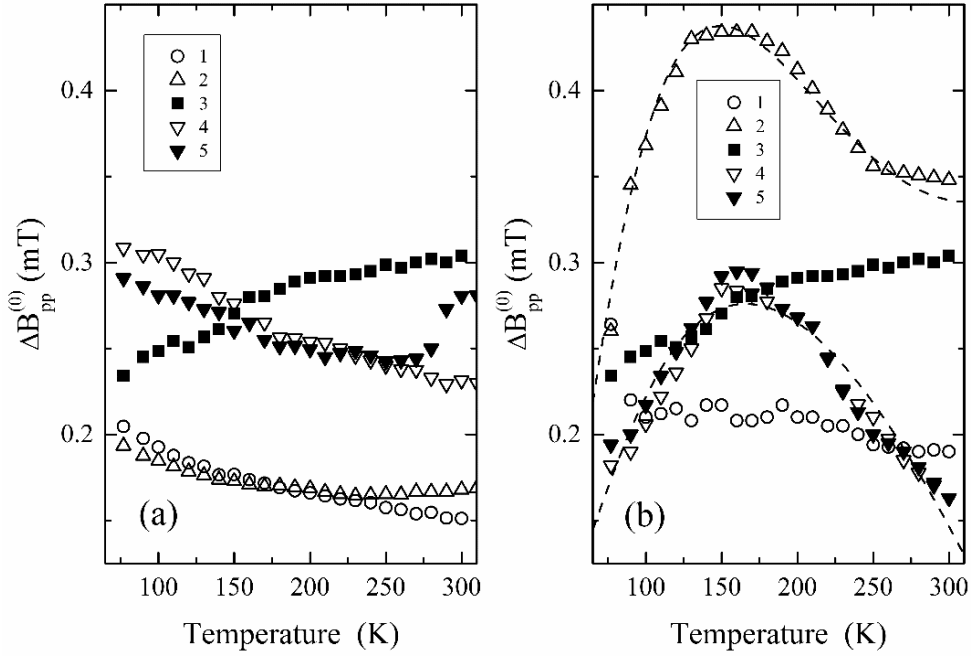
Figure 30. Temperature dependence of peak-to-peak linewidth $\Delta B_{pp}^{(0)}$ determined for domestic polarons $P_1^{\bullet+}$ stabilized in the initial PANI-ES backbones (*1*), PANI-ES/P3DDT:PC$_{61}$BM composites (*2*), polarons $P_2^{+\bullet}$ background photo initiated by white light in the P3DDT:PC$_{61}$BM BHJ (*3*), as well as polarons $P_2^{+\bullet}$ stabilized in the darkened (*4*) and irradiated by white light (*5*) PANI-ES/P3DDT:PC$_{61}$BM composites with A$^-$ ≡ SA (*a*) and A$^-$ ≡ *p*TSA (*b*) counter-ions. The upper (0) symbol in $\Delta B_{pp}^{(0)}$ implies this parameter to be measured far from the spectrum microwave saturation. Dashed lines show the dependences calculated from Eq.(A.19) with $\omega_{hop}^0 = 1.2 \times 10^9$ s^{-1}, $E_r = 0.006$ eV (above line), $\omega_{hop}^0 = 1.3 \times 10^9$ s^{-1}, $E_r = 0.12$ eV (below line), $J_{ex} = 0.110$ eV, and $n_g = 1.2 \times 10^{-4}$.

Figure 30,a shows temperature dependences of effective absorption peak-to-peak linewidth ΔB_{pp} of polarons $P_1^{+\bullet}$ stabilized in the PANI:SA, $P_2^{+\bullet}$ photo initiated in P3DDT:PC$_{61}$BM BHJ, and these values obtained for darkened and illuminated PANI:SA/P3DDT:PC$_{61}$BM composite. It is seen that the EPR linewidth for both polarons stabilized in these systems depends on structure of a polymer matrix. Indeed, the heating of the initial PANI:SA samples is accompanied by a monotonic decrease in ΔB_{pp} of polarons $P_1^{+\bullet}$ stabilized on their chains. However, this parameter for polarons $P_2^{+\bullet}$ photo initiated in the P3DDT:PC$_{61}$BM BHJ evidences an opposite temperature dependence as compared with that for polarons $P_1^{+\bullet}$ (Figure 30). This effect can be explained by different interaction of these polarons with appropriate polymer lattice (see below). The formation of the PANI:SA/P3DDT:PC$_{61}$BM composite does not noticeably changes the linewidth for paramagnetic centers $P_1^{+\bullet}$. However, this originates the change in the temperature dependence of $P_2^{+\bullet}$ charge carriers photo initiated in the P3DDT matrix (see Figure 30,a).

Spin properties of both polaronic reservoirs in the PANI-ES/P3DDT:PC$_{61}$BM composites are strongly governed by the conformation of PANI-ES chains which determines its main electronic properties (Wessling 2010). As the PANI:SA matrix is replaced by the PANI:pTSA one, both polarons $P_1^{+\bullet}$ and $P_2^{+\bullet}$ start to demonstrate extreme temperature dependent linewidths characterized by appropriate critical point $T_{ex} \approx 150$ K. A similar effect was observed in the EPR study of exchange interaction of polarons with guest oxygen biradicals $^{\bullet}O - O^{\bullet}$ in PANI-ES highly doped with hydrochloric acid (Houze and Nechtschein 1996) and pTSA (Krinichnyi, Roth, et al. 2006, Krinichnyi, Tokarev, et al. 2006, Krinichnyi 2014a). This effect was identified as exchange interaction in quasi-pairs formed by guest spins with domestic mobile polarons hopping between sites of polymer chain with rate ω_{hop} across energy barrier E_r. Thus, the data, presented in Figure 30,b can perfectly be described in terms of the spin-spin exchange interaction of polarons $P_1^{+\bullet}$ and $P_2^{+\bullet}$ hopping in the nearly located solitary polymer chains. The collision of both type spins should additionally broaden the absorption term of EPR line by the value described by Eq.(A.19). In this case the extreme temperature dependence should indicate strong and weak spin interaction limits at $T \leq T_c$ and $T \geq T_c$, respectively ($T_c = 150 - 160$ K). In particular, it is an evidence of a stronger interaction of polarons with own microenvironment in P3DDT as compared with PANI-ES.

Assuming activation character of polaron motion in both polymer matrices and $n_P = 1.2 \times 10^{-4}$ obtained for P3DDT:PC$_{61}$BM BHJ (Krinichnyi, Yudanova, and Spitsina 2010), the linewidth of the polarons $P_1^{+\bullet}$ and $P_2^{+\bullet}$ can be fitted by Eq.(A.19) with $E_r = 0.006$ and 0.012 eV, respectively, at $J_{ex} = 0.110$ eV (see Figure 30,b). J_{ex} is less than that (0.360 eV) determined for air-filled PANI:pTSA (Krinichnyi, Roth, et al. 2006, Krinichnyi, Tokarev, et al. 2006) due probably to less number of guest radical and higher interpolaron distance.

Figure 31,a and Figure 31,b show the temperature dependence of spin susceptibility χ with contributions due to polarons $P_1^{+\bullet}$, $P_2^{+\bullet}$ and methanofullerene radical anions $mC_{61}^{-\bullet}$ forming spin pairs in the P3DDT:PC$_{61}$BM BHJ stabilized in the darkened and background illuminated PANI:SA/P3DDT:PC$_{61}$BM and PANI:pTSA/P3DDT:PC$_{61}$BM composites. The dependences obtained are important to reveal mobile or localized character of spins and their possible interaction. Indeed, for non-interacting and localized (or slightly delocalized) electrons in disordered phase, susceptibility normally follows the Curie law $\chi_C \propto 1/T$, whereas polarons delocalized in the conduction band of ordered crystallites cause temperature-independent Pauli behavior, χ_P. However, such simple picture has been questioned especially for polyaniline and other conducting polymers because most of the spins are localized (Mizoguchi and Kuroda 1997, Raghunathan et al. 1998). Disorder localizes electron spins and conducting polymer systems exhibit significant disorder. Therefore, we have to interpret the results obtained for the composites in terms of the model of exchange of $N_s/2$ coupled spin pairs with an uniform distribution originating the last term in Eq.(A.4). It is seen that the curves calculated from Eq.(A.4) with C, a_d, and J values determined for polarons carrying a charge in the initial PANI-ES and respective PANI-ES/P3DDT:PC$_{61}$BM composites (Krinichnyi, Yudanova, and Wessling 2013) provide excellent fits to all the experimental data sets within all temperature range used. Spin susceptibility obtained for $P_1^{+\bullet}$ is close to that obtained for PANI highly doped by sulfuric (Kahol 2000) and hydrochloric (Wang, Ray, et al. 1991) acids. The latter parameter is normally a function of distance. When polymer chains vibrate, J for polarons diffusing along neighboring chains would oscillate and should be

described by a stochastic process (Adrain and Monchick 1979). However, such effect appears at low temperatures, when $k_B T \ll J$. Thus, it can be neglected within all temperature range used. Nevertheless, this constant increases as polarons $P_1^{+\bullet}$ start to interact with polarons $P_2^{+\bullet}$ and, on the side, SA counter ions are replaced by pTSA ones (Krinichnyi, Yudanova, and Wessling 2013). This is additional evidence of strong interaction of polarons stabilized in both PANI-ES and P3DDT matrices. When the Fermi energy ε_F is close to the mobility edge, the temperature dependence of spin susceptibility gradually changes from Curie-law behavior $\chi_C \propto 1/T$ to temperature-independent Pauli-type behavior with increasing temperature. Corresponding density of states $n(\varepsilon_F)$ for both spin directions per monomer unit at ε_F can be determined from the analysis of the $\chi(T)T$ dependence for all polarons stabilized in both polymers (see inserts in Figure 31). It is seen that the pTSA-treated system is characterized by higher $n(\varepsilon_F)$ as compared with PANI:SA. This can be explained by the difference in their above mentioned metallic properties and also by on-site electron-electron interaction (Ginder et al. 1987).
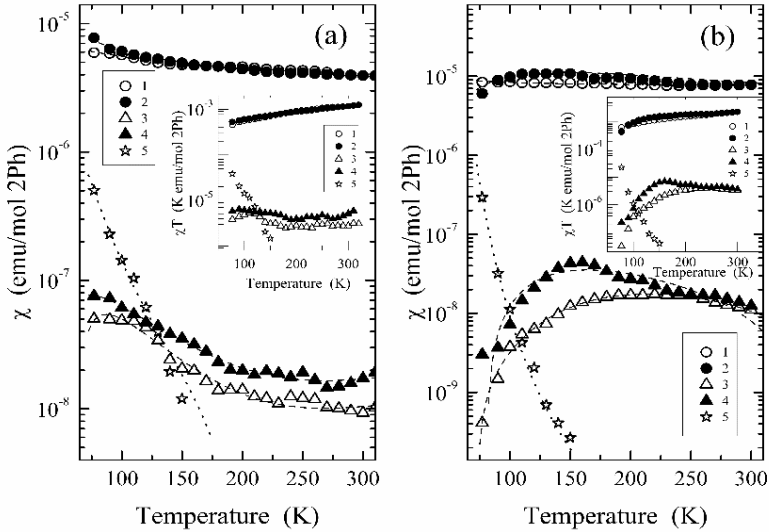
Figure 31. Temperature dependences of spin susceptibility χ and χT product (inserts) obtained for domestic polarons $P_1^{\bullet+}$ stabilized in the initial PANI-ES network (*1*) and respective PANI-ES/P3DDT:PC$_{61}$BM composite (*2*), polarons $P_2^{+\bullet}$ stabilized in the darkened (*3*) and illuminated by white light (*4*) PANI-ES/P3DDT/PCBM composites, as well as methanofullerene radical anions mC$_{61}^{-\bullet}$ (*5*) photo initiated in these composites with SA (*a*) and pTSA (*b*) counter-ions. Dashed lines show the dependences calculated from last term of Eq.(A.4) with respective C, a_d, and J constants. The dotted lines show the dependences calculated from Eq.(A.12) with $E_r = 0.024$ (*a*) and 0.050 (*b*) eV.

Spin susceptibility obtained for methanofullerene radical anions mC$_{61}^{-\bullet}$ in both composites demonstrates sharper temperature dependence (Figure 31). This can be explained by fast recombination of the polaron-methanofullerene radical pairs $P_2^{+\bullet}$—mC$_{61}^{-\bullet}$ whom spectrum is shown in Figure. 29,d. During background illumination of the P3DDT:PC$_{61}$BM BHJ, two processes are realized simultaneously, namely, photo initiation and recombination of spin pairs. As a result, we detected only net (effective) spin concentration. Therefore,

effective paramagnetic susceptibility of both charge carriers photo initiated in P3DDT:PC$_{61}$BM BHJ should inversely depend on the probability of their recombination. Such process is also governed by multi-stage activation Q1D polaron hopping between polymer units (Yan et al. 2000). Positive charge on a polaron is not required to be recombined with the first negatively charged methanofullerene radical anion. Activation traveling of a polaron near such a center localized near a polymer chain should interact with its unpaired electron with the above probability p_f expressed by Eq.(A.11). In this case, effective spin susceptibility of such interacting spin sub-pairs can finally be described by Eq.(A.12). The dependences calculated from Eq.(A.12) with $E_r = 0.024$ and 0.050 eV are also presented in Figure 31. The latter value is higher than $E_r = 0.012$ eV obtained from Eq.(A.19) for polaron diffusion in the respective system. It can probably be explained by more complex exchange interaction of methanofullerene radical anion with polarons in both the PANI:*p*TSA and P3DDT backbones. Equation (A.12) fits well the experimental data presented in Figure 31. Therefore, the decay of long-lived charge carriers originated from initial spin pairs photo induced in the PANI-ES/P3DDT:PC$_{61}$BM composites can successfully be described in terms of the above model in which the low-temperature recombination rate is strongly governed by temperature and the width of energy distribution of trap sites.

It is seen from Figure 31 that spin susceptibility of polarons $P_1^{+\bullet}$ stabilized in both initial PANI-ES samples is characterized by weak temperature dependence without any anomaly. This also holds for polarons $P_2^{+\bullet}$ photo initiated in the PANI:SA/P3DDT:PC$_{61}$BM composite. The shape of $\chi(T)$ changes dramatically as SA counter ions are replaced by *p*TSA ones. Such a replacement provokes extremal χ vs. T dependence obtained for polarons $P_1^{+\bullet}$ and $P_2^{+\bullet}$ (see Figure 31,b). This is evidence of the above mentioned exchange interaction between these polarons formed on neighboring PANI and P3DDT chains. Such interaction increases the overlapping of their wave functions (which, however, slightly decreases at further light flashing) and the energy barrier which overcomes the polaron crossing a BHJ. This affects the polaron intrachain mobility and, therefore, probability of its recombination with fullerene anion. However, the character of the $mC_{61}^{-\bullet}$ quasi-rotation changes weakly under such a replacement (see Figure 31).

The analysis of electron spin relaxation of charge carriers can expand the information about spin localization, matrix dimensionality and spin-assisted electronic processes carrying out in the polymer systems. The EPR linewidth is determined mainly by spin-spin relaxation time. Spin-lattice relaxation also shortens the lifetime of a spin state and broadens the line. So, the effective linewidth can be expressed by Eq.(A.16) taking into account all contributions due to the structural, conformational and electronic properties of polarons' microenvironment. So, it would be important to analyze also how spin exchange affect spin-lattice relaxation. The interaction of polarons $P_1^{+\bullet}$ stabilized in the PANI:SA matrix was appeared to be depending weakly on the presence of guest spins. Their dominantly contribute in an effective spin susceptibility of the composites under study. So, a spin-lattice relaxation of these charge carriers in the PANI:*p*TSA and PANI:*p*TSA/P3DDT:PC$_{61}$BM BHJ can be analyzed with more degree of certainty.

Figure 32 exhibits temperature dependencies of both the T_1 and T_2 values of polarons $P_1^{+\bullet}$ stabilized in shadowed PANI:*p*TSA and PANI:*p*TSA/P3DDT:PC$_{61}$BM composites. Spin-spin relaxation was shown above to be governed by the spin-spin exchange interaction. RT spin-

lattice relaxation time of the samples was measured to be 0.45×10^{-7} and 0.33×10^{-7} s, respectively. These values are in good agreement with $T_1 = 0.98 \times 10^{-7}$ s obtained by Wang at all. (Wang et al. 1992) for polyaniline highly doped by hydrochloric acid. It is seen, that spin-lattice relaxation of $P_1^{+\bullet}$ stabilized in the initial polymer changes weakly as the temperature increases up to ~180 K that is typical for organic ordered systems. This process accelerating suddenly near $T \sim 210$ K possibly to a phase transition and then plateaus at higher temperatures. The latter value differs from T_c mentioned above because they characterize different processes. As $P_1^{+\bullet}$ start to interact with other paramagnetic centers in the PANI:pTSA/P3DDT:PC$_{61}$BM composite, their spin-lattice relaxation strongly accelerates and becomes more temperature-dependent (Figure 32). It is once more evidence of the exchange between polarons stabilized in neighboring polymer chains. Figure 32 demonstrates then T_1 tends to T_2 at high temperatures. This is typical for organic systems of lowed dimensionality and can be explained by the defrosting of macromolecular dynamics.
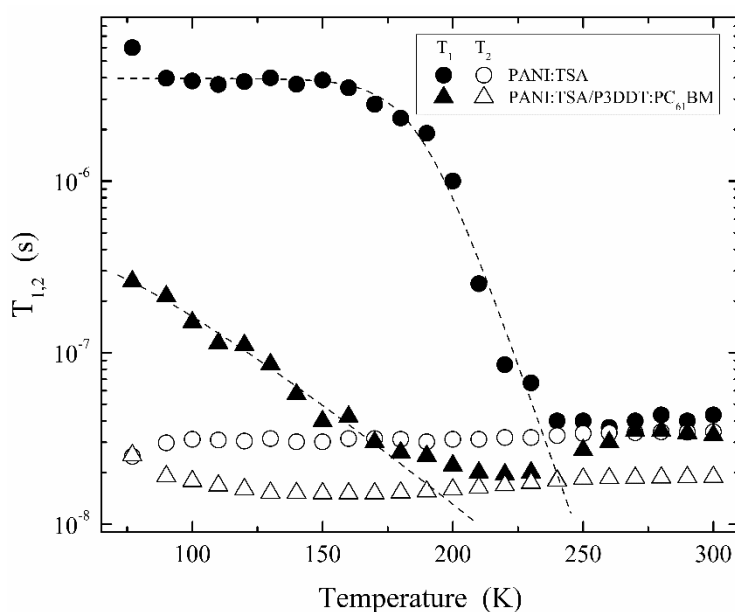
Figure 32. Temperature dependence of spin-lattice, T_1, and spin-spin, T_2, relaxation times determined for polarons $P_1^{+\bullet}$ stabilized in the PANI:pTSA backbone (*1*) and respective PANI:pTSA/P3DDT:PC$_{61}$BM composite (*2*) without light illumination.

So, light excitation of P3DDT:PC$_{61}$BM BHJ in the PANI-ES/P3DDT:PC$_{61}$BM composites leads to charge separation and transfer from a P3DDT chain to a methanofullerene molecule. This is accompanied by the excitation of two paramagnetic centers with clearly resolved LEPR spectra, namely, the positively charged polaron $P_2^{+\bullet}$ on the polymer backbone and the negatively charged radical anion $mC_{61}^{-\bullet}$ located between polymer chains. Both radicals are spatially separated due to fast Q1D diffusion of the former, so that they become non-interacting. After the forming and separation, spin charge carriers tend to recombine in polymer backbone. This process is governed by structure and

morphology of polymer matrix and anion radical inserted. Polarons $P_2^{+\bullet}$ moving in P3DDT solitary chains interact with $P_1^{+\bullet}$ stabilized on neighboring PANI-ES chains due to overlapping of their wave functions. Such interaction is governed mainly by nanomorphology of PANI-ES subdomains and defines insulating and conducting forms of PANI:SA and PANI:pTSA, respectively. Spin exchange and transverse relaxation of polarons is governed by Q1D activation hopping $P_2^{+\bullet}$ along P3DDT chains and strongly increase as PANI:SA polymer is replaced by PANI:pTSA one in the triple composite. Spin-lattice relaxation of polarons stabilized in PANI:pTSA is also accelerated by their exchange interaction with guest spin ensemble. Paramagnetic susceptibility of these polarons is realized according the model of exchange coupled spin pairs differently distributed in appropriate polymer matrices. This deepens overlapping of wave functions of these charge carriers and leads to the increase in the energy barrier which overcomes the polaron under its crossing through a BHJ. It is evident that separate EPR investigation of spin properties of domestic and photo excited paramagnetic centers in the polymer:dopant/polymer:fullerene composite and its ingredients may give a possibility to control its texture and other structural properties over the entire range of temperatures studied. The data obtained for such model systems can contribute to open new horizon in creation of flexible and scalable organic molecular devices with spin-assisted electronic properties. The results described suggest an important role played by interchain coupling of different spin charge carriers on a handling of charge transfer in BHJ of PANI-ES/P3DDT:PC$_{61}$BM composite. Photo initiation of additional spins allows making such handling more delicate that is a critical strategy in creating systems with spin-assisted charge transfer. The correlations established between dynamics, electronic and structural parameters of these systems can be used for controllable synthesis of various organic spintronic devices with optimal properties. Since coherent spin dynamics in organic semiconductors is anisotropic, our strategy seems to make it possible obtaining complex correlations of anisotropic electron transport and spin dynamics for the further design of progressive molecular electronics. Electronic properties of such devices seem to be improved by the use of more ordered composites. The use, for example, of PCDTBT modified by C$_{70}$-based methanofullerene instead of the P3DDT:PC$_{60}$BM system described should facilitate the excitation to reach the polymer:fullerene interface for charge separation before it becomes spatially self-localized and bound within an exciton (Moon, Jo, and Heeger 2012). Therefore, the main properties of an exciton are irrelevant to ultrafast charge transfer and do not limit effective charge transfer in such composite.

It was shown that charge transfer in the PCDTBT:PC$_{61}$BM composite depends not only on the polymer structure and morphology but also on the number and nature of guest spin ensemble. In order to obtain all parameters of such system in details, the main magnetic resonance and dynamics parameters of PC in its ingredients should be first studied. Figure 33,a shows X-band EPR dark spectrum of the PANI:pTSA measured at $T = 77$ K. This spectrum consists of two components contributed by polarons $P_{11}^{+\bullet}$ and $P_{12}^{+\bullet}$ stabilized in different phases of polymer backbone. Linewidth and concentration of these PC differ by three and eight times, respectively. X-band LESR sum spectrum and its contributions due to polarons pinned by deep traps $P_2^{+\bullet}$ and mobile polaron-methanofullerene radical quasi-pairs $P_2^{+\bullet}$— mC$_{61}^{-\bullet}$ photo initiated by white light with color temperature 5500 K in the PCDTBT:PC$_{61}$BM composite are shown in the same Figure. Sum LEPR spectrum and the

contributions of these PC photo initiated in the PANI:*p*TSA/PCDTBT:PC$_{61}$BM composite are depicted in Figure 33,c. It should be noted some conclusions from the analysis of the data presented. First of them is the increase of relative number of polarons $P_{12}^{+\bullet}$ stabilized in crystalline, more ordered PANI phase of such multispin composite. An interaction of mobile fullerene anion radicals with other spin ensembles decreases in this complex system. These effects can be due to the increase in exchange interaction between all spin ensembles stabilized and photo initiated in the polymer composite. They can be used for the handling of charge transport in polymer composites by using of spin interactions. Electronic properties of multispin composite are also governed by the energy of initiated photons $h\nu_{ph}$.
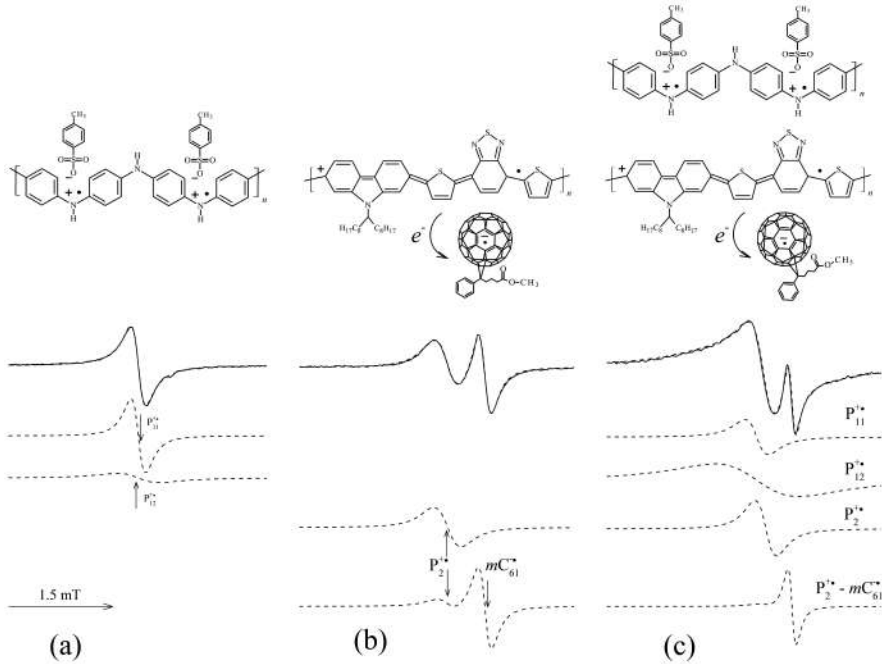
Figure 33. (*a*) X-Band EPR spectra of polarons $P_{p1}^{+\bullet}$ and $P_{p2}^{+\bullet}$ stabilized in fully doped with *para*-toluenesulfuric acid, PANI:*p*TSA. Dashed lines show the sum spectrum and both its contributions calculated with $\Delta B_{pp}^{p1} = 0.21$ mT, $\Delta B_{pp}^{p2} = 0.61$ mT, and $[P_{p1}^{+\bullet}]/[P_{p2}^{+\bullet}] = 1{:}8.2$. (*b*) X-band LESR spectrum of PCDTBT:PC$_{61}$BM BHJ illuminated by white light with color temperature 5500 K. Dashed lines show the sum spectrum and its contributions due to polaronspinned by deep traps $P_{p2}^{+\bullet}$ and mobile polaron-methanofullerene radical quasi-pairs $P_{p2}^{+\bullet}$ — $mC_{61}^{-\bullet}$ calculated with $\Delta B_{pp}^{P} = 0.21$ mT, $\Delta B_{pp}^{F} = 0.13$ mT, $[P_{p2}^{+\bullet}]/[mC_{61}^{-\bullet}] = 1.1{:}1.0$, and respective *g*-factors presented in Table 1. (*c*) X-band LESR spectrum of PANI:*p*TSA/PCDTBT:PC$_{61}$BM multispin composite illuminated by achromatic white light with color temperature 5500 K at $T = 77$ K. Dashed lines show the sum spectrum and it's the above contributions with $\Delta B_{pp}^{p1} = 0.33$ mT, $\Delta B_{pp}^{p2} = 1.22$ mT, $\Delta B_{pp}^{P} = 0.28$ mT, $\Delta B_{pp}^{F} = 0.12$ mT, and $[P_{p1}^{+\bullet}]{:}[P_{p2}^{+\bullet}]{:}[P_{p2}^{+\bullet}]{:}[mC_{61}^{-\bullet}] = 51.4{:}8556{:}5.4{:}1.0$, and respective *g*-factors presented in Table 1. The positions of paramagnetic centers are shown as well. Structures of the PANI:*p*TSA (*a*), PCDTBT:PC$_{61}$BM BHJ (*b*), as well as multispin composite PANI:*p*TSA/PCDTBT:PC$_{61}$BM (*c*) are shown schematically. The formation of positive charged polaron in the PCDTBT backbone due to photoinitiated charge separation and transfer to the fullerene globe is also shown schematically (*b*,*c*).

Figure 34 demonstrates the dependence of the main properties of polaronic charge carriers in the PANI:pTSA/PCDTBT:PC$_{61}$BM composite on the photon energy. One can to note non-linear dependence of the number of mobile and pinned polarons photoinitiated in the PCDTBT:PC$_{61}$BM BHJ on $h\nu_{ph}$. This parameter of both charge carriers demonstrates dependences with explicit extremes lying near 1.8 and 2.7 eV. The former value lies near the PCDTBT bandgap, $2\Delta = 1.87$ eV (Park et al. 2009, Kim et al. 2014). Such a peculiarity can probably be as result of specific morphology and band structure of the samples with inhomogeneously distributed spin traps. It is quite clear that the higher concentration ratio $[P_{mob}^{+\bullet}]/[P_{loc}^{+\bullet}]$, the better efficiency of energy conversion should be expected for respective system. This ratio weakly depends on the light photon energy. Once PANI:pTSA is introduced into the composite, this ratio becomes more sensitive to the photon energy with extremum at $h\nu_{ph} \approx 1.8$ eV. Besides, the insert of the guest spin ensemble into the initial composite increases the selectivity of its polarons to the photon energy. This can be also used in novel elements of polymer electronics for spin-assisted energy conversion.

Figure 34 demonstrates how polaron dynamics in both composites is governed by photon energy and changes due to spin-spin interaction. Both the constants of spin intrachain and interchain diffusion in the PCDTBT:PC$_{61}$BM composite are shown in Figure 34,c as function of $h\nu_{ph}$. These values as well as the anisotropy of spin dynamics (D_{1D}/D_{3D}) demonstrate weak dependence on the photon energy. Dynamics of all spin packets becomes sensitive to the photon energy in the PANI:pTSA/PCDTBT:PC$_{61}$BM BHJ (Figure 34,d). It is seen that all the constants of spin diffusion change extremely with characteristic energy $h\nu_{ph} \approx 1.8 - 2.0$ eV. The system ordering or dimensionality proportional to the ratio D_{3D}/D_{1D} changes extremely in this point as well. Such effect can be used for constructing of molecular device with spin-assisted charge transport properties. It should be noted that the main change in spin concentration and dynamics occurs at $h\nu_{ph} \approx 1.8$ eV. According the Eq.(A.34), the effective charge transport is determined by the product of the number of charge carriers by their mobility. Therefore, the photons with such energy should mainly influence spin-controlled charge transport in the multispin composite described.

So, the results described show that the main part of these carriers transfers the charge through PCDTBT:PC$_{61}$BM BHJ, whereas some quantity of polarons is captured by deep spin traps reversibly initiated in polymer backbone. The spatial distribution, number, and energy depth of such traps depend on a structure, morphology of polymer matrix as well as on the energy of initiating photons. Magnetic resonance, relaxation and dynamics parameters of mobile and fixed charge carriers are governed by their exchange interaction and, therefore, all the process carrying out in the copolymer composites become spin-assisted. Besides, these parameters were shown to be governed by the number and energy of initiating photons. Concentration of both charge carriers in the systems studied shows extreme dependence on the photon energy with explicit extremes around 1.8 and 2.8 eV. Such a peculiarity can appears as a result of specific morphology and band structure of the composite matrix with spin traps inhomogeneously distributed in its bulk. Dynamics of polarons photoinitiated in the PCDTBT:PC$_{61}$BM composite weakly depends on the photon energy. At the inserting of guest spin ensemble into the PCDTBT:PC$_{61}$BM composite, dynamics parameters become stronger dependent on the photon energy demonstrating extremes around 1.8 eV. The sensitivity of polaron properties to the energy of photons can be used for creation of perspective molecular electronic elements with spin-light-assisted magnetic and electronic characteristics. The

methodology described can be used also for the study of electronic properties of other organic multispin polymer composites.
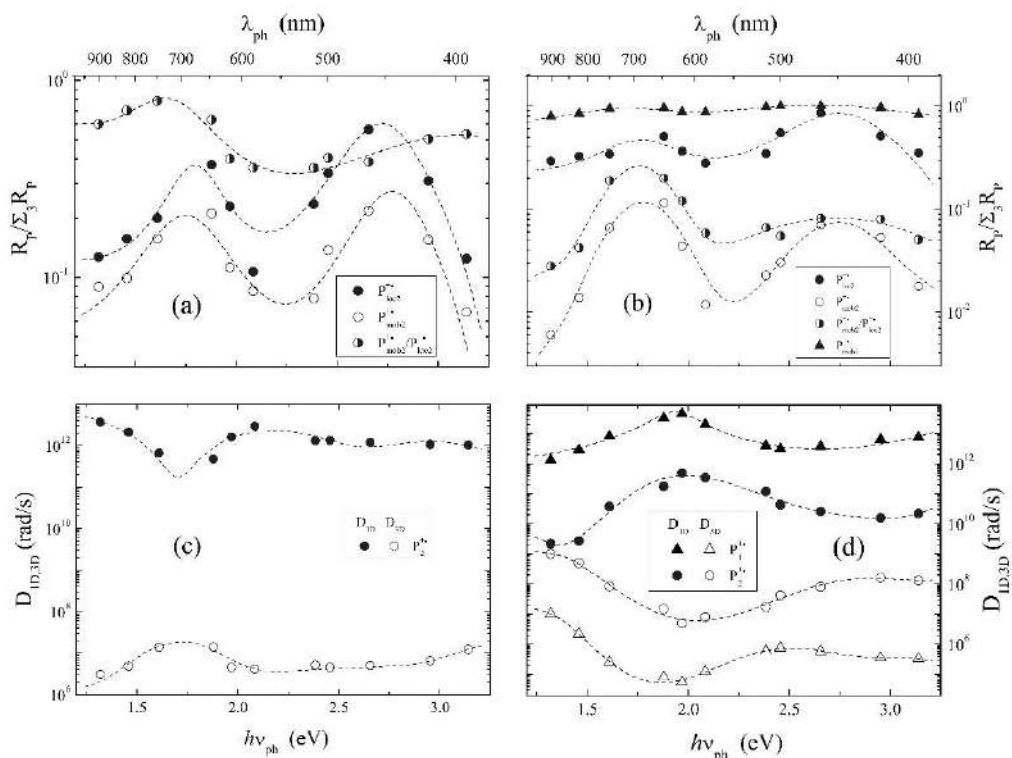
Figure 34. Relative concentrations of polarons, $[P_{1,2}^{+\bullet}]/\Sigma[P_i^{+\bullet}]$ and $[P_{mob2}^{+\bullet}/[P_{loc2}^{+\bullet}]$ (*a,b*) as well as intrachain, D_{1D}, and interchain, D_{3D}, diffusion coefficients (*c,d*) of polarons $P_1^{\bullet+}$ and $P_2^{+\bullet}$ photoinduced in the PCDTBT:PC$_{61}$BM (*a,c*) and PANI:TSA/PCDTBT:PC$_{61}$BM (*b,d*) composites as a function of photon energy $h\nu_{ph}$. The values obtained were normalized to the luminous emittance of the light sourses. The dashed lines are drawn arbitrarily only for illustration to guide the eye.

CONCLUSION

The results presented show principal advantage of the multifrequency EPR spectroscopy in obtaining qualitatively new information on molecular dynamics, transfer mechanism of polarons in conjugated polymers and their nanocomposites. The method enables to detect such charge carriers with close magnetic resonant characteristics, to provide their reliable identification and to establish the correlation of their structural, dynamics and magnetic parameters in such systems. Besides, the interaction between different spin-packets is waned significantly in high magnetic fields, so then they may be considered as noninteracting and their parameters can be determined more precessionaly. It takes qualitatively new information on metrology, relaxation and mobility of polarons as well as matrix's morphology, polarity, etc.

Polarons are stabilized in conjugated polymers as dimerization distortion of their chains. They possess a spin, elemental charge and are characterized by high mobility along polymer chains. The main properties of such charge carriers depend on various factors, e.g., method of synthesis, structure and morphology of an initial and modified polymer. The pairing of polarons into diamagnetic bipolarons with slower dynamics and higher effective mass can occurs with the increase of doping level of a polymer. Besides, the doping process leads to the change in charge transfer mechanism. Spin and charge dynamics in initial and weakly nanomodified conjugated polymer is realized mainly by interchain tunneling of the "small polarons," which highly interact with phonons of polymer lattice. Once the doping level of a polymer increases and its matrix becomes more ordered, these mechanisms ceases to dominate and the charge can be transferred in result of its thermal activation from widely separated localized states in the bandgap to close localized states in the tails of both the valence and conjugated bands. This stipulates the formation in some matrices of complex quasi-particles, namely the molecular-lattice polarons, due to libron-phonon interactions analogously to that as it is realized in organic molecular crystals. Polaron dynamics in conjugated polymers are *a priori* highly anisotropic due their lower dimensionality. In heavily doped samples crytalline Q3D clasters are formed in bulk of polymer matrix. Polaron transport in such systems is realized in terms of Q1D spin hopping between Q3D clasters characterizing by its strong interaction with lattice phonons. Polarons diffusing along a polymer chains interact with other spin charge carriers stabilized on neighboring chains and/or with radicals embedded into polymer matrix as counter anions. Such exchange interaction complicates charge transport in polymer:fullerene and polymer:dopant/polymer:fullerene multispin nanocomposites. Charge dynamics in these systems is also realized in the above mentioned mechanisms which tangled by spin exchange interaction. These spin-assisted processes are governed mainly by the structure of ingredients of a composite as well as by the nature and dynamics of photoinduced charge carriers. The specific morphology of polymer nanocomposites changes their energy levels and shifts the competition between excited states in their BHJ. Correlations obtained for polymer:fullerene and polymer:dopant/polymer:fullerene composites and their ingredients by direct EPR method can be used for a further development and optimization of nanomodified polymer photovoltaic devices.

The spin of a polaron plays a key role in coupling of different polarons stabilized in close polymer chains. This can be used for a handling of charge transfer through BHJ of multispin nanocomposite. Such spin-assisted charge transfer can be more delicate under initiation of polarons by different photons. The correlations established between dynamics, electronic and structural parameters of these systems at wide region of spin precession frequency can be used for the further controllable synthesis of various conjugated polymers with optimal properties. This will open new horizon in creation of flexible and scalable organic devices with field- and spin-assisted electronic properties. Such organic systems can also play the role of efficient spin injectors and detectors, which can potentially eliminate ferromagnetic materials in spin devices. Solitary spin carriers trapped in bulk of darkened polymer matrix can in principle be used as elemental dots for quantum computing. Since coherent spin dynamics in such organic BHJ is anisotropic, our strategy seems to make it possible obtaining complex correlations of anisotropic electron transport and spin dynamics for the further design of progressive molecular electronics and spintronics.

APPENDIX

EPR method is based on the excitation of unpaired electron spin to the higher energy level upon an external magnetic field and MW radiation. Electrons possess a property called "spin," resulting in an angular momentum. Because the electron is charged, there is associated with the angular momentum a magnetic moment which points in the opposite direction to the angular momentum vector. In an external magnetic field, the spin precesses around the field direction at the Larmor frequency and thus a component of the magnetic moment is either parallel or anti-parallel to the field direction. If a microwave field of this frequency is applied to a spin containing sample, then the spins can change their direction relative to the magnetic field. This results in absorption of the microwave field, which may be measured. Spin reorientation is also affected by microenvironment. Microwave absorption depends on fundamental properties of spin reservoir described above. Thus, EPR spectra can yield detail information not only about spin properties of a sample but also about its structure and composition.

A.1. Theoretical Backgrounds of Electron Paramagnetic Resonance of Polarons in Conjugated Polymers

A.1.1. Landé Factor

The main magnetic resonance parameters directly obtained by the continuous wave (CW) EPR spectroscopy for paramagnetic centers in condensed systems are the Landé factor (or *g*-factor that is the ratio of electron mechanic momentum to a magnetic moment), spin susceptibility, as well as line shape and width. The first of them is characterized by the Zeeman interaction of an unpaired electron with external magnetic field. If the fundamental resonance condition (Assenheim 2014).

$$\hbar\,\omega_e = \gamma_e\,\hbar\,B_0 = g\mu_B B_0 \tag{A.1}$$

is fulfilled (here μ_B is the Bohr magneton), an unpaired electron absorbs an energy quantum and is transferred to a higher excited state. It can be seen that the higher B_0 (or ω_e) value, the higher excited state an electron can reach and the higher spectral resolution can therefore be realized. It is stipulated by the distribution of spin density in polymer unit, the energy of exited configurations and its interaction with nearest nuclear. If spin of polaron weakly interacts with own environments, its Landé-factor lies near *g*-factor of free electron, $g_e = 2.00232$. At higher interaction, environmental nuclei induce an additional magnetic field resulting tensoric character of its Landé-factor (Buchachenko, Turton, and Turton 1995, Misra 2011, 2014),

$$\mathbf{g} = \begin{vmatrix} g_{xx} & & \\ & g_{yy} & \\ & & g_{zz} \end{vmatrix} = \begin{vmatrix} 2\left(1 + \dfrac{\lambda\rho(0)}{\Delta E_{n\pi*}}\right) & & \\ & 2\left(1 + \dfrac{\lambda\rho(0)}{\Delta E_{\sigma\pi*}}\right) & \\ & & 2 \end{vmatrix},$$

(A.2)

where λ is the spin-orbit coupling constant, $\rho(0)$ is the spin density, $\Delta E_{n\pi*}$ and $\Delta E_{\sigma\pi*}$ are the energies of the unpaired electron $n \to \pi*$ and $\sigma \to \pi*$ transitions, respectively. Normally, polarons in organic conjugated polymers require a small energy of $n \to \pi*$ transition. This leads to deviation of its g_{xx} and g_{yy} values from g_e, so then the inequality $g_{xx} > g_{yy} > g_{zz} \approx g_e$ holds for these PC.

Weak interaction of an unpaired electron delocalized on polaron over L lattice units with heteroatoms involved in a polymer backbone provokes rhombic symmetry of spin density and, therefore, anisotropy of its magnetic resonance parameters. Since the backbone of a polymer can be expected to lie preferably parallel to the film substrate (Kim et al. 2006), the lowest principal g-value is associated with the polymer backbone. The macromolecule can take any orientation relative to the z-axis, i.e., the polymer backbone direction as is derives from the presence of both the g_{xx} and g_{yy} components in the spectra for all orientations of the film. Thus, the g-factor anisotropy is the result of inhomogeneous distribution of additional fields in such systems along the x and y directions within the plane of their σ-skeleton rather than along its perpendicular z direction. Multifrequency EPR spectroscopy allows to resolve some paramagnetic centers with near g-factors or spectral components of paramagnetic centers with anisotropic g-factor (Krinichnyi 1995, 2000a, 2006, Misra 2011, 2014). Harmonic librations of polymer chains with localized polarons can modulate the charge transfer integrals in polymer composites as it is typical for organic molecular ordered systems (Silinsh, Kurik, and Chapek 1988). This should change effective g-factor as

$$g = g_0 + \frac{A}{\hbar\omega_l}\coth\left(\frac{\hbar\omega_l}{2k_B T}\right),$$

(A.3)

where g_0 and A are constants, $\omega_l = \omega_0\exp(-E_l/k_B T)$ is librational frequency, E_l is the energy required for activation of such a motion, and T is the temperature.

A.1.2. Spin Susceptibility

A static paramagnetic susceptibility χ is also important characteristic of a paramagnetic system. Generally, this parameter of N spins consists of temperature independent Pauli susceptibility of the Fermi gas χ_P and temperature dependent contributions of localized Curie paramagnetic centers χ_C (Vonsovskii 1974). However, such simple picture has been questioned especially for conjugated polymers and their composites. These systems are characterized by significant disorder which localizes spins (Mizoguchi and Kuroda 1997, Raghunathan et al. 1998). This originates the appearance in effective χ of additional contribution χ_{ST} coming due to a possible singlet-triplet spin equilibrium in the system

(Vonsovskii 1974), contribution χ_{ECP} described in terms of an exchange coupled pairs (ECP) model of spin exchange interaction in pairs randomly distributed in a polymer matrix (Kahol and Mehring 1986, Clark and Tippie 1979) and contribution χ_m coming due to polaron Q1D mobility characterizing by mid-gap energy $E_g = 2E_a$ near the Fermi level ε_F (Jonston 1984, Barnes 1981). Finally, one can write the equation for sum χ as

$$\chi=\chi_P+\chi_C+\chi_{ST}+\chi_m+\chi_{ECP}= N_A\mu_{eff}^2\, n(\varepsilon_F) + \frac{C}{3k_BT} + \frac{k_1}{T}\left[\frac{\exp(-J_{af}/k_BT)}{1+3\exp(-J_{af}/k_BT)}\right]^2 +$$

$$\frac{Ca_d}{3k_BT}\left[3+\exp\left(-\frac{2J}{k_BT}\right)\right]^{-1} + C(1-a_d)\left\{\frac{J}{3k_BT}+\ln\left[3+\exp\left(-\frac{2J}{k_BT}\right)\right]\right\} + k_2\sqrt{\frac{E_a}{k_BT}}\exp\left(1-\frac{E_a}{k_BT}\right), \quad \text{(A.4)}$$

where N_A is the Avogadro's number, $n(\varepsilon_F)$ is the density of states per unit energy (in eV) for both spin orientations per monomer unit at ε_F, $\mu_{eff} = \mu_B g \sqrt{S(S+1)}$ is the effective magneton, S is a spin normally equal to ½ for paramagnetic centers in organic polymers, $C = N\mu_B^2 g^2 S(S+1)$ is the Curie constant per mole-C/mole-monomer, k_1 and k_2 are constants, J is the exchange coupling constant, and a_d is a fraction of spin pairs interacting in disordered polymer regions.. The contributions of these terms to the total paramagnetic susceptibility depend on various factors, for example, on the nature and mobility of charge carriers can vary at the system modification. A small value of J corresponds to spin localization in a strongly disordered matrix and it increases at overlapping of wave functions of interacting spins in more ordered regions.

In most polymer semiconductors, polarons are formed as very stable quasi-particles in result of their doping and/or treatment, e.g., by annealing or irradiation. Such charge carriers can also be excited on polymer chains quite reversibly, and such effect is used for conversion of solar light (Sun and Sariciftci 2005, Brabec, Scherf, and Dyakonov 2014). The treatment of polymer semiconductors modified by some electron acceptor normally leads to the transfer of electron from their chains to the acceptor that is accompanied by the formation of polarons on polymer chains and anion-radicals on acceptors. Paramagnetic carriers charged positively and negatively recombine after an irradiation down. Therefore, an effective spin susceptibility of such system is sum of these two alternating processes (Krebs 2012).

In polymer:fullerene composites, both initiated charges diffusing to the opposite electrodes must reach them prior to recombination. If these chargers after their transfer are still bound by the Coulomb potential, which is typical for the compounds with low-mobile charge carriers described here, they cannot escape from each other's attraction and will finally recombine. When the carrier dissipation distance is longer than the Coulomb radius, the excitons initiated, e.g., by light in their heterojunctions can be split into positive and negative charge carriers. To fulfill this condition, the Coulomb field must be shielded or charge carrier hopping distance must exceed the Coulomb radius. In this case charges are transferred to the electrodes either by the diffusion of appropriate carriers or by the drift induced by the electric field. In order to excite a radical pair by each photon, charge carrier transit time t_{tr} should be shorter considerably than the lifetime of a radical pair τ, i.e., $t_{tr} \ll \tau$. The former value is determined by charge carrier mobility μ, sample thickness d, and electric field E inside the film, $t_{tr} = d/\mu E$. If photocurrent is governed by the carrier drift in the applied electric field, the drift distance $l_{dr} = \mu\tau E$. If this current is governed by carrier diffusion, the diffusion distance

$l_{\text{diff}} = (D\tau)^{1/2} = (\mu\tau k_B T/e)^{1/2}$, where D is the diffusion coefficient, and e is the elemental electron charge. Thus, the $\mu\tau$ product governs the average distance passed by the charge carrier before recombination and, therefore, is an important parameter determining whether the efficiency of solar cells is limited by charge transport and recombination. The latter, generally, is described as a thermally activated bimolecular recombination (2003) which consists of temperature-independent fast and exponentially temperature-dependent slow steps (Westerling, Osterbacka, and Stubb 2002).

Let a polaron possessing a positive charge multihops along a polymer chain from one initial site i to other available site j close to a position occupied by a negatively charged fullerene globule. A charge hops easier between fullerenes than from polaron and fullerene, and an effective charge recombination is still limited by the transport of polarons towards fullerene molecules. The recombination is mainly stipulates by sequential charge transfer by polaron along a polymer chain and its transfer from polymer chain to a site occupied by a fullerene. Polaronic dynamics in undoped and slightly doped conjugated polymers is highly anisotropic (Krinichnyi 2000a). Therefore, the probability of a charge transfer along a polymer chain exceeds considerably that of its transfer between polymer macromolecules.

According to the tunneling model (Nelson 2003), positive charge on a polaron can tunnel from this carrier toward a fullerene and recombine with its negative charge during the time

$$\tau(R_{ij}^{|}) = \frac{\ln X}{\nu_{\text{pn}}} \exp\left(\frac{2R_{ij}^{|}}{a_0} \right), \tag{A.5}$$

where $R_{ij}^{|}$ is the spatial separation of sites i and j, a_0 is the effective localization (Bohr) radius, X isa random number between 0 and 1, and ν_{pn} is the attempt to jump frequency for positive charge tunneling from polymer chain to fullerene. The charge can also be transferred by the polaron thermally assisted multistep tunneling through energy barrier $\Delta E_{ij} = E_j - E_i$, so then

$$\chi(R_{ij}, E_{ij}) = \chi_0 \frac{\ln X}{\nu_{\text{pp}}} \exp\left(\frac{2R_{ij}}{a_0} \right) \exp\left(\frac{\Delta E_{ij}}{k_B T} \right), \tag{A.6}$$

where ν_{pp} is the attempt frequency for a hole tunneling between the polymer chains. The values in the couples ν_{pn}, ν_{pp} and $R_{ij}^{|}$, R_{ij} may be different due, for instance, to the different electronic orbits.

Undoubtedly, both charge carriers have different localization radii. The localization radius for a negative charged carrier should be on the order of the radius of the fullerene globule. The distance R_0 should depend, e.g., on the length of a side alkyl chain substitute in a polymer:fullerene matrix (Tanaka et al. 2007). Polaron stabilized in conjugated polymers is normally covers 3 - 5 monomer units (Devreux et al. 1987, Westerling, Osterbacka, and Stubb 2002, Niklas et al. 2013). The nearest-neighbor distance of spin pair with the typical radiative lifetime τ_0 changes with time t as

$$R_0(t) = \frac{a}{2} \ln\left(\frac{t}{\tau_0} \right). \tag{A.7}$$

Assuming that photoexcitation is turned off at some initial time $t_0 = 0$ at a charge carrier concentration n_0 and taking into account a time period of geminate recombination t_1- t_0, one can write for concentration of charge carriers

$$n(R) = \frac{n}{1 + \frac{4\pi}{3} n_1 \left(R_0^3 - R_1^3 \right)},$$ (A.8)

where R_0 is specified by Eq.(A.8), $R_1 = R(t_1)$ describes the distance between the nearest-neighbor charge carriers at time t_1 after which solely non-geminate recombination is assumed, and n_1 is the charge carrier concentration at time t_1. It follows from Eq.(A.8) that the time dependence of residual carrier concentration does not follow a simple exponential decay but shows a more logarithmic time behavior. After very long times, i.e., at large R_0, one obtains $n(R_0) = (3/4\pi)R_0^{-3}$ which is independent of the initial carrier density n_1 and also n_0. It follows from Eq.(A.5) that photoexcited charge carriers have comparable long lifetimes which are solely ascribed to the large distances between the remaining trapped charge carriers. The excited carrier concentration n_1 follows directly from light induced EPR (LEPR) measurements, whereas the a and τ_0 values can be guessed in a physically reasonable range. Finally, the concentration of spin pairs should follow the relation (Schultz et al. 2001)

$$\frac{n(t)}{n_0} = \frac{\frac{n_1}{n_0}}{1 + \left(\frac{n_1}{n_0} \right) \frac{\pi}{6} n_0 a^3 \left[\ln^3 \left(\frac{t}{\tau_0} \right) - \ln^3 \left(\frac{t_1}{\tau_0} \right) \right]}.$$ (A.9)

The analysis showed that the spin concentration initially photoexcited at $t = 0$ is governed by some factors. One of them is the number and distribution of spin traps inversely formed in polymer matrix under irradiation. A number and a depth of such traps depend on the photon energy $h\nu_{ph}$ (Krinichnyi 2009, Krinichnyi, Yudanova, and Spitsina 2010, Krinichnyi 2016b, a). At the latter step, polaronic charge carrier can either be retrapped by vacant trap site or recombine with electron on fullerene anion radical. Trapping and retrapping of a polaron reduces its energy that results in its localization into deeper trap and in the increase in number of localized polarons with time. So, the decay curves presented can be interpreted in terms of bulk recombination between holes and electrons during their repeated trapping into and detrapping from trap sites with different depths in energetically disordered semiconductor (Tachiya and Seki 2010). Analysing LEPR spectra, it becomes possible to separate the decay of mobile and pinned spin charge carriers excited in the composite. The traps in such a system should be characterized by different energy depths and energy distribution E_0. Polarons fast translative diffuse along a polymer backbone, and fullerene anion radicals can be considered to be immobilized between polymer chains. This approach predicts the following law for decay of charge carriers (Tachiya and Seki 2010):

$$\frac{n(t)}{n_0} = \frac{\pi \alpha \delta (1 + \alpha) \nu_d}{\sin(\pi \alpha)} t^{-\alpha},$$ (A.10)

where n_0 is the initial number of polarons at $t = 0$, δ is the gamma function, $\alpha = k_B T / E_0$, ν_d is the attemptjump frequency for polaron detrapping.

Positive charge on polaron is not required to be recombined with the first negative charge on subsequent acceptor. Thus, the probability of annihilation of charges can differ from the unit. Q1D hopping of positively charged polaron from site i to site j with the frequency ω_{hop} may collide with the acceptor located near the polymer matrix. While polaron is mobile, the molecule of acceptor can be considered as a translative fixed, but librating near own main molecular axis. In this case the spin flip-flop probability p_{ff} during a collision should depend on the amplitude of exchange and ω_{hop} value as (Molin, Salikhov, and Zamaraev 1980, Houze and Nechtschein 1996)

$$p_{ff} = k_1 \cdot \frac{\alpha^2}{1 + \alpha^2}, \tag{A.11}$$

where k_1 is constant equal to ½ and 16/27 for $S = ½$ and $S = 1$, respectively, $\alpha = (3/2)\, 2\pi J_{ex}/\hbar$ ω_{hop} and J_{ex} is the constant of exchange interaction of spins in a radical pair. In the polymer composites weak and strong exchange limits can be realized when the increase of ω_{hop} may result in decrease or increase in exchange frequency, respectively. If the ratio $J_{ex}/\hbar$ exceeds the frequency of collision of both types of spins, the condition of strong interaction is realized in the system leading to the direct relation of spin-spin interaction and polaron diffusion frequencies, so then $\lim(p) = 1/2$. In the opposite case $\lim(p) = 9/2$ $(\pi/\hbar)^2 (J_{ex}/\omega_{hop})^2$. It is evident that the longer both the above tunneling times or/and the lesser the probability p_{ff}, the smaller the number of ion-radical pairs possible to recombine and, therefore, higher spin susceptibility should be reached. A combination of Eq.(A.6) and Eq.(A.11) gives

$$\chi_p = \chi_{pn} + \chi_P^0 \frac{\hbar}{J_{ex}}\left(\alpha + \frac{1}{\alpha}\right)\exp\left(\frac{\Delta E_r}{k_B T}\right). \tag{A.12}$$

Assuming the above introduced activation character for polaron multistep hopping with the frequency $\omega_{hop} = \omega_{hop}^0 \exp(-\Delta E_r/k_B T)$ and the absence of dipole-dipole interaction between fullerene anion-radicals, one can determine ΔE_r from temperature dependences of paramagnetic susceptibility.

A.1.3. Spectral Line Shape and Width

In contrast with a solitary and isolated spin characterized by δ-function absorption spectrum, the spin interaction with own environment in a real system leads typically to the change in line shape and increase of linewidth. Analyzing the shape and intensity of experimental spectrum it is possible to obtain direct information on electronic processes in polymer systems. It is known that an electron spin is affected by local magnetic fields, induced by another nuclear and electron n r_{ij}-distanced spins (Roth, Keller, and Schneider 1984):

$$B_{\text{loc}}^2 = \frac{1}{4n}\gamma_e^2 \hbar^2 S(S+1)\sum_{i,j}\frac{\left(1-3\cos^2\theta_{ij}\right)}{r_{ij}^6} = \frac{M_2}{3\gamma_e^2}, \tag{A.13}$$

where M_2 is the second moment of a spectral line. If a line broadening is stipulated by local magnetic field fluctuating faster than the rate of interaction of a spin with nearest environment, the first derivative of the Lorentzian resonant line with a distance between positive and negative peaks $\Delta B_{\text{pp}}^{\text{L}}$ and maximum intensity between these peaks $I_{\text{L}}^{'(0)}$ is registered at resonance frequency $\omega_e^{(0)}$ (Blumenfeld, Voevodski, and Semenov 1962, Weil, Bolton, and Wertz 2007)

$$I_{\text{L}}' = \frac{16}{9}I_{\text{L}}^{'(0)}\frac{(B-B_0)}{\Delta B_{\text{pp}}^{\text{L}}}\left[1+\frac{4}{3}\frac{(B-B_0)^2}{\left(\Delta B_{\text{pp}}^{\text{L}}\right)^2}\right]^{-2}, \tag{A.14}$$

whereas at slower fluctuation of an additional local magnetic field the spectrum is defined by Gaussian function of distribution of spin packets

$$I_{\text{G}}' = \sqrt{e}\; I_{\text{G}}^{'(0)}\frac{(B-B_0)}{\Delta B_{\text{pp}}^{G}}\exp\left[-\frac{2(B-B_0)^2}{\left(\Delta B_{\text{pp}}^{G}\right)^2}\right]. \tag{A.15}$$

The EPR line shape due to dipole or hyperfine broadening is normally Gaussian. An exchange interaction between the spins in real system may result in the appearance of more complicated line shape, described by a convolution of Lorentzian and Gaussian distribution function. This takes a possibility from the analysis of such a line shape to define the distribution, composition and local concentrations of spins in such a system. For example, if equivalent paramagnetic centers with concentration n are arranged chaotically or regularly in the system their line shape is described by the Lorentzian and Gaussian distribution function, respectively, with the width $\Delta B_{\text{pp}}^{\text{L}} = \Delta B_{\text{pp}}^{\text{G}} = 4\gamma_e\hbar\,n$ (Lebedev and Muromtsev 1972). In the mixed cases the line shape transforms to Lorentzian at a distance from the center $\delta B \leq 4\gamma_e\hbar\,/r^3$ (here r is a distance between magnetic dipoles) with the width $\Delta B_{\text{pp}}^{\text{L}} = 4\gamma_e\hbar\,n$ in the center and becomes Gaussian type on the tails at $\delta B \geq \gamma_e\hbar\,/r^3$ with the width $\Delta B_{\text{pp}}^{\text{G}} = \gamma_e\hbar\sqrt{n/r^3}$.

Linewidth is mainly determined by transverse (spin-spin) relaxation time T_2. However, there are several relaxation processes in a polymer composites which cause the shortening of T_2 and hence the broadening of the EPR line. One of them is spin longitudinal (spin-lattice) relaxation on the lattice phonons with time T_1, which shortens the lifetime of a spin state and therefore broadens the line. Representing all other possible relaxation processes by the time $T_2^{|}$, one can write for effective peak-to-peak linewidth ΔB_{pp} as (Wertz and Bolton 2013)

$$\Delta B_{\text{pp}} = \Delta B_{\text{pp}}^0 + \frac{2}{\sqrt{3}\gamma_e}\cdot\frac{1}{T_2} = \Delta B_{\text{pp}}^0 + \frac{2}{\sqrt{3}\gamma_e}\cdot\left(\frac{1}{T_2^{|}}+\frac{1}{2T_1}\right), \tag{A.16}$$

where ΔB_{pp}^0 is the linewidth at the absence of spin dynamics and interaction. The collision of these paramagnetic centers should to broad EPR spectrum by (Molin, Salikhov, and Zamaraev 1980, Houze and Nechtschein 1996)

$$\delta(\Delta B_{\mathrm{pp}}) = p_{\mathrm{ff}}\,\omega_{\mathrm{hop}}n_{\mathrm{g}} = k_1\omega_{\mathrm{hop}}n_{\mathrm{g}}\left(\frac{\alpha^2}{1+\alpha^2}\right), \tag{A.17}$$

where p_{ff} is the flip-flop probability inserted above and n_{g} is the number of guest paramagnetic centers per each polymer unit. In this case the guest spin acts as a nanoscopic probe of the polaron dynamics. Note, that the n_{g} parameter is temperature dependent that should be taken into account when calculating the effective linewidth. According to the spin exchange fundamental concepts (Molin, Salikhov, and Zamaraev 1980), if exchange interaction changes between weak and strong exchange limits (see above), an appropriate $\delta(\Delta\omega)(T)$ dependency may demonstrate extremal dependence with characteristic temperature T_{c}. This should evidence the realization of high and low of spin-spin interaction at $T \le T_{\mathrm{c}}$ and $T \ge T_{\mathrm{c}}$, respectively, realized, e.g., in highly doped polyaniline samples (Houze and Nechtschein 1996, Krinichnyi, Roth, et al. 2006, Krinichnyi, Tokarev, et al. 2006, Krinichnyi, Yudanova, and Wessling 2013).

The rate of charge hopping between two adjacent polymer units can be estimated to a good approximation using a semiclassical Marcus theory adopted for conjugated polymers (Van Vooren, Kim, and Cornil 2008, Lan and Huang 2008)

$$\omega_{hop} = \frac{4\pi^2}{\hbar}\frac{t_{\mathrm{1D}}^2}{\sqrt{4\pi E_{\mathrm{r}}k_{\mathrm{B}}T}}\exp\left(-\frac{E_{\mathrm{r}}}{4k_{\mathrm{B}}T}\right), \tag{A.18}$$

where t_{1D} is electronic coupling between initial and final states (intrachain transfer integral) and E_{r} is both the inner- and outer-sphere reorganization energy of charge carriers due to their interaction with the lattice phonons. The t_{1D} value decreases slightly with temperature, whereas its distribution broadens a line due to thermal motion of polymer units (Cheung, McMahon, and Troisi 2009) similar to that happening in organic crystals (Troisi and Orlandi 2006, Kirkpatrick et al. 2007). Note, that the n_{g} parameter is temperature dependent that should be included into finalized equation. Combination of Eq.(A.17) and Eq.(A.18) yields

$$\delta(\Delta\omega) = \frac{\pi t_{\mathrm{1D}}^2 n_{\mathrm{g}}(T)}{\hbar\sqrt{\dfrac{E_{\mathrm{r}}k_{\mathrm{B}}T}{\pi}}}\cdot\frac{\exp\left(-\dfrac{E_{\mathrm{r}}}{4k_{\mathrm{B}}T}\right)}{1+\left[\dfrac{3J_{\mathrm{ex}}}{2t_{\mathrm{1D}}^2}\sqrt{\dfrac{E_{\mathrm{r}}k_{\mathrm{B}}T}{\pi}}\exp\left(\dfrac{E_{\mathrm{r}}}{4k_{\mathrm{B}}T}\right)\right]^{-2}}. \tag{A.19}$$

Except fast electron spin diffusion, EPR line can also be broadened by the acceleration of molecular dynamics processes, for example oscillations or slow torsion librations of the polymer macromolecules. The approach of random walk treatment provides (Butler, Walker, and Soos 1976), that such Q1D, Q2D, and Q3D spin diffusion with respective diffusion coefficients D_{1D}, D_{2D} and D_{3D} in the motionally narrowed regime changes the respective linewidth of a spin-packet as (Krasicky, Silsbee, and Scott 1982)

$$\Delta B_{pp} \approx \frac{\gamma_e^{1/3}(\Delta B_{pp}^0)^{4/3}}{D_{1D}^{1/3}}, \tag{A.20}$$

$$\Delta B_{pp} \approx \frac{\gamma_e(\Delta B_{pp}^0)^2}{\sqrt{D_{1D}D_{3D}}}, \tag{A.21}$$

$$\Delta B_{pp} \approx \frac{\gamma_e(\Delta B_{pp}^0)^2}{D_{3D}}. \tag{A.22}$$

This theory postulates that at the transition from Q1D to Q2D and then to Q3D spin motion the shape of the EPR line should transform from Gaussian to Lorentzian. This approach allows evaluating an effective dimension of the system under study, say from an analysis of temperature dependence of its EPR spectrum linewidth. For spin Q3D motion or exchange, the line shape becomes close to Lorentzian shape, corresponding to an exponential decay of transverse magnetization with time t, proportional to exp(-ηt); for a Q1D spin motion, this value is proportional to exp(-ρt) (here η and ρ are constants (Hennessy, McElwee, and Richards 1973). In order to determine the type of spin dynamics in Q1D system appropriate anamorphoses $I_0^{\downarrow}/I(B)$ vs. $[(B - B_0)/\Delta B_{1/2}]^2$ and $I_0^{\downarrow}/I(B)$ vs. $[(B - B_0)/\Delta B_{pp}]^2$ (here $\Delta B_{1/2}$ is the half-width of an integral line) (Hennessy, McElwee, and Richards 1973) should be analyzed.

A.1.4. Electron Relaxation and Spin Dynamics

As the magnetic term B_1 of the steady-state microwave field increases, the linewidth ΔB_{pp} of a LEPR spectrum broadens and its intensity I_L first increases linearly, plateaus starting from some B_1 value and then decreases. This occurs due to manifestation of the microwave steady-state saturation effect in the LEPR spectrum of composite. Polaron and fullerene anion radical are non-interacting and, therefore, independent of one another. This allows us to use such effects for separate estimation of their spin-lattice T_1 and spin-spin T_2 relaxation times from relations (Poole 1983)

$$\Delta B_{pp} = \Delta B_{pp}^{(0)} \sqrt{1 + \gamma_e^2 B_1^2 T_1 T_2} \tag{A.23}$$

and

$$I_L = I_L^{(0)} B_1 \left(1 + \gamma_e^2 B_1^2 T_1 T_2\right)^{-3/2}, \tag{A.24}$$

where $I_L^{(0)}$ is intensity of non-saturated spectrum and $T_2 = 2/\sqrt{3}\gamma_e \Delta B_{pp}^{(0)}$. Normally, the inflection point characteristic for polarons' saturation curve is distinct from that obtained for fullerene anion radicals. This is evidence of different relaxation parameters of these paramagnetic centers and confirms additionally their mutual independence.

The mechanism and the rate of electron relaxation depend on the structure and conformation of an initial and modified polymer:fullerene composites in which radical pairs

are photoinduced in differently ordered domains with respective band-gaps. Various spin-assisted dynamic processes occur in polymer:fullerene composites, e.g., polaron diffusion along and between polymer chains with coefficients D_{1D} and D_{3D}, respectively, and librative rotational motion of fullerene anion radical near own main molecular axis with coefficient D_{rot}. These processes induce additional magnetic fields in the whereabouts of electron and nuclear spins which, in turn, accelerates relaxation of both spin ensembles. Relaxation of the whole spin reservoir in organic conjugated polymers is defined mainly by dipole-dipole interaction between electron spins (Krinichnyi et al. 1992), so then these coefficients can be determined from the following equations (Carrington and McLachlan 1967):

$$T_1^{-1}(\omega_e) = \langle \omega^2 \rangle [2J(\omega_e) + 8J(2\omega_e)], \tag{A.25}$$

$$T_2^{-1}(\omega_e) = \langle \omega^2 \rangle [3J(0) + 5J(\omega_e) + 2J(2\omega_e)], \tag{A.26}$$

where $\langle \omega^2 \rangle = 1/10 \, \gamma_e^4 \hbar^2 S(S+1) n \Sigma_{ij}$ is the constant of dipole-dipole interaction for powder, n is a number of polarons per each monomer, Σ_{ij} is the lattice sum for powder-like sample, $J(\omega_e) = (2D_{1D}^| \omega_e)^{-1/2}$ (at $D_{1D}^| \gg \omega_e \gg D_{3D}$), $J(0) = (2D_{1D}^| D_{3D})^{-1/2}$ (at $D_{3D} \gg \omega_e$) are the spectral density functions for polaron longitudinal diffusion, and $J(\omega_e) = \tau_c/(1 + \tau_c^2 \omega_e^2)$ is the spectral density function for fullerene rotational libration with correlation time τ_c, $D_{1D}^| = 4D_{1D}/L^2$, and L is a factor of spin delocalization over a polaron equal approximately to five monomer units in P3AT (Devreux et al. 1987, Westerling, Osterbacka, and Stubb 2002).

Spinless charge carrier induces at a distinct point with a guest charge an electric field with a potential (Buchachenko 1984)

$$E_d = \frac{k_B T (x \coth x - 1)}{\mu_u}, \tag{A.27}$$

where $x = 2\mu_u \mu_v (\pi \varepsilon \varepsilon_0 k_B T r^3)^{-1}$, μ_v and μ_u are the dipole moments of the domestic and guest charge carriers, respectively, ε and ε_0 are the dielectric constants for a carrier and vacuum respectively, and r is the distance between both charge carriers. Such a field may change magnetic parameters of guest spin, and such variation can also be registered by EPR method.

A.1.5. Mechanism of Charge Transport in Polymer Systems

Different theoretical models can be used for explanation of spin dynamics in condensed systems.

To describe electron transfer in amorphous metals Mott developed the variable range hopping (VRH) model (Mott and Davis 2012). This theory balances the likelihood of tunneling between random energy electron potential wells with the likelihood of gaining enough thermal energy to move to a nearby site. In this hopping process of a charge transfer each state can have only one electron of one spin direction. If the localization of a charge carrier is very strong, it will hop to the nearest state with the probability proportional to $\exp(-\Delta E_{ij}/k_B T)$ (see the respective term of Eq.(A.6). As the temperature is decreased, fewer states fall within the allowed energy range and the average hopping distance increases. This

results in the following temperature and frequency dependence of spin diffusion coefficient in such system (Austin and Mott 1969)

$$D_{ac}(\omega,T) = D_0 \omega_e T^2 \left(\ln \frac{\omega_0}{\omega_e} \right)^4, \tag{A.28}$$

where ω_0 is the hopping attempt frequency.

Polaron dynamics in some polymer composites can be characterized by strong temperature dependence. This can probably be due to the scattering of polarons on the lattice phonons of crystalline domains embedded into an amorphous matrix. According to the model proposed for charge dynamics in crystalline domains of doped conjugated polymers, such scattering should affect polaron intrachain diffusion with an appropriate coefficient (Pietronero 1983, Kivelson and Heeger 1988)

$$D_{3D}(T) = \frac{\pi^2 M t_0^2 k_B^2 T^2}{h^3 \alpha_{eph}^2} \cdot \left[\sinh\left(\frac{E_{ph}}{k_B T} \right) - 1 \right] = D_{3D}^{(0)} T^2 \cdot \left[\sinh\left(\frac{E_{ph}}{k_B T} \right) - 1 \right], \tag{A.29}$$

where M is the mass of a polymer unit, t_0 is the transfer integral equal for π-electron to ~2.5 – 3 eV, α_{eph} is a constant of electron-phonon interaction, and E_{ph} is phonon energy.

Spin dynamics in less ordered polymer matrix of composites can be realized in the frames of the Elliot model based on spin hopping over energetic barrier E_b (Long and Balkan 1980). This model predicts the following temperature dependencies for diffusion coefficients of a charge carrier at alternating current

$$D_{ac}(\omega,T) = D_{ac}^0 T^2 \omega_e^s \exp\left(\frac{E_b}{k_B T} \right), \tag{A.30}$$

where the exponent $s = 1 - \alpha k_B T / E_b$ reflects system dimensionality and α is a constant. Comparison of spin dynamic parameters obtained at direct current and at different spin precession frequencies ω_e allowed one to determine more precisely details of charge transfer in organic polymer systems (Krinichnyi 1995, 2000a, 2006).

If spin traps are initiated in polymer matrix, the dynamics of spin charge carriers can be explained in terms of the Hoesterey-Letson formalism modified for amorphous low-dimensional systems containing spin traps with concentration n_t and depth E_t (Fishchuk et al. 2002). In the frames of such approach, the coefficient of trap-assisted spin diffusion in the case of low trap concentration limit can be

$$D_t(T) = \nu_0 \left(\frac{R_{ij}}{d} \right)^2 \exp\left(-\frac{2R_{ij}}{r} \right) \exp\left(\frac{E_t}{2k_B T_{cr}} \right) \exp\left[-\frac{E_t}{2k_B T} \left(\frac{\sigma_0}{k_B T} \right)^2 \right], \tag{A.31}$$

where ν_0 is hopping attempt frequency, d is the lattice constant, $T_{cr} = E_t / 2k_B \ln(n_t)$ is critical temperature at which the transition from trap-controlled to trap-to-trap hopping transport regimes occurs, and σ_0 is the width of intrinsic energetic distributions of hopping states in the absence of traps.

Diffusion of small polaron may correlate with the dynamics of polymer matrix. According to the Friedman-Holstein model (Friedman and Holstein 1963), in an adiabatic regime this

should lead to the following temperature dependence of such charge carrier diffusion coefficient (Nagels 1980)

$$D_{sp} = \frac{\omega_0}{4\pi} \; f(T) \; \exp\left(-\frac{E_h - t_h}{3k_B T}\right), \tag{A.32}$$

where d_i is the distance between neighboring hopping sites, $f(T) = 1$ for $t_h \ll k_B T$, and $f(T) = k_B T / t_h$ for $t_h \gg k_B T$, E_h is the hopping activation energy, and t_h is the hopping transfer integral. In a non-adiabatic regime, small polaron cannot follow the lattice oscillations and the time required for its hopping from one site to another is large compared to the duration of a coincidence even between two polaron sites. For this case the latter Equation should be written as (Nagels 1980)

$$D_{sp} = \frac{t_h}{2h}\left(\frac{\pi k_B T}{4E_h}\right)^{1/2} \exp\left(-\frac{E_h}{3k_B T}\right). \tag{A.33}$$

The conductivity of a conjugated polymer due to dynamics of N_i polarons can be calculated from the modified Einstein relation

$$\sigma_{1,3D} = N_i e^2 \mu = \frac{N_i e^2 D_{1,3D} d_{1,3D}^2}{k_B T}, \tag{A.34}$$

where μ is the charge carrier mobility and $c_{1,3D}$ is the respective lattice constant.

A.1.6. Dysonian EPR Spectral Contribution

EPR line of paramagnetic centers in conducting composites can be complicated by the fact that the magnetic term B_1 of MW field used to excite resonance sets up eddy currents in the material bulk. These currents effectively confine the magnetic flux to a surface layer of thickness of order of the "skin depth". The appearance of such skin layer on various surfaces is shown in inserts of Figure A.1. This phenomenon affects the absorption of microwave energy incident upon a sample and results in the less intensity of electron absorption per unit volume of material for large particles than for small ones. This also leads to the appearance of asymmetric Dyson-like contribution (Dyson 1955) in EPR spectra of some polymer systems containing ordered domains embedded into their amorphous phase (Krinichnyi 1995, 2006, 2009, 2014b, 2016b, a, 2017, Konkin et al. 2014) (see Figure A.1). Such effect appears when the skin-layer thickness δ becomes comparable or thinner than a characteristic size of a sample, e.g., due to the increase of conductivity. In this case the time of charge carrier diffusion through the skin-layer becomes essentially less than a spin relaxation time and the Dysonian line with characteristic asymmetry factor *A/B* (the ratio of intensities of the spectral positive peak to negative one) is registered. Such line shape distortion is accompanied by the line shift into higher magnetic fields and the drop of sensitivity of EPR technique.
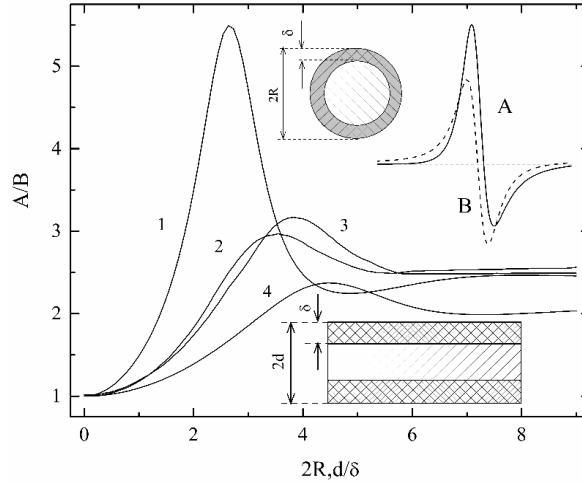
Figure A.1. The dependence of the spectrum asymmetry factor A/B on the thickness of skin-layer δ formed on the conjugated plate (*1*), shank with square (*2*) and circular (*3*) section, and sphere (*4*). In the insert are shown EPR spectra of PC in insulating (dashed line, $D/A = 0$, $A/B = 1$) and conducting (solid line, $D/A = 0.8$, $A/B = 2.2$) materials with characteristic diameter and thickness size.

Generally, the Dysonian line consists of dispersion $\chi^{|}$ and absorption $\chi^{\|}$ terms, therefore one can write for its first derivative the following relation (Chapman, Rhodes, and Seymour 1957):

$$\frac{d\chi}{dB} = A\frac{2x}{(1+x^2)^2} + D\frac{1-x^2}{(1+x^2)^2},\tag{A.35}$$

where $x = 2(B\text{-}B_0)/\sqrt{3}\Delta B_{pp}^{L}$. The line asymmetry parameter A/B is correlated with the above coefficients A and D simply as $A/B = 1 + 1.5\, D/A$ independently on the EPR linewidth. Organic polymers are usually studied as powder and film. Appropriate coefficients of absorption A and dispersion D in Eq.(A.35) for skin-layer on the surface of a spherical powder particle with radius R and intrinsic *ac* conductivity σ_{ac} can be calculated from equations:

$$\frac{4A}{9} = \frac{8}{p^4} - \frac{8\,(\sinh p + \sin p)}{p^3(\cosh p - \cos p)} + \frac{8\,\sinh p\,\sin p}{p^2(\cosh p - \cos p)^2} + \frac{(\sinh p - \sin p)}{p\,(\cosh p - \cos p)} - \frac{(\sinh^2 p - \sin^2 p)}{(\cosh p - \cos p)^2} + 1,\tag{A.36}$$

$$\frac{4D}{9} = \frac{8\,(\sinh p - \sin p)}{p^3(\cosh p - \cos p)} - \frac{4\,(\sinh^2 p - \sin^2 p)}{p^2(\cosh p - \cos p)^2} + \frac{(\sinh p + \sin p)}{p\,(\cosh p - \cos p)} - \frac{2\sinh p\,\sin p}{(\cosh p - \cos p)^2},\tag{A.37}$$

where $p = 2R/\delta$, $\delta = \sqrt{2/\mu_0\omega_e\sigma_{ac}}$, and μ_0 is the magnetic permeability for vacuum. In case of the formation of skin-layer on the flat plate with a thickness of $2d$ the above coefficients can be determined from relations

$$A = \frac{\sinh p + \sin p}{2p \ (\cosh p + \cos p)} + \frac{1 + \cosh p \ \cos p}{(\cosh p + \cos p)^2},$$ (A.38)

$$D = \frac{\sinh p - \sin p}{2p \ (\cosh p + \cos p)} + \frac{\sinh p \ \sin p}{(\cosh p + \cos p)^2},$$ (A.39)

where $p = 2d/\delta$.

Figure A.1 depicts the dependence of the spectrum asymmetry factor A/B on the thickness of skin-layer δ formed in different conducting bulks. The analysis of multifrequncy EPR spectra with Dysonian term allows determining directly *ac* conductivity of crystalline domains embedded into amorphous polymer matrix at spin precession frequency ω_e.

A.2. EPR Techniques

The study of spin properties of spin topological distortions in organic substances is mainly carried out by using X-band EPR technique operating at $\omega_e/2\pi \approx 9.7$ GHz and $B_0 \approx 0.33$ T. This is due mainly to the availability starting from the 1940s of an appropriate element base and a relative simplicity of the experiments at this waveband. Typical X-band CW EPR spectrometer is drawn schematically in Figure A2. The main parts of this device are MW power oscillator *1*, magnet *9*, and MW reflecting cavity (resonator) *11*. The EPR spectrum is usually measured keeping constant MW frequency during sweeping the magnetic field strength. If the energy of the MW quants equals the energy splitting of the spin states, the resonance condition (A.1) is fulfilled and MW radiation is absorbed. Typically, the EPR spectrum is given as the first derivative of the absorption peak, resulting from magnetic field modulation necessary for the use of a lock-in amplifier. The field modulation determines among others the time resolution of the EPR spectrometer. It is limited to the inverse of the field modulation frequency. Usually a modulation frequency of 100 kHz is used which would result in a maximum time resolution of 10 ps. MW power is generated by oscillator *1* previously based on vacuum klystron or backward wave oscillator and then on solid-state Gunn diode. This part contains also appropriate automatic frequency control circuit. MW power is splitted and transmitted to the two branches of the MW bridge. The referent branch of the bridge consists of MW attenuator *2* and MW phase shifter *3*, whereas the signal measuring part contains more precession MW attenuator *6*, one-way MW circulator *7* and MW reflecting cavity (resonator) *11* situated between the magnet poles *9*. The sample under study in quartz ampoule is placed at the centre of the MW cavity *11* and both the branches are tuned to reach balanced zero signal at the output of the MW diode *4*. Once the Eq.(A.1) is fulfilled for PC analyzed, they absorb a little part of MW energy in the measuring branch and are excited to the higher energy level. This causes imbalance in the MW bridge and appearance at its output of resonant *ac* signal under a scanning of a sample in an external magnetic field B_0. This signal is transformed into a resulting *dc* EPR response by phase detector *5*. Normally, the cavity and magnet of the spectrometer are provided with a hole through which the PC can be initiated in the sample under its direct irradiation or illumination by appropriated source *8*. The more spins are stabilized or/and initiated in the sample the higher integral signal is registered on the device output. One of the simple exemplary devices,

portable X-band EPR spectrometer PS 100X operating at 9.72 GHz is characterized by a sensitivity of 4×10^{11} spin/mT, resonance instability of 3×10^{-5} per a hour, maximal MW power 150 mW inducing $B_1 = 48$ μT in center of the cavity with an unloaded quality factor $Q \approx$ 5,000 and mode H_{102}.
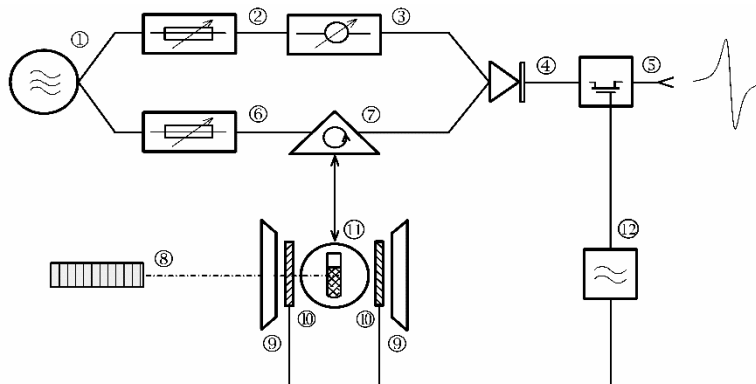
Figure A2. The sketch of X-band EPR spectrometer: *1* - MW oscillator, *2* - MW attenuator, *3* - MW phase shifter, *4* - MW detector, *5 – ac* phase detector, *6 – MW* attenuator, *7 – MW* circulator, *8 –* light source (laser), *9* - magnet pole, *10 - ac* modulation coils, *11* - MW cavity with a sample, *12 - ac* oscillator.

If some spin ensembles with near magnetic parameters are stabilized in a sample, their lines can overlap. The width of individual EPR lines of most organic radicals usually amounts to 0.1-1.0 mT, and *g*-factor value differs from g_e by $(1-10)\times10^{-4}$. Therefore the spectral resolution or splitting of lines of different radicals, $\delta B \cong \delta g B_0/g \cong 10$ - 100 mT, is smaller than their width at X-band, resulting in the overlapping of their EPR spectra. This complicates the identification of such radials in solids and the analysis of structural and dynamic properties of microenvironment by using their *g*-factors (Misra 2011). This means that in order to attain the satisfactory resolution of free radicals' EPR spectra the condition $\delta B/B_0 < 2\times10^{-5}$ should be valid. If the linewidth of PC do not changes with registration frequency ω_e, such condition is fulfilled at millimeter wavebands EPR. The separation in field of two lines with different *g*-factors will scale with the field, so if the linewidths remain constant, then the lines will eventually be resolved as the field is increased. Besides, the susceptibility of the method also increases at high spin precession frequency ω_e (Krinichnyi 2006, Misra 2011, Krinichnyi 2016b). The operating frequency was defined in most cases by the investigation purposes and physical properties of the objects under study. Except X-band (of frequences extending from 8 up to 12 GHz), such investigations are also carried out at K- (18 − 26.5 GHz), Q- (30 − 50 GHz), W- (75 − 110 GHz), and D- (110 − 170 GHz) bands EPR. The main advantages of the high-frequency/field CW EPR spectroscopy may be compiled as following:

- Increase in spectral resolution due to the higher magnetic field
- Increase in detection sensitivity for samples of limited quantity due to higher resonator filling factor
- Increase in orientation selectivity in the investigation of disordered systems

- Accessibility of spin systems with larger zero-field splitting due to the larger microwave quantum energy
- Implification of spectra due to the reduction of second-order effects at high fields.

The basic block-scheme of the CW D-band EPR spectrometer (Galkin et al. 1977, Krinichnyi 1991a, b) is drawn in Figure A.3. This device is assembled as a direct amplification circuit with H_{011} type reflecting cavity, a double MW T-bridge and *n*-SbIn bolometer operating as MW detector at temperature of liquid helium (4.2 K). The main part of the spectrometer includes the MW klystron or Gunn diode oscillator *11* with appropriate elements of the waveguide section, a cryostat *1* with a superconducting solenoid *2* and MW bolometric *n*-SbIn sensor *14*. In the center of the cryostat is placed the tunable MW cavity *4* with a sample *5* encircled by modulating *3* and temperature-sensitive *6* copper coils. A sample filled into a quartz capillary with the external diameter and length of 0.6 and 7 mm, respectively, is placed into the center of the cavity between two cylindrical pistons. The temperature of the sample can be controlled within 6 − 380 K region by helium or nitrogen gaseous flow. The quality factor Q of the cavity with the inner diameter of 3.5 mm and operation length of 1.5 mm lies near 2,000. The value of microwave field magnetic component B_1 in the center of the cavity is equal to 20 μT. The magnetic field inhomogeneity in the point of sample arrangement does not exceed 10 μT/mm. The absolute point-sample sensitivity of the spectrometer is 5×10^8 spin/mT at room temperature that is unique for EPR spectroscopy. The latter value is three orders of magnitude lower than N_{min} calculated (Krinichnyi 2016b) due to the smaller P and Q_0 values as compared with X-band. The concentration sensitivity for aqueous samples is 6×10^{13} spin/mT cm^3.
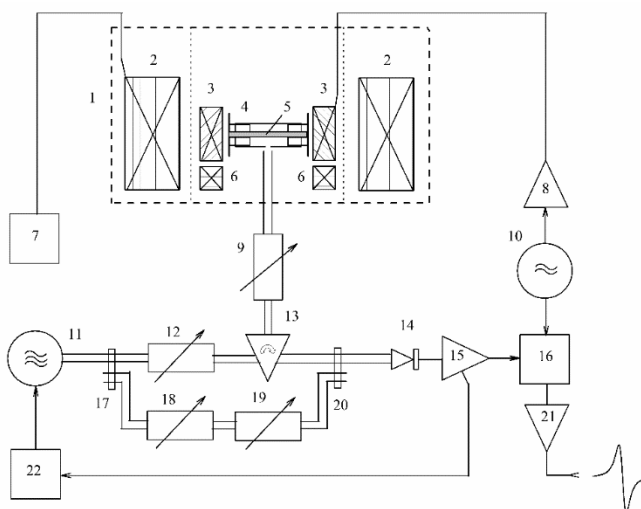
Figure A3. The sketch of D-band EPR spectrometer: *1* - helium cryostat, *2* - superconducting solenoid, *3 – ac* modulation coil, *4 –* MW cavity with two cylindrical side tuning and fixed pistons, *5 –* quartz capillary with a sample, *6* - temperature-sensitive coil, *7* - solenoid current supply, *8 – ac* modulator amplifier, *9* and *19 –* MW phase shifter, *10* - ac oscillator, *11* - MW oscillator, *12* and *18* - MW attenuators, *13* - MW circulator, *14 –* MW superlow temperature (4.2 K) barretter, *15 - 21 - ac* preamplifiers, *16* - phase detector, *17* and *20* - directional MW couplers, *22 –* MW oscillator power supply with a section of MW frequency auto adjustment.

The first CW D-band EPR investigation of PC stabilized in different biopolymers and organic conjugated polymers showed the growth of sensitivity and resolution of the method at this waveband (Krinichnyi 1991a, b, 1995). It was demonstrated that the study of these systems at higher registration frequencies allows increasing sufficiently the efficiency of the method, to obtain qualitative new information on these and other objects and to solve various scientific problems. During the last decade, multi frequency EPR spectroscopy allowed us to study the main properties of polarons and other PC in conjugated polymers and their nanocomposites (Krinichnyi 2006, 2009, 2014b, a, 2016b, a). During this time, the variety of EPR technique, pulse, combined, has been expanded (Misra 2011).

REFERENCES

Adrain, F.J., and L. Monchick. 1979. "Theory of chemically induced magnetic polarization. Effects of S–T$_{\pm 1}$ mixing in strong magnetic fields." *Journal of Chemical Physics* 71 (6):2600-2610.

Aguirre, A., P. Gast, S. Orlinskii, I. Akimoto, E. J. J. Groenen, H. El Mkami, E. Goovaerts, and S. Van Doorslaer. 2008. "Multifrequency EPR analysis of the positive polaron in I$_2$-doped poly(3-hexylthiophene) and in poly[2-methoxy-5-(3,7-dimethyloctyloxy)]-1,4-phenylenevinylene." *Physical Chemistry Chemical Physics* 10 (47):7129-7138.

Ahlskog, M., R. Menon, A. J. Heeger, T. Noguchi, and T. Ohnishi. 1997. "Metal-insulator transition in oriented poly(p-phenylenevinylene)." *Physical Review B* 55 (11):6777-6787.

Ahlskog, M., M. Reghu, and A. J. Heeger. 1997. "The temperature dependence of the conductivity in the critical regime of the metal-insulator transition in conducting polymers." *Journal of Physics -Condensed Matter* 9 (20):4145-4156.

Al Ibrahim, M., H. K. Roth, M. Schrödner, A. Konkin, U. Zhokhavets, G. Gobsch, P. Scharff, and S. Sensfuss. 2005. "The influence of the optoelectronic properties of poly(3-alkylthiophenes) on the device parameters in flexible polymer solar cells." *Organic Electronics* 6 (2):65-77.

Altshuler, S. A., and B. M. Kozirev. 1972. Электронный парамагнитный резонанс соединений элементов промежуточных групп [*Electron paramagnetic resonance of compounds of elements of intermediate groups*]. Academic Press. Original edition, M.: Наука, 1972, 670 с.

Ashwell, G. J., ed. 1992. *Molecular Electronics*. Edited by G. J. Ashwell. New York: John Wiley.

Assenheim, H.M. 2014. *Introduction to Electron Spin Resonance*: Springer.

Audebert, P., G. Binan, M. Lapkowski, and Limosin. 1987. "Grafting, ionomer composites, and auto-doping of conductive polymers." In *Electronic Properties of Conjugated Polymers, Springer Series in Solid State Sciences*, edited by H. Kuzmany, M. Mehring and S. Roth, 366. Berlin: Springer-Verlag.

Austin, I. G., and N. F. Mott. 1969. "Polarons in crystalline and non-crystalline materials." *Advances in Physics* 18 (71):41-102.

Banerji, N., S. Cowan, M. Leclerc, E. Vauthey, and A. J. Heeger. 2010. "Exciton formation, relaxation, and decay in PCDTBT." *Journal of the American Chemical Society* 132 (49):17459-17470.

Barnes, S. E. 1981. "Theory of electron spin resonance of magnetic ions in metals." *Advances in Physics* 30 (6):801-938.

Barta, P., S. Niziol, P. Leguennec, and A. Pron. 1994. "Doping-Induced magnetic phase-transition in poly(3-alkylthiophenes)." *Physical Review B* 50 (5):3016-3024.

Bartle, A., L. Dunsch, H. Naarmann, D. Schmeisser, and W. Gopel. 1993. "ESR studies of polypyrrole films with a two-dimensional microstructure." *Synthetic Metals* 61(1-2):167-170.

Baunsgaard, D., M. Larsen, N. Harrit, J. Frederiksen, R. Wilbrandt, and H. Stapelfeldt. 1997. "Photophysical properties of 2,3,6,7,10,11-hexakis(n-hexylsulfanyl)triphenylene and 2,3,6,7,10,11-hexakis(n-hexylsulfonyl)triphenylene insolution." *Journal of the Chemical Society, Faraday Transactions* 93 (10):1893-1901.

Beau, B., J. P. Travers, and E. Banka. 1999. "NMR evidence for heterogeneous disorder and quasi-1D metallic state in polyaniline CSA." *Synthetic Metals* 101 (1-2):772-775.

Beau, B., J. P. Travers, F. Genoud, and P. Rannou. 1999. "NMR study of aging effects in polyaniline CSA." *Synthetic Metals* 101 (1-2):778-779.

Bernier, P. 1986. "The magnetic properties of conjugated polymers: ESR studies of undoped and doped systems." In *Handbook of Conducting Polymers*, edited by T. E. Scotheim, 1099-1125. New York: Marcel Dekker, Inc.

Blakemore, J. S. 1985. *Solid State Physics*. 2 ed. Cambridge: Cambridge University Press.

Blank, A., R. Kastner, and H. Lebanon. 1998. "Exploring new active materials for low noise, room temperature, microwave amplifiers and other devices." *IEEE Transactions of Microwave Theory and Techniques* 46 (12):2137-2144.

Bleier, H., S. Roth, Y. Q. Shen, and D. Schafer-Siebert. 1988. "Photoconductivity in trans-polyacetylene: Transport and recombination of photogenerated charged excitations." *Physical Review B* 38:6031-6040.

Blumenfeld, L. A., V. V. Voevodski, and A. G. Semenov. 1962. *Application of Electron Paramagnetic Resonance in Chemistry (Russ)*. Novosibirsk: Izdat. SO AN SSSR. Original edition, [Л.А. Блюменфельд, В.В. Воеводский, А.Г. Семёнов, Применение электронного парамагнитного резонанса в химии], Новосибирск, Издат. СА АН СССР, 1962, c.

Bobacka, J., A. Ivaska, and A. Lewenstam. 1999. "Plasticizer-free all-solid-state potassium-selective electrode based on poly(3-octylthiophene) and valinomycin." *Analytica Chimica Acta* 385 (1-3):195-202.

Bock, H., P. Rittmeyer, A. Krebs, K. Schultz, J. Voss, and B. Kopke. 1984. "Radical ions. 56. One-electron oxidation of 1,2-dithiete derivatives." *Phosphorus Sulfur and Silicon and the Related Elements* 19:131-136.

Brabec, C., V. Dyakonov, J. Parisi, and N. S. Sariciftci. 2003. *Organic Photovoltaic: Concepts and Realization*, *Springer Series in Materials Science*. Berlin: Springer.

Brabec, C., U. Scherf, and V. Dyakonov, eds. 2014. *Organic Photovoltaics: Materials, Device Physics, and Manufacturing Technologies*. 2- ed. Vol. 1. Weinheim: Wiley-VCH.

Brédas, J. L. 1986. "Electronic structure of highly conducting polymers." In *Handbook of Conducting Polymers*, edited by T. E. Scotheim, 859-913. New York: Marcel Dekker, Inc.

Brédas, J. L., and R. R. Chance, eds. 1990. *Conjugated Polymeric Materials: Opportunities in Electronics, Optoelectronics, and Molecular Electronics*. Edited by J. L. Brédas and R. R. Chance, *NATO Advanced Study Series*. Dordrecht: Kluwer Academic Publishers.

Brédas, J. L., R. R. Chance, R. H. Baughman, and R. Silbey. 1982. "Abinitio effective Hamiltonian study of the electronic properties of conjugated polymers." *Journal of Chemical Physics* 76 (7):3673-3678.

Brédas, J. L., C. Quattrocchi, J. Libert, A. G. MacDiarmid, J. M. Ginder, and A. J. Epstein. 1991. "Influence of ring-torsion dimerization on the band-gap of aromatic conjugated polymers." *Physical Review B* 44 (12):6002-6010.

Brédas, J. L., and G. B. Street. 1985. "Polarons, bipolarons, and solitons in conducting polymers." *Accounts of Chemical Research* 18 (10):309-315.

Breiby, D. W., S. Sato, E. J. Samuelsen, and K. Mizoguchi. 2003. "Electron spin resonance studies of anisotropy in semiconducting polymeric films." *Journal of Polymer Science Part B-Polymer Physics* 41 (23):3011-3025.

Buchachenko, A. L. 1984. *Complexes of Radicals and Molecular Oxygen with Organic Molecules (Russ)*. Moscow: Nauka. Original edition, [Бучаченко, А. Л., Комплексы радикалов и молекулярного кслорода с органическими молекулами], М.: Химия, 1984.

Buchachenko, A. L., C.N. Turton, and T.I. Turton. 1995. *Stable Radicals*. New York: Consultants Bureau.

Buchachenko, A. L., and A. M. Vasserman. 1973. *Stable Radicals (Russ)*. Moscow: Khimija. Original edition, [Бучаченко, А.Л., Вассерман, А.М., Стабильные радикалы, М.: Химия], 1973.

Butler, M. A., L. R. Walker, and Z. G. Soos. 1976. "Dimensionality of spin fluctuations in highly anisotropic TCNQ salts." *Journal of Chemical Physics* 64 (9):3592-3601.

Cameron, T. S., R. C. Haddon, S. M. Mattar, S. Parsons, J. Passmore, and A. P. Ramirez. 1991. "The synthsis, characterization, X-ray crystal-structure and solution ESR-spectrum of the paramagnetic solid, 4,5-bis(trifluoromethyl)-1,2,3-trithiolium hexafluorarsenate - Implication for the identity of 1,2-dithiete cations." *Journal of the Chemical Society-Chemical Communications* (6):358-360.

Cameron, T. S., R. C. Haddon, S. M. Mattar, S. Parsons, J. Passmore, and A. P. Ramirez. 1992. "Preparation and crystal-structure of the paramagnetic solid $F_3CCSSSCCF_3ASF_6$ - Implication for the identity of RCSSCR-bullet$^+$." *Journal of the Chemical Society-Dalton Transactions* (9):1563-1572.

Carrington, F., and A. D. McLachlan. 1967. *Introduction to Magnetic Resonance with Application to Chemistry and Chemical Physics*. New York, Evanston, London: Harrer & Row, Publishers.

Carter, F. L., ed. 1982. *Molecular Electronic Devices II*. Edited by F. L. Carter. Vol. 2. New York: Marcel Dekker.

Chakrabarti, S., B. Das, P. Banerji, D. Banerjee, and R. Bhattacharya. 1999. "Bipolaron saturation in polypyrrole." *Physical Review B* 60 (11):7691-7694.

Chang, Y. H., K. Lee, R. Kiebooms, A. Aleshin, and A. J. Heeger. 1999. "Reflectance of conducting poly(3,4-ethylenedioxythiophene)." *Synthetic Metals* 105 (3):203-206.

Chapman, A. C., P. Rhodes, and E. F. W. Seymour. 1957. "The effect of eddy currents on nuclear magnetic resonance in metals." *Proceedings of the Physical Society* B 70 (4):345-360.

Chatterjee, A., and S. Mukhopadhyay, eds. 2018. *Polarons and Bipolarons: An Introduction*, *Chapman & Hall Pure and Applied Mathematics*. Boca Raton: CRC Press.

Chen, J., A. J. Heeger, and F. Wudl. 1986. "Confined soliton pairs (bipolarons) in polythiophene - *insitu* magnetic-resonance measurements." *Solid State Communications* 58 (4):251-257.

Chen, T. A., X. M. Wu, and R. D. Rieke. 1995. "Regiocontrolled synthesis of poly(3-alkylthiophenes) mediated by Rieke zink - their characterization and solid-state properties." *Journal of the American Chemical Society* 117 (1):233-244.

Cheung, D. L., D. P. McMahon, and A. Troisi. 2009. "Computational study of the structure and charge-transfer parameters in low-molecular-mass P3HT." *Journal of Physical Chemistry B* 113 (28):9393–9401.

Cik, G., F. Sersen, L. Dlhan, I. Cerven, A. Stasko, and D. Vegh. 2002. "Study of magnetic properties of copolymer of 3-dodecylthiophene and 2,3-R,R-thieno[3,4-b]pyrazine." *Synthetic Metals* 130 (2):213-220.

Cik, G., F. Sersen, L. Dlhan, L. Szabo, and J. Bartus. 1995. "Anomaly in magnetic properties of poly(3-alkylthiophene)s depending on alkyl chain length." *Synthetic Metals* 75 (1):43-48.

Cinchetti, M., K. Heimer, J. P. Wustenberg, O. Andreyev, M. Bauer, S. Lach, C. Ziegler, Y. L. Gao, and M. Aeschlimann. 2009. "Determination of spin injection and transport in a ferromagnet/organic semiconductor heterojunction by two-photon photoemission." *Nature Materials* 8:115-119.

Clark, W. G., and L. C. Tippie. 1979. "Exchange-coupled pair model for the random-exchange Heisenberg antiferromagnetic chain." *Physical Review B* 20 (7):2914-2923.

Conwell, E. M. 1997. "Transport in conducting polymers." In *Handbook of Organic Conductive Molecules and Polymers*, edited by H. S. Nalwa, 1-45. Chichester: John Wiley & Sons.

Conwell, E. M., C. B. Duke, A. Paton, and S. Jeyadev. 1988. "Molecular conformation of polyaniline oligomers: optical absorption and photoemission of three-phenyl molecules." *Journal of Chemical Physics* 88 (5):3331-3337.

Dediu, V. A., L. E. Hueso, I. Bergenti, and C. Taliani. 2009. "Spin routes in organic semiconductors." *Nature Materials* 8:707 - 716.

Deibel, C., D. Mack, J.Gorenflot, A.Schöll, S. Krause, F.Reinert, D.Rauh, and V. Dyakonov. 2010. "Energetics of excited states in the conjugated polymer poly(3-hexylthiophene)." *Physical Review B* 81 (8):085202 - 085206.

Demirboga, B., and A. M. Onal. 2000. "ESR and conductivity investigations on electrochemically synthesized polyfuran and polythiophene." *Journal of Physics and Chemistry of Solids* 61 (6):907-913.

Devreux, F., F. Genoud, M. Nechtschein, and B. Villeret. 1987. "On polaron and bipolaron formation in conducting polymers." In *Electronic Properties of Conjugated Polymers*, edited by H. Kuzmany, M. Mehring and S. Roth, 270-276. Berlin: Springer-Verlag.

Devreux, F., and H. Lecavelier. 1987. "Evidence for anomalous diffusion in a conducting polymer." *Physical Review Letters* 59 (22):2585-2587.

Dubois, M., A. Merlin, and D. Billaud. 1999. "Electron spin resonance in lithium and sodium electrochemically intercalated poly(paraphenylene)." *Solid State Communications* 111 (10):571-576.

Dyson, F. J. 1955. "Electron spin resonance absorbtion in metals. II. Theory of electron diffusion and the skin effect." *Physical Review B* 98 (2):349-359.

Eaton, G.R., S.S. Eaton, D.P. Barr, and R.T. Weber. 2010. *Quantitative EPR*. Wien, New York: Springer.

Elliott, R. J. 1954. "Effect of spin-orbit coupling on paramagnetic resonance in semi-conductors." *Physical Review* 96:266-279.

Elsenbaumer, R. L., and L. W. Shacklette. 1986. "Phenylene-Based conducting polymers." In *Handbook of Conducting Polymers*, edited by T. E. Scotheim, 213-263. New York: Marcel Dekker, Inc.

Emin, D. 2013. *Polarons*. Cambridge: Cambridge University Press.

Epstein, A. J. 2007. "Conducting polymers: Electrical conductivity." In *Physical Properties of Polymers. Handbook*, edited by J. E. Mark, 725-744. Springer.

Faridbod, F., M. R. Ganjali, R. Dinarvand, and P. Norouzi. 2008. "Developments in the field of conducting and non-conducting polymer based potentiometric membrane sensors for ions over the past decade." *Sensors* 8 (4):2331-2412.

Fishchuk, I. I., A. K. Kadashchuk, H. Bässler, and D. S. Weiss. 2002. "Nondispersive charge-carrier transport in disordered organic materials containing traps." *Physical Review B* 66 (20):205208/01 - 205208/12.

Friedman, L., and T. Holstein. 1963. "Studies of polaron motion. Part III: The Hall mobility of the small polaron." *Annals of Physics* 21 (3):494-549.

Galkin, A. A., O. Y. Grinberg, A. A. Dubinskii, N. N. Kabdin, V. N. Krymov, V. I. Kurochkin, Y. S. Lebedev, L. G. Oransky, and V. F. Shuvalov. 1977. "EPR spectrometer in 2-mm range for chemical research." *Instruments and Experimental Techniques* 20 (4):1229-1229.

Garnica, M., D. Stradi, S. Barja, F. Calleja, C. Diaz, M. Alcami, N. Martin, de Parga Vazquez, L. Amadeo, F. Martin, and R. Miranda. 2013. "Long-range magnetic order in a purely organic 2D layer adsorbed on epitaxial graphene." *Nature Physics* 9 (6):368-374.

Gebeyehu, D., C. J. Brabec, F. Padinger, T. Fromherz, J. C. Hummelen, D. Badt, H. Schindler, and N. S. Sariciftci. 2001. "The interplay of efficiency and morphology in photovoltaic devices based on interpenetrating networks of conjugated polymers with fullerenes." *Synthetic Metals* 118 (1-3):1-9.

Gebeyehu, D., F. Padinger, T. Fromherz, J. C. Hummelen, and N. S. Sariciftci. 2000. "Photovoltaic properties of conjugated polymer/fullerene composites on large area flexible substrates." *Bulletin of the Chemical Society of Ethiopia* 14 (1):57-68.

Ginder, J. M., A. F. Richter, A. G. MacDiarmid, and A. J. Epstein. 1987. "Insulator-to-metal transition in polyaniline." *Solid State Communications* 63 (2):97-101.

Goldenberg, L. M., A. E. Pelekh, V. I. Krinichnyi, O. S. Roshchupkina, A. F. Zueva, R. N. Lyubovskaja, and O. N. Efimiv. 1990. "Investigation of poly(*p*-phenylene) obtained by electrochemical oxidation of benzene in a BuPyCl-AlCl$_3$melt." *Synthetic Metals* 36 (2):217-228.

Goldenberg, L. M., A. E. Pelekh, V. I. Krinichnyi, O. S. Roshchupkina, A. F. Zueva, R. N. Lyubovskaja, and O. N. Efimiv. 1991. "Investigation of poly(*para*-phenylene) obtained in electrochemical oxidation of benzene in the BuPyCl-AlCl$_3$ melt and in organic solvents with oleum." *Synthetic Metals* 43 (1-2):3071-3074.

Grinberg, O. Y., A. A. Dubinskii, and Y. S. Lebedev. 1983. "Electron-Paramagnetic Resonance of free radicals in a 2-millimeter range of wave-length." *Russian Chemical Reviews* 52 (9):1490-1513.

Gronowitz, S., ed. 1991. *Thiophene and its Derivatives*. Edited by S. Gronowitz. Vol. 44, *The Series of Heterocyclic Compounds*. New York: Wiley.

Gruber, H., H. K. Roth, J. Patzsch, and E. Fanghänel. 1990. "Electrical-Properties of poly(tetrathiafulvalenes)." *Makromolekulare Chemie-Macromolecular Symposia* 37:99-113.

Harigaya, K. 1998. "Long-range excitons in conjugated polymers with ring torsions: poly(para-phenylene) and polyaniline." *Journal of Physics -Condensed Matter* 10 (34):7679-7690.

Hayashi, S., K. Kaneto, K. Yoshino, R. Matsushita, and T. Matsuyama. 1986. "Electrical-Conductivity and Electron-Spin-Resonance studies in iodine-doped polythiophene from semiconductor to metallic regime." *Journal of the Physical Society of Japan* 55 (6):1971-1980.

Heeger, A. J., S. Kivelson, J. R. Schrieffer, and W. P. Su. 1988. "Solitons in conducting polymers." *Reviews of Modern Physics* 60 (3):781-850.

Heeger, A. J., N. S. Sariciftci, and E. B. Namdas. 2010. *Semiconducting and Metallic Polymers*. London: Oxford Univertsity Press.

Hempel, G., A. M. Richter, E. Fanghänel, and H. Schneider. 1990. "NMR-Untersuchungen zu Struktur und Beweglichkeit von substituierten Polyacetylenen." *Acta Polymerica* 41 (10):522-527.

Hennessy, Michael J., Carl D. McElwee, and Peter M. Richards. 1973. "Effect of interchain coupling on electron-spin resonance in nearly one-dimensional systems." *Physical Review B* 7 (3):930-947.

Hinh, L. V., G. Schukat, and E. Fanghänel. 1979. "Tetrathiafulvalene. VII [1]. Arylenverbrückte polymere Tetrathiafulvalene." *Journal für Praktische Chemie* 321 (2):299-307.

Hotta, S. 1997. "Molecular conductive materials: polythiophenes and oligothiophenes." In *Handbook of Organic Conductive Molecules and Polymers*, edited by H. S. Nalwa, 309-387. Chichester, New York: John Wiley & Sons.

Houze, E., and M. Nechtschein. 1996. "ESR in conducting polymers: Oxygen-induced contribution to the linewidth." *Physical Review B* 53 (21):14309-14318.

Hyde, J. S., and L. R. Dalton. 1979. "Saturation-transfer spectroscopy." In *Spin Labeling II: Theory and Application*, edited by L. J. Berliner, 1-70. New York: Academic.

Iida, M., T. Asaji, R. Ikeda, M. B. Inoue, M. Inoue, and D. Nakamura. 1992. "Electron-Paramagnetic Resonance study of intrinsic paramagnetism in poly(aniline trifluoromethanesulfonate), $[(—C_6H_4NH—)(CF_3SO_3)_{0.5} \cdot 0.5H_2O]_x$" *Journal of Materials Chemistry* 2 (3):357-360.

Iida, M., T. Asaji, M. B. Inoue, and M. Inoue. 1993. "EPR study of polyaniline perchlorates - Spin species-related to charge-transport." *Synthetic Metals* 55 (1):607-612.

Im, C., J. M. Lupton, P. Schouwink, S. Heun, H.Becker, and H. Bassler. 2002. "Fluorescence dynamics of phenyl-substituted polyphenylenevinylene–trinitrofluorenone blend systems." *Journal of Chemical Physics* 117:1395-1402.

Janssen, R. A. J., D. Moses, and N. S. Sariciftci. 1994. "Electron and energy transfer processes of photoexcited oligothiophenes onto tetracyanoethylene and C60." *Journal of Chemical Physics* 101 (11):9519-9527.

Jeffries-El, M., and R. D. McCullough. 2007. "Regioregular Polythiophenes." In *Handbook of Conducting Polymers*, edited by T. E. Scotheim and J. R. Reynolds, 9-1 - 9-49. Boca Raton: CRC Press.

Jonston, D. C. 1984. "Thermodynamics of charge-density waves in quasi one-dimensional conductors." *Physical Review Letters* 52 (23):2049-2052.

Kaeriyama, K. 1997. "Synthesis and properties of processable polythiophenes." In *Handbook of Organic Conductive Molecules and Polymers*, edited by H. S. Nalwa, 271-308. Chichester, New York: John Wiley & Sons.

Kahol, P. K. 2000. "Magnetic susceptibility of polyaniline and polyaniline-polymethylmethacrylate blends." *Physical Review B* 62 (21):13803-13804.

Kahol, P. K., and M. Mehring. 1986. "Exchange-coupled pair model for the non-curie-like susceptibility in conducting polymers." *Synthetic Metals* 16 (2):257-264.

Kahol, P. K., A. Raghunathan, B. J. McCormick, and A. J. Epstein. 1999. "High temperature magnetic susceptibility studies of sulfonated polyanilines." *Synthetic Metals* 101 (1-3):815-816.

Kanemoto, K., and J. Yamauchi. 2000a. "Doping-induced variation of electron spin relaxation behavior in polypyrroles." *Synthetic Metals* 114 (1):79-84.

Kanemoto, K., and J. Yamauchi. 2000b. "Electron-spin dynamics of polarons in lightly doped polypyrroles." *Physical Review B* 61 (2):1075-1082.

Kanemoto, K., and J. Yamauchi. 2001. "ESR broadening in conducting polypyrrole because of oxygen: Application to the study of oxygen adsorption." *Journal of Physical Chemistry B* 105 (11):2117-2121.

Kaneto, K., S. Hayashi, S. Ura, and K. Yoshino. 1985. "Electron-Spin-Resonance and transport studies in electrochemically doped polythiophene film." *Journal of the Physical Society of Japan* 54 (3):1146-1153.

Kaniowski, T., S. Niziol, J. Sanetra, M. Trznadel, and A. Proń. 1998. "Optical studies of regioregular poly(3-octylthiophene)s under pressure." *Synthetic Metals* 94 (1):111-114.

Kapil, A., M. Taunk, and S. Chand. 2010. "Preparation and charge transport studies of chemically synthesized polyaniline." *Journal of Materials Science-Materials in Electronics* 21 (4):399-404.

Kawai, T., H. Mizobuchi, S. Okazaki, H. Araki, and K. Yoshino. 1996. "Ferromagnetic tendency of TDAE-fullerene-conducting polymer system." *Japanese Journal of Applied Physics Part 2-Letters* 35 (5B):L640-L643.

Kim, D. H., H. J. Song, S. W. Heo, K. W. Song, and D. K. Moon. 2014. "Enhanced photocurrent generation by high molecular weight random copolymer consisting of benzothiadiazole and quinoxaline as donor materials." *Solar Energy Materials and Solar Cells* 120:94-101.

Kim, Y., S. Cook, S. M. Tuladhar, S. A. Choulis, J. Nelson, J. R. Durrant, D. D. C. Bradley, M. Giles, I. McCulloch, C. S. Ha, and M. Ree. 2006. "A strong regioregularity effect in self-organizing conjugated polymer films and high-efficiency polythiophene: fullerene solar cells." *Nature Materials* 5 (3):197-203.

Kirkpatrick, J., V. Marcon, J. Nelson, K. Kremer, and D. Andrienko. 2007. "Charge mobility of discotic mesophases: A multiscale quantum and classical study." *Physical Review Letters* 98 (22):227402/01–227402/04.

Kivelson, S. 1980. "Hopping conduction and the continuous-time random-walk model." *Physical Review B* 21 (12):5755-5767.

Kivelson, S., and A. J. Heeger. 1988. "Intrinsic conductivity of conducting polymers." *Synthetic Metals* 22 (4):371-384.

Kobayashi, S., and K. Müllen, eds. 2015. *Encyclopedia of Polymeric Nanomaterials*: Springer.

Kon'kin, A. L., V. G. Shtyrlin, R. R. Garipov, A. V. Aganov, A. V. Zakharov, V. I. Krinichnyi, P. N. Adams, and A. P. Monkman. 2002. "EPR, charge transport, and spin dynamics in doped polyanilines." *Physical Review B* 66 (7):075203/01-075203/11.

Kondawar, Subhash B., and Hemlata J. Sharma, eds. 2017. *Conducting Polymer Nanocomposites: Synthesis, Characterizations and Applications*: Studera Press.

Konkin, A., U. Ritter, P. Scharff, G. Mamin, A. Aganov, S. Orlinskii, V. I. Krinichnyi, D. A. M. Egbe, G. Ecke, and H. Romanus. 2014. "Multifrequency X-, W-band ESR study on photo-induced ion radical formation in solid films of mono- and di-fullerenes embedded in conjugated polymers." *Carbon* 77:11-17.

Konkin, A., U. Ritter, P. Scharff, H.-K. Roth, A. Aganov, N. S. Sariciftci, and D. A. M. Egbe. 2010. "Photo-induced charge separation process in (PCBM-C$_{120}$O)/(M3EH-PPV) blend solid film studied by means of X and K-bands ESR at 77 and 120 K" *Synthetic Metals* 160 (5-6):485-489.

Krasicky, P. D., R. H. Silsbee, and J. C. Scott. 1982. "Studies of a polymeric chromium phosphinate - Electron-Spin Resonance and spin dynamics." *Physical Review B* 25 (9):5607-5626.

Krebs, F. C. 2012. *Stability and Degradation of Organic and Polymer Solar Cells*. Chichester, UK: John Wiley & Sons.

Krinichnyi, V. I. 1991a. "Investigation of biological systems by high-resolution 2-mm wave band ESR" *Journal of Biochemical and Biophysical Methods* 23 (1):1-30.

Krinichnyi, V. I. 1991b. "Investigation of biological systems by high resolution 2-mm wave band EPR." *Applied Magnetic Resonance* 2 (1):29-60.

Krinichnyi, V. I. 1995. *2-mm Wave Band EPR Spectroscopy of Condensed Systems*. Boca Raton, FL: CRC Press. Book.

Krinichnyi, V. I. 1996. "The nature and dynamics of nonlinear excitations in conducting polymers. Heteroaromatic polymers." *Russian Chemical Reviews* 65 (6):521-536.

Krinichnyi, V. I. 2000a. "2-mm Waveband electron paramagnetic resonance spectroscopy of conducting polymers (Review)." *Synthetic Metals* 108 (3):173-222.

Krinichnyi, V. I. 2000b. "The nature and dynamics of nonlinear excitations in conducting polymers. Polyaniline." *Russian Chemical Bulletin* 49 (2):207-233.

Krinichnyi, V. I. 2006. "High Field ESR Spectroscopy of Conductive Polymers." In *Advanced ESR Methods in Polymer Research*, edited by S. Schlick, 307-338. Hoboken, NJ: Wiley.

Krinichnyi, V. I. 2008a. "2-mm Waveband saturation transfer electron paramagnetic resonance of conducting polymers." *Journal of Chemical Physics* 129 (13):134510-134518.

Krinichnyi, V. I. 2008b. "The 140-GHz (D-band) saturation transfer electron paramagnetic resonance studies of macromolecular dynamics in conducting polymers." *Journal of Physical Chemistry B* 112 (32):9746-9752.

Krinichnyi, V. I. 2009. "LEPR spectroscopy of charge carriers photoinduced in polymer/fullerene composites." In *Encyclopedia of Polymer Composites: Properties,*

Performance and Applications, edited by M. Lechkov and S. Prandzheva, 417-446. Hauppauge, New York: Nova Science Publishers.

Krinichnyi, V. I. 2014a. "Dynamics of spin charge carriers in polyaniline." *Applied Physics Reviews* 1 (2):021305/01 – 021305/40.

Krinichnyi, V. I. 2014b. "Relaxation and dynamics of spin charge carriers in polyaniline." In *Advances in Materials Science Research*, edited by M. C. Wythers, 109-160. Hauppauge, New York: Nova Science Publishers.

Krinichnyi, V. I. 2016a. "EPR spectroscopy of polymer:fullerene nanocomposites." In *Spectroscopy of Polymer Nanocomposites*, edited by S. Thomas, D. Rouxel and D. Ponnamma, 202-275. Amsterdam: Elsevier.

Krinichnyi, V. I. 2016b. *Multi Frequency EPR Spectroscopy of Conjugated Polymers and Their Nanocomposites*. Boca Raton, FL: CRC Press Taylor & Francis Group. Book.

Krinichnyi, V. I., and A. A. Balakai. 2010. "Light-induced spin localization in poly(3-dodecylthiophen)/PCBM composite." *Applied Magnetic Resonance* 39 (3):319-328.

Krinichnyi, V. I., S. D. Chemerisov, and Y. S. Lebedev. 1997. "EPR and charge-transport studies of polyaniline." *Physical Review B* 55 (24):16233-16244.

Krinichnyi, V. I., N. N. Denisov, H. K. Roth, E. Fanghänel, and K. Lüders. 1998. "Dynamics of paramagnetic charge carriers in poly(tetrathiafulvalene)." *Polymer Science, Series A* 40 (12):1259-1269.

Krinichnyi, V. I., O. Y. Grinberg, I. B. Nazarova, G. I. Kozub, L. I. Tkachenko, M. L. Khidekel, and Y. S. Lebedev. 1985. "Polythiophene and polyacetylene conductors in the 3-cm and 2-mm electron spin resonance bands." *Bulletin of the Academy of Sciences of the USSR, Division of Chemical Science* 34 (2):425-427.

Krinichnyi, V. I., R. Herrmann, E. Fanghänel, W. Mörke, and K. Lüders. 1997. "Spin relaxation and magnetic properties of benzo-1,2,3- trithiolium radical cations." *Applied Magnetic Resonance* 12 (2-3):317-327.

Krinichnyi, V. I., A. L. Konkin, and A. Monkman. 2012. "Electron paramagnetic resonance study of spin centers related to charge transport in metallic polyaniline." *Synthetic Metals* 162 (13-14):1147–1155.

Krinichnyi, V. I., I. B. Nazarova, L. M. Goldenberg, and H. K. Roth. 1998. "Spin dynamics in conducting poly(aniline)." *Polymer Science, Series A* 40 (8):835-843.

Krinichnyi, V. I., A. E. Pelekh, H. K. Roth, and K. Lüders. 1993. "Spin relaxation studies on conducting poly(tetrathiafulvalene)." *Applied Magnetic Resonance* 4 (3):345-356.

Krinichnyi, V. I., A. E. Pelekh, L. I. Tkachenko, and G. I. Kozub. 1992. "Study of spin dynamics intrans -polyacetylene at 2-mm waveband EPR." *Synthetic Metals* 46 (1):1-12.

Krinichnyi, V. I., and H. K. Roth. 2004. "EPR study of spin and charge dynamics in slightly doped poly(3-octylthiophene)" *Applied Magnetic Resonance* 26:395-415.

Krinichnyi, V. I., H. K. Roth, G. Hinrichsen, F. Lux, and K. Lüders. 2002. "EPR and charge transfer in H$_2$SO$_4$-doped polyaniline." *Physical Review B* 65 (15):155205/01-155205/14.

Krinichnyi, V. I., H. K. Roth, and M. Schrödner. 2002. "Spin charge carrier dynamics in poly(*bis*-alkylthioacetylene)" *Applied Magnetic Resonance* 23:1-17.

Krinichnyi, V. I., H. K. Roth, M. Schrödner, and B. Wessling. 2006. "EPR study of polyaniline highly doped by*p*-toluenesulfonic acid" *Polymer* 47 (21):7460-7468.

Krinichnyi, V. I., H. K. Roth, S. Sensfuss, M. Schrödner, and M. Al Ibrahim. 2007. "Dynamics of photoinduced radical pairs in poly(3-dodecylthiophene)/fullerene composite." *Physica E* 36 (1):98-101.

Krinichnyi, V. I., S. V. Tokarev, H. K. Roth, M. Schrödner, and B. Wessling. 2006. "EPR study of charge transfer in polyaniline highly doped by *p*-toluenesulfonic acid." *Synthetic Metals* 156 (21-24):1368-1377.

Krinichnyi, V. I., P. A. Troshin, and N. N. Denisov. 2008. "The effect of fullerene derivative on polaronic charge transfer in poly(3-hexylthiophene/fullerene compound." *Journal of Chemical Physics* 128 (16):164715/01 - 164715/7.

Krinichnyi, V. I., E. I. Yudanova, and N. N. Denisov. 2014. "The role of spin exchange in charge transfer in low-bandgap polymer:fullerene bulk heterojunctions." *Journal of Chemical Physics* 141 (4):044906/01 - 044906/11.

Krinichnyi, V. I., E. I. Yudanova, and N. G. Spitsina. 2010. "Light-induced EPR study of poly(3-alkylthiophene)/fullerene composites." *Journal of Physical Chemistry C* 114 (39):16756–16766.

Krinichnyi, V. I., E. I. Yudanova, and B. Wessling. 2013. "Influence of spin–spin exchange on charge transfer min PANI-ES/P3DDT/PCBM composite." *Synthetic Metals* 179:67–73.

Krinichnyi, V. I. 2017. *2-mm Wave Band EPR Spectroscopy of Condensed Systems*. Boca Raton, FL: CRC Press Taylor & Francis Group. Book.

Kuivalainen, P., H. Stubb, P. Raatikainen, and C. Holmstrom. 1983. "Electron Spin Resonance studies of magnetic defects in $FeCl_3$-doped polyparaphenylene (p-C_6H_4)$_x$." *Journal de Physique Colloques* 44:C3-757-C3-760.

Kunugi, Y., Y. Harima, K. Yamashita, N. Ohta, and S. Ito. 2000. "Charge transport in a regioregular poly(3-octylthiophene) film." *Journal of Materials Chemistry* 10 (12):2673-2677.

Kuroda, S. 2002. "ESR and ENDOR spectroscopy of solitons and polarons in conjugated polymers." In *EPR in the 21st Century: Basics and Applications to Material, Life and Earth Sciences*, edited by A. Kawamori, J. Yamauchi and H. Ohta, 113-124. Amsterdam, Tokio: Elsevier Science B.V.

Lacaze, P. C., S. Aeiyach, and J. C. Lacroix. 1997. "Poly(*p*-phenylenes): preparation, techniques and properties." In *Handbook of Organic Conductive Molecules and Polymers*, edited by H. S. Nalwa, 205-270. Chichester, New York: Wiley.

Lan, Y. K., and C. I. Huang. 2008. "A theoretical study of the charge transfer behavior of the highly regioregular poly-3-hexylthiophene in the ordered state." *Journal of Physical Chemistry B* 112 (47):14857-14862.

Launay, J. P., and M. Verdaguer. 2013. *Electrons in Molecules: From Basic Principles to Molecular Electronics*. Oxford, New York: Oxford University Press.

Lebedev, Y. S., and V. I. Muromtsev. 1972. *EPR and Relaxation of Stabilized Radicals (Russ)*. Moscow: Khimija. Original edition, [Я.С. Лебедев, В.И. Муромцев, ЭПР и релаксация стабилизированных радикалов, М.: Химия], 1972, 256 с.

Lee, C. H., G. Yu, D. Moses, K. Pakbaz, C. Zhang, N. S. Sariciftci, A. J. Heeger, and F. Wudl. 1993. "Sensitization of the photoconductivity of conducting polymers by C-60 - photoinduced electron-transfer." *Physical Review B* 48 (20):15425-15433.

Lee, K. H., A. J. Heeger, and Y. Cao. 1993. "Reflectance of polyaniline protonated with camphor sulfonic acid - Disordered metal on the metal-insulator boundary."*Physical Review B* 48 (20):14884-14891.

Lee, K. H., R. A. J. Janssen, N. S. Sariciftci, and A. J. Heeger. 1994. "Direct evidence of photoinduced electron-transfer in conducting-polymer-C60 composites Infrared photoexcitation spectroscopy." *Physical Review B* 49 (8):5781-5784.

Lee, K., A. J. Heeger, and Y. Cao. 1995. "Reflectance spectra of polyaniline." *Synthetic Metals* 72 (1):25-34.

List, E. J. W., U. Scherf, K. Mullen, W. Graupner, C. H. Kim, and J. Shinar. 2002. "Direct evidence for singlet-triplet exciton annihilation in π-conjugated polymers." *Physical Review B* 66 (23):235203-235207.

Little, W. A. 1964. "Possibility of synthesizing an organic superconductor." *Physical Review* 134 (6A):1416-1424.

Lloyd, M. T., Y. F. Lim, and G. G. Malliaras. 2008. "Two-step exciton dissociation in poly(3-hexylthiophene)/fullerene heterojunctions." *Applied Physics Letters* 92 (14):143308-143310.

Lloyd, S. 1993. "A potentially realizable quantum computer." *Science* 261:1569-1571.

Long, A. R., and N. Balkan. 1980. "AC loss in amorphous germanium" *Philosophical Magazine B* 41(3):287-305.

Long, S. M., K. R. Cromack, A. J. Epstein, Y. Sun, and A. G. MacDiarmid. 1994. "ESR of pernigraniline base solutions revisited." *Synthetic Metals* 62 (3):287-289.

Lu, Y., ed. 1988. *Solitons and Polarons in Conducting Polymers*. River Edge, NJ, Singapore: World Scientific.

Lupton, J. M., D. R. McCamey, and C. Boehme. 2010. "Coherent spin manipulation in molecular semiconductors: Getting a handle on organic spintronics." *Chemical Physics Chemistry* 11 (14):3040-3058.

Łuźny, W., M. Trznadel, and A. Proń. 1996. "X-Ray diffraction study of reoregular poly(3-alkylthiophenes)" *Synthetic Metals* 8171-74.

Madhukar, A., and W. Post. 1977. "Exact solution for the diffusion of a particle in a medium with site diagonal and off-diagonal dynamic disorder." *Physical Review Letters* 39 (22):1424-1427.

Maekawa, S., ed. 2006. *Concepts in Spin Electronics*. Oxford: Oxford University Press.

Marchant, S., and P. J. S. Foot. 1995. "Poly(3-hexylthiophene)-zinc oxide rectifying junctions."*Journal of Materials Science-Materials in Electronics* 6 (3):144-148.

Mardalen, J., E. J. Samuelsen, O. R. Konestabo, M. Hanfland, and M. Lorenzen. 1998. "Conducting polymers under pressure: synchrotron x-ray determined structure and structure related properties of two forms of poly(octyl-thiophene)." *Journal of Physics - Condensed Matter* 10:7145-7154.

Marumoto, K., Y. Muramatsu, N. Takeuchi, and S. Kuroda. 2003. "Light-induced ESR studies of polarons in regioregular poly(3-alkylthiophene)-fullerene composites." *Synthetic Metals* 135 (1-3):433-434.

Marumoto, K., N. Takeuchi, T. Ozaki, and S. Kuroda. 2002. "ESR studies of photogenerated polarons in regioregular poly(3-alkylthiophene)-fullerene composite."*Synthetic Metals* 129:239-247.

Masters, J. G., J. M. Ginder, A. G. MacDiarmid, and A. J. Epstein. 1992. "Thermochromism in the insulating forms of polyaniline - role of ring-torsional conformation." *Journal of Chemical Physics* 96 (6):4768-4778.

Masubuchi, S., R. Imai, K. Yamazaki, S. Kazama, J. Takada, and T. Matsuyama. 1999. "Structure and electrical transport property of poly(3-octylthiophene)." *Synthetic Metals* 101 (1-3):594-595.

Masubuchi, S., S. Kazama, K. Mizoguchi, M. Honda, K. Kume, R. Matsushita, and T. Matsuyama. 1993. "Metallic transport-properties in electrochemically as-grown and heavily-doped polythiophene and poly(3-methylthiophene)." *Synthetic Metals* 57 (2-3):4962-4967.

Matthews, M. J., M. S. Dresselhaus, N. Kobayashi, T. Enoki, M. Endo, and K. Nishimura. 1999. "Localized spins in partially carbonized polyparaphenylene." *Physical Review B* 60 (7):4749-4757.

McCullough, R. D., R. D. Lowe, M. Jayaraman, P. C. Ewbank, and D. L. Anderson. 1993. "Synthesis and physical-properties of regiochemically well-defined, head-to-tail coupled poly(3-alkylthiophenes)." *Synthetic Metals* 55 (2-3):1198-1203.

Menon, R. 1997. "Charge Transport in Conducting Polymers." In *Handbook of Organic Conductive Molecules and Polymers*, edited by H. S. Nalwa, 47-145. Chichester: John Wiley & Sons.

Menon, R., C. O. Yoon, D. Moses, and A. J. Heeger. 1997. "Metal-Insulator transition in doped conducting polymers." In *Handbook of Conducting Polymers*, edited by T. A. Skotheim, R. L. Elsenbaumer and J. R. Reynolds, 27-84. New York: Marcel Dekker.

Misra, S. K., ed. 2011. *Multifrequency Electron Paramagnetic Resonance. Theory and Applications*. 2 vols. Vol. 2. Weinheim: Wiley-VCH.

Misra, S. K., ed. 2014. *Handbook of Multifrequency Electron Paramagnetic Resonance: Data and Techniques*. Weinheim, Germany: Wiley-VCH.

Mizoguchi, K., M. Honda, S. Masubuchi, S. Kazama, and K. Kume. 1994. "Study of spin dynamics and electronic-structure in polythiophene heavily-doped with ClO_4." *Japanese Journal of Applied Physics Part 2-Letters* 33 (9A):L1239-L1241.

Mizoguchi, K., and S. Kuroda. 1997. "Magnetic properties of conducting polymers." In *Handbook of Organic Conductive Molecules and Polymers*, edited by H. S. Nalwa, 251-317. Chichester, New York: John Wiley & Sons.

Molin, Y. N., K. M. Salikhov, and K. I. Zamaraev. 1980. *Spin Exchange*. Berlin: Springer. [К. И. Замараев, Ю. Н. Молин, К. М. Салихов, Спиновыйобмен. Теория и физико-химические приложения, Наука СО: Новосибирск, 1977, 320 с.].

Moon, J. S., J. Jo, and A. J. Heeger. 2012. "Nanomorphology of PCDTBT:$PC_{70}BM$ bulk heterojunction solar cells." *Advanced Energy Materials* 2 (3):304-308.

Moraes, F., D. Davidov, M. Kobayashi, T. C. Chung, J. Chen, A. J. Heeger, and F. Wudl. 1985. "Doped poly(thiophene) - Electron-Spin Resonance determination of the magnetic susceptibility." *Synthetic Metals* 10 (3):169-179.

Mott, N. F., and E. A. Davis. 2012. *Electronic Processes in Non-Crystalline Materials*, *Oxford Classic Texts in the Physical Sciences*. Oxford: Clarendon Press.

Nagels, P. 1980. *The Hall Effect and its Application*. New York: Plenum.

Nalwa, H. S., ed. 1997. *Handbook of Organic Conductive Molecules and Polymers*. Edited by H. S. Nalwa. 1-4 vols. Vol. 1-4. Chichester, New York: John Wiley & Sons.

Nalwa, H. S., ed. 2001. *Advanced Functional Molecules and Polymers: Electronic and Photonic Properties*. Edited by H. S. Nalwa. Vol. 3. Boca Raton: CRC Press.

Nechtschein, M. 1997. "Electron spin dynamics." In *Handbook of Conducting Polymers*, edited by T. A. Skotheim, R. L. Elsenbaumer and J. R. Reynolds, 141-163. New York: Marcel Dekker.

Nelson, J. 2003. "Diffusion-limited recombination in polymer-fullerene blends and its influence on photocurrent collection." *Physical Review B* 67 (15):155209/01-155209/10.

Niklas, Jens, Kristy L. Mardis, Brian P. Banks, Gregory M. Grooms, Andreas Sperlich, Vladimir Dyakonov, Serge Beauprě, Mario Leclerc, Tao Xu, Luping Yue, and Oleg G. Poluektov. 2013. "Highly-efficient charge separation and polaron delocalization in polymer–fullerene bulk-heterojunctions: a comparative multi-frequency EPR and DFT study." *Physical Chemistry Chemical Physics* 15 (24):9562-9574.

Obrzut, J., and K. A. Page. 2009. "Electrical conductivity and relaxation in poly(3-hexylthiophene)." *Physical Review B* 80 (19):195211/01 - 195211/07.

Österbacka, R., C. P. An, X. M. Jiang, and Z. V. Vardeny. 2001. "Delocalized polarons in self-assembled poly(3-hexylthiophene) nanocrystals." *Synthetic Metals* 116 (1-3):317-320.

Owens, J. 1977. "Evidence for zero-field fluctuations in Cr^{3+} near the phase transition in $NH_4Al(SO_4)_2 \cdot 12H_20$." *Physica Status Solidi B* 79 (2):623-628.

Pagliaro, M., G. Palmisano, and R. Ciriminna. 2008. *Flexible Solar Cells*: Wiley-WCH.

Park, S. H., A. Roy, S. Beaupre, S. Cho, N. Coates, J. S. Moon, D. Moses, M. Leclerc, K. Lee, and A. J. Heeger. 2009. "Bulk heterojunction solar cells with internal quantum efficiency approaching 100%." *Nature Photonics* 3:297-302.

Parneix, J. P., and M. El Kadiri. 1987. "Frequency- and temperature-dependent dielectric losses in lightly doped conducting polymers." In *Electronic Properties of Conjugated Polymers*, edited by H. Kuzmany, M. Mehring and S. Roth, 23-26. Berlin: Springer-Verlag.

Patzsch, J. 1991. "Elektrische Eigenschaften von polymeren Tetrathiafulvalen (PTTF)." Ph.D., Technische Hochschule Leipzig.

Patzsch, J., and H. Gruber. 1992. "Small Polarons in Polymeric Polytetrathiafulvalenes (PTTF)." In *Electronic Properties of Polymers*, edited by H. Kuzmany, M. Mehring and S. Roth, 121-124. Berlin: Springer-Verlag.

Peierls, R. E. 1996. *Quantum Theory of Solids*. London, U.K.: Oxford University Press.

Pelekh, A. E., L. M. Goldenberg, and V. I. Krinichnyi. 1991. "Study of dopped polypyrrole by the spin probe method at 3-cm and 2-mm waveband EPR." *Synthetic Metals* 44 (2):205-211.

Pietronero, L. 1983. "Ideal conductivity of carbon π-polymers and intercalation compounds." *Synthetic Metals* 8:225-231.

Poluektov, O. G., S. Filippone, N. Martín, A. Sperlich, C. Deibel, and V. Dyakonov. 2010. "Spin signatures of photogenerated radical anions in polymer-[70]fullerene bulk heterojunctions: High frequency pulsed EPR spectroscopy." *Journal of Physical Chemistry B* 114 (45):14426-14429.

Poole, Ch P. 1983. *Electron Spin Resonance, A Comprehensive Treatise on Experimental Techniques*. New York: John Wiley & Sons.

Poortmans, J., and V. Arkhipov, eds. 2006. *Thin Film Solar Cells: Fabrication, Characterization and Applications* Edited by J. Poortmans and V. Arkhipov. West Sussex: Wiley.

Pratt, F. L., S. J. Blundell, W. Hayes, K. Nagamine, K. Ishida, and A. P. Monkman. 1997. "Anisotropic polaron motion in polyaniline studied by muon spin relaxation." *Physical Review Letters* 79 (15):2855-2858.

Quang, T. 1987. PhD, *Chemical*, Carl Schorlemmer Technical University Merseburg.

Raghunathan, A., P. K. Kahol, J. C. Ho, Y. Y. Chen, Y. D. Yao, Y. S. Lin, and B. Wessling. 1998. "Low-temperature heat capacities of polyaniline and polyaniline polymethylmethacrylate blends." *Physical Review B* 58 (24):R15955-R15958.

Ranby, B., and J. F. Rabek. 2011. *ESR Spectroscopy in Polymer Research Series: Polymers - Properties and Applications (Book 1)*: Springer.

Reddoch, A., and S. Konishi. 1979. "The solvent effect on di-tert- butyl nitroxide. A dipole-dipole model for polar solutes in polar solvents." *Journal of Chemical Physics* 70:2121.

Reufer, M., P. G. Lagoudakis, M. J. Walter, J. M. Lupton, J. Feldmann, and U. Scherf. 2006. "Evidence for temperature-independent triplet diffusion in a ladder-type conjugated polymer." *Phys. Rev. B* 74 (24):241201-241204.

Richter, A. M., J. M. Richter, N. Beye, and E. Fanghänel. 1987. "Organische Elektronenleiter und Vorstufen. V. Synthese von Poly(organylthio-acetylenen)." *Journal Praktische Chemie* 329 (5):811-816.

Rodriguez, J., H. J. Grande, and T. F. Otero. 1997. "Polypyrroles: From basic research to technological applications." In *Handbook of Organic Conductive Molecules and Polymers*, edited by H. S. Nalwa, 415-468. Chichester, New York: Wiley.

Roth, H. K., W. Brunner, G. Volkel, M. Schrödner, and H. Gruber. 1990. "ESR and ESE studies on polymer semiconductors of weakly doped poly(tetrathiafulvalene)." *Makromolekulare Chemie-Macromolecular Symposia* 34:293-307.

Roth, H. K., H. Gruber, E. Fanghänel, and Trinh vu Quang. 1988. "ESR on polymer semiconductors of poly(tetrathiafulvalene)." *Progress in Colloid Polymer Science* 78:75-78.

Roth, H. K., H. Gruber, E. Fanghänel, A. M. Richter, and W. Horig. 1990. "Laser-Induced generation of highly conducting areas in poly(*bis*-alkylthioacetylenes)." *Synthetic Metals* 37:151-164.

Roth, H. K., H. Gruber, G. Voelkel, W. Brunner, and E. Fanghänel. 1989. "Electron spin resonance and relaxation studies on conducting poly(tetrathiafulvalenes)." *Progress in Colloid and Polymer Science* 80 (1):254-263.

Roth, H. K., F. Keller, and H. Schneider. 1984. *Hochfrequenzspectroskopie in der Polymerforschung*. Berlin: Academie Verlag.

Roth, H. K., and V. I. Krinichnyi. 2003. "Spin and charge transport in poly(3-octylthiophene)." *Synthetic Metals* 137 (1-3):1431-1432.

Roth, H. K., V. I. Krinichnyi, M. Schrödner, and R. I. Stohn. 1999. "Electronic properties of laser modified poly(*bis*-alkylthio-acetylene)" *Synthetic Metals* 101 (1-3):832-833.

Rouxel, Didier, Sabu Thomas, and Deepalekshmi Ponnamma, eds. 2016. *Spectroscopy of Polymer Nanocomposites*. 1 ed. Oxford, Cambridge, Amsterdam: Elsevier. Original edition, Spectroscopy of Polymer Nanocomposites.

Sakamoto, H., N. Kachi, K. Mizoguchi, K. Yoshioka, S. Masubuchi, and S. Kazama. 1999. "Origin of ESR linewidth for polypyrrole." *Synthetic Metals* 101 (1-3):481-481.

Salamone, J. C., ed. 1996. *Polymeric Material Encyclopedia*. Edited by J. C. Salamone. 12 vols. Boca Raton, Fl.: CRC Press.

Salaneck, W. R., D. T. Clark, and E. J. Samuelsen, eds. 1991. *Science and Applications of Conducting Polymers, Papers from the Sixth European Industrial Workshop*. Edited by W. R. Salaneck, D. T. Clark and E. J. Samuelsen. New York (Bristol): Adam Hilger.

Samuelsen, E. J., and J. Mardalen. 1997. "Structure of polythiophenes." In *Handbook of Organic Conductive Molecules and Polymers*, edited by H. S. Nalwa, 87-120. Chichester, New York: John Wiley.

Sariciftci, N. S., and A. J. Heeger. 1995. "Photophysics of semiconducting polymer C-60 composites - A comparative-study." *Synthetic Metals* 70 (1-3):1349-1352.

Sariciftci, N. S., A. J. Heeger, and Y. Cao. 1994. "Paramagnetic susceptibility of highly conducting polyaniline - Disordered metal with weak electron-electron interactions (Fermi glass)." *Physical Review B* 49 (9):5988-5992.

Sariciftci, N. S., A. C. Kolbert, Y. Cao, A. J. Heeger, and A. Pines. 1995. "Magnetic resonance evidence for metallic state in highly conducting polyaniline." *Synthetic Metals* 69 (1-3):243-244.

Saunders, B. R., R. J. Fleming, and K. S. Murray. 1995. "Recent advances in the physical and spectroscopic properties of polypyrrole films, particularly those containing transition-metal complexes as counteranions." *Chemistry of Materials* 7 (6):1082-1094.

Sauvajol, J. L., D. Bormann, M. Palpacuer, J. P. Lere-Porte, J. J. E. Moreau, and A. J. Dianoux. 1997. "Low and high-frequency vibrational dynamics as a function of structural order in polythiophene." *Synthetic Metals* 84 (1-3):569-570.

Scharli, M., H. Kiess, G. Harbeke, W. Berlinger, K. W. Blazey, and K. A. Muller. 1987. "ESR of BF4-doped poly(3-methylthiophene)." In *Electronic Properties of Conjugated Polymers*, edited by H. Kuzmany, M. Mehring and S. Roth, 277-280. Berlin: Springer-Verlag.

Schlick, S., ed. 2006. *Advanced ESR Methods in Polymer Research*. Edited by S. Schlick. New York: John Wiley & Sons Inc.

Schmeisser, D., A. Bartl, L. Dunsch, H. Naarmann, and W. Gopel. 1998. "Electronic and magnetic properties of polypyrrole films depending on their one-dimensional and two-dimensional microstructures." *Synthetic Metals* 93 (1):43-58.

Schultz, N. A., M. C. Scharber, C. J. Brabec, and N. S. Sariciftci. 2001. "Low-temperature recombination kinetics of photoexcited persistent charge carriers in conjugated polymer/fullerene composite films." *Physical Review B* 64 (24):245210/01-245210/07.

Scotheim, T. E., R. L. Elsenbaumer, and J. R. Reynolds, eds. 1997. *Handbook of Conducting Polymers*. Edited by T. E. Scotheim, R. L. Elsenbaumer and J. R. Reynolds. New York: Marcel Dekker.

Scotheim, T. E., and J. R. Reynolds, eds. 2007. *Handbook of Conducting Polymers*. Edited by T. E. Scotheim and J. R. Reynolds. Vol. 3d. Boca Raton: CRC Press.

Scott, J. C., P. Pfluger, M. T. Kroumbi, and G. B. Street. 1983. "Electron-spin-resonanse studies of pyrrole polymers: Evidence for bipolarons" *Physical Review B* 28 (4):2140-2145.

Scrosati, B., ed. 1993. *Application of Electroactive Polymers*. Edited by B. Scrosati. London: Chapman & Hall.

Sersen, F., G. Cik, and P. Veis. 2003. "Study of conformational changes in poly(3-dodecylthiophene) dependent on backbone stereoregularity using a spin-probe technique." *Journal of Applied Polymer Science* 88 (9):2215-2223.

Shaheen, S. E., C. J. Brabec, N. S. Sariciftci, F. Padinger, T. Fromherz, and J. C. Hummelen. 2001. "2.5% Efficient organic plastic solar cells." *Applied Physics Letters* 78 (6):841-843.

Sharma, G. D. 2010. "Advances in nano-structured organic solar cells." In *Physics of Nanostructured Solar Cells*, edited by V. Badescu and M. Paulescu, 361−460. New York: Nova Science Publishers.

Shchegolikhin, A. N., I. V. Yakovleva, and M. Motyakin. 1995. "Optical-Properties of poly(diacetylene) block-copoly(ether-urethanes), containing covalently bound nitroxyl spin labels in the main-chain." *Synthetic Metals* 71 (1-3):2091-2092.

Shen, L., M. Zeng, Q. Wu, Z. Bai, and Y. P. Feng. 2014. "Graphene spintronics: Spin generation and manipulation in graphene." In *Graphene Optoelectronics: Synthesis, Characterization, Properties, and Applications*, edited by Rashid bin Mohd Yusoff, 167-188. Weinheim: Wiley.

Silinsh, E. A., M. V. Kurik, and V. Chapek. 1988. *Electronic Processes in Organic Molecular Crystals: The Phenomena of Localization and Polarization (Russian)*. Riga: Zinatne. Original edition, [Силиньш, Э.А., Курик, М.В., Чапек, В., Электронные процессы в органических молекулярных кристаллах: Явления локализации и поляризации, Рига: Зинатне], 1988, 329 с.

Singleton, J. 2001. *Band Theory and Electronic Properties of Solids*, *Oxford Master Series in Condensed Matter Physics*. Oxford: Oxford University Press.

So, F., J. Kido, and P. Burrows. 2008. "Organic light-emitting devices for solid-state lighting." *Materials Research Society Bulletin* 33 (7):663−669.

Springborg, M. 1992. "The electronic-properties of polythiophene." *Journal of Physics - Condensed Matter* 4 (1):101-120.

Stafstrom, S., and J. L. Brédas. 1988. "Band-Structure calculations for the polaron lattice in the highly doped regime of polyacetylene, polythiophene, and polyaniline." *Molecular Crystals and Liquid Crystals* 160:405-420.

Stafström, S., and J. L. Brédas. 1988. "Evolution of the electronic-structure of polyacetylene and polythiophene as a function of doping level and lattice conformation." *Physical Review B* 38 (6):4180-4191.

Sun, S. S., and N. S. Sariciftci, eds. 2005. *Organic Photovoltaics: Mechanisms, Materials, and Devices (Optical Engineering)*. Edited by S. S. Sun and N. S. Sariciftci, *Optical Science and Engineering Series*. Boca Raton: CRC Press.

Tachiya, M., and K. Seki. 2010. "Theory of bulk electron-hole recombination in a medium with energetic disorder."*Physical Review B* 82 (8):085201/01 - 085201/08.

Taka, T., O. Jylha, A. Root, E. Silvasti, and H. Osterholm. 1993. "Characterization of undoped poly(3-octylthiophene)." *Synthetic Metals* 55 (1):414-419.

Takeda, K., H. Hikita, Y. Kimura, H. Yokomichi, and K. Morigaki. 1998. "Electron spin resonance study of light-induced annealing of dangling bonds in glow discharge hydrogenated amorphous silicon: Deconvolution of electron spin resonance spectra." *Japanese Journal of Applied Physics Part 1-Regular Papers Short Notes & Review Papers* 37 (12A):6309-6317.

Tanaka, H., N. Hasegawa, T. Sakamoto, K. Marumoto, and S. I. Kuroda. 2007. "Light-induced ESR studies of quadrimolecular recombination kinetics of photogenerated charge carriers in regioregular poly(3-alkylthiophene)/C-60 composites: Alkyl chain

dependence." *Japanese Journal of Applied Physics Part 1-Regular Papers Brief Communications & Review Papers* 46 (8A):5187-5192.

Taunk, M., and S. Chand. 2014. "Variable range hopping transport in polypyrrole composite films." In *Physics of Semiconductor Devices*, edited by V. K. Jain and A. Verma, 903-904. Heidelberg New York Dordrecht London: Springer.

Tourillon, G., D. Gourier, F. Garnier, and D. Vivien. 1984. "Electron spin resonance study of electrochemically generated poly(thiophene) and derivatives." *Journal of Physical Chemistry* 88:1049.

Traven', V. F. 1989. *Electronic Structure and Properties of Organic Molecules (Russian)*. Moscow: Khimija. Original edition, [Травень, В. Ф. "Электронная структура и свойства органических молекул." Москва: Химия]. 1989.

Trinh, V. Q., L. V. Hinh, G. Shukat, and E. Fanghänel. 1989. "Tetrathiafulvalene. XXV [1]. Konjugativ verknüpfte polymere Tetrathiafulvalene (TTF)." *Journal für Praktische Chemie* 331 (5):826-834.

Troisi, A., and G. J. Orlandi. 2006. "Dynamics of the intermolecular transfer integral in crystalline organic semiconductors." *Journal of Physical Chemistry A* 110 (11):4065–4070.

Van Vooren, A., J.-S. Kim, and J. Cornil. 2008. "Intrachain versus interchain electron transport in poly(fluorene-alt-benzothiadiazole): A quantum-chemical insight." *Chem Phys Chem* 9 (7):989-993.

Vonsovskii, S. V. 1974. *Magnetism. Magnetic Properties of Dia-, Para-, Ferro-, Antiferro-, and Ferrimagnetics*. 2 vols. Vol. 1,2. New York: John Wiley & Sons. Original edition, [Вонсовский, С.В., Магнетизм, Магнитные свойства диа-, пара-, ферро-, антиферро- и ферримагнетиков, М.: Наука], 1971, 1032 с.

Wan, M. X. 2008. *Conducting Polymers with Micro or Nanometer Structure*. Berlin, Heidelberg, New York: Springer.

Wang, Z. H., C. Li, E. M. Scherr, A. G. MacDiarmid, and A. J. Epstein. 1991. "3 Dimensionality of metallic states in conducting polymers - Polyaniline." *Physical Review Letters* 66 (13):1745-1748.

Wang, Z. H., A. Ray, A. G. MacDiarmid, and A. J. Epstein. 1991. "Electron localization and charge transport inpoly(*o*-toluidine) - A model polyaniline derivative." *Physical Review B* 43 (5):4373-4384.

Wang, Z. H., E. M. Scherr, A. G. MacDiarmid, and A. J. Epstein. 1992. "Transport and EPR studies of polyaniline - A quasi-one-dimensional conductor with 3-dimensional metallic states." *Physical Review B* 45 (8):4190-4202.

Weil, J. A., J. R. Bolton, and J. E. Wertz. 2007. *Electron Paramagnetic Resonance: Elementary Theory and Practical Applications*. Vol. 2d. New York: Wiley-Interscience.

Wertz, J. E., and J. R.Bolton. 2013. *Electron Spin Resonance: Elementary Theory and Practical Applications*: Springer Verlag.

Wessling, B. 1997. "Metallic properties of conductive polymers due to dispersion." In *Handbook of Organic Conductive Molecules and Polymers*, edited by H. S. Nalwa, 497-632. Chichester: John Wiley & Sons.

Wessling, B. 2010. "New insight into organic metal polyaniline morphology and structure." *Polymers* 2:786-798.

Wessling, B., D. Srinivasan, G. Rangarajan, T. Mietzner, and W. Lennartz. 2000. "Dispersion-induced insulator-to-metal transition in polyaniline." *European Physical Journal E* 2 (3):207-210.

Westerling, M., R. Osterbacka, and H. Stubb. 2002. "Recombination of long-lived photoexcitations in regioregular polyalkylthiophenes." *Physical Review B* 66 (16):165220/01 - 165220/07.

Williams, J. M., J. R. Ferraro, R. J. Thorn, K. D. Carlson, U. Geiser, H. H. Wang, A. M. Kini, and M. H. Whangboo. 1992. *Organic Superconductors (Including Fullerenes): Synthesis, Structure, Properties, and Theory*. New Jersey: Prentice-Hall, Inc., Englewood Cliffs.

Winter, H., G. Sachs, E. Dormann, R. Cosmo, and H. Naarmann. 1990. "Magnetic-Properties of spin-labeled polyacetylene." *Synthetic Metals* 36 (3):353-365.

Wohlgenannt, M., K. Tandon, S. Mazumdar, S. Ramasesha, and Z. V. Vardeny. 2001. "Formation cross-sections of singlet and triplet excitons in p-conjugated polymers." *Nature* 409:494-497.

Wolf, S. A., D. D. Awschalom, R. A. Buhrman, J. M. Daughton, S. von Molnar, M. L. Roukes, A. Y. Chtchelkanova, and D. M. Treger. 2001. "Spintronics: A spin-based electronics vision for the future." *Science* 294 (5546):1488-1495.

Wong, C. P., ed. 1993. *Polymers for Electronic & Photonic Application*. Boston, USA: Elsevier - Academic Press Inc.

Wu, T. M., H. L. Chang, and Y. W. Lin. 2009. "Synthesis and characterization of conductive polypyrrole/multi-walled carbon nanotubes composites with improved solubility and conductivity." *Composites Science and Technology* 69 (5):639-644.

Xie, S. J., L. M. Mei, and D. L. Lin. 1994. "Transitio between bipolaron and polaron states in doped heterocycle polymers." *Physical Review B* 50 (18):13364-13370.

Yamauchi, T., H. M. Najib, Y. W. Liu, M. Shimomura, and S. Miyauchi. 1997. "Positive temperature coefficient characteristics of poly(3-alkylthiophene)s." *Synthetic Metals* 84 (1-3):581-582.

Yan, B., N. A. Schultz, A. L. Efros, and P. C. Taylor. 2000. "Universal distribution of residual carriers in tetrahedrally coordinated amorphous semiconductors." *Physical Review Letters* 84 (18):4180-4183.

Yanilkin, V. V., N. V. Nastapova, V. I. Morozov, V. P. Gubskaya, F. G. Sibgatullina, L. S. Berezhnaya, and I. A. Nuretdinov. 2007. "Competitive conversions of carbonyl-containing methanofullerenes induced by electron transfer." *Russian Journal of Electrochemistry* 43 (2):184-203.

Yazawa, K., Y. Inoue, T. Shimizu, M. Tansho, and N. Asakawa. 2010. "Molecular dynamics of regioregular poly(3-hexylthiophene) investigated by NMR relaxation and an interpretation of temperature dependent optical absorption." *Journal of Physical Chemistry B* 114 (3):1241-1248.

Yudanova, E. I., V.R. Bogatyrenko, and V. I. Krinichnyi. 2016. "EPR Study of spin interactions in poly(3-dodecylthiophene):fullerene/polyaniline:*p*-toluenesulfonic acid composite." *High Energy Chemistry* 50 (2):132-138.

Zanardi, C., F. Terzi, L. Pigani, and R. Seeber. 2009. Electrode coatings consisting of polythiophene-based composites containing metal centres. In *Encyclopedia of Polymer Composites: Properties, Performance and Applications*, edited by M. Lechkov and S. Prandzheva. Hauppauge, NY: Nova Science Publishers.

Zaumseil, J. 2014. "P3HT and other polythiophene field-effect transistors." In *P3HT Revisited: From Molecular Scale to Solar Cell Devices*, edited by S. Ludwigs, 107-137.

Zuppiroli, L., S. Paschen, and M. N. Bussac. 1995. "Role of the dopant counterions in the transport and magnetic-properties of disordered conducting polymers." *Synthetic Metals* 69 (1-3):621-624.

ABOUT THE AUTHOR

Victor I. Krinichnyi
Institute of Problems of Chemical Physics,
Chernogolovka, Russian Federation
Email: kivirus@gmail.com

Victor I. Krinichnyi was born in Kazan, USSR, in 1953. He received the diploma in radiophysics and electronics from the Kazan State University, USSR, in 1975. He was employed as an engineer (1975-1979), a principal engineer (1979-1982), a young scientific researcher (1982-1987), a scientific researcher (1987-1992), a senior scientific researcher (1992-1996) and a leading scientific researcher (1997-present) in the former Institute of Chemical Physics in Chernogolovka RAS, currently the Institute of Problems of Chemical Physics RAS, Chernogolovka, Moscow Region, Russia. He received the Ph.D. (in 1986) and Sci.D. (in 1993) degrees in physics and mathematics from the Institute of Problems of Chemical Physics RAS. His research interests resulting from practical application of multifrequency EPR spectroscopy include the relaxation and dynamics of non-linear charge carriers, solitons and polarons, in conjugated polymers and their nanocomposites, mechanism of charge transport in molecular crystals, spin phenomena in condensed systems as well as organic molecular electronics, photonics and spintronics. He collaborated as invited summer researcher in the Center of Atomic Energy (1994), Grenoble, France, Merseburg (1994), Jena (1997), Stuttgart (2001) and Ilmenau (2010, 2017) Universities, Institute for Physical High Technology (2004), Jena, and Polymer Research Institute (1998, 2000, 2002, 2003, 2004, 2005), Rudolstadt, Germany. He is the author of two monographs, "2-mm Wave Band EPR Spectroscopy of Condensed Systems" (Boca Raton, Fl.: CRC Press, 1995) and "Multi Frequency EPR Spectroscopy of Conjugated Polymers and Their Nanocomposites" (Boca Raton, Fl.: CRC Press, 2016), five contributions in edited books, eleven reviews and more than 100 articles. Dr.Sci. Krinichnyi is a member of the International EPR (ESR) Society since 1992.